Analysis of bacterial-host interactions in *Wolbachia* infection

A Dissertation
SUBMITTED TO THE FACULTY OF
UNIVERSITY OF MINNESOTA
BY

Yang Li

IN PARTIAL FULFILLMENT OF THE REQUIREMENTS
FOR THE DEGREE OF
DOCTOR OF PHILOSOPHY

Ann Fallon, Advisor

May 2016

Acknowledgements

First I'd like to thank my Ph.D. advisor, Dr. Ann Fallon, for granting me the opportunity and supporting me to pursue all my studies presented herein. Dr. Fallon has been an extremely easy-going and helpful mentor to me. She generously allowed me to begin Ph.D. researches in her lab despite the lack of a master degree in my education. She has been always available to me whenever I bugged her, and very open to my sometimes irregular schedule. She has been very patient in listening to and understanding my ideas, needs and complaining, and very good at offering me accurate encouragement and help with her sharp vision to push my research forward smoothly. Dr. Fallon has also been super supportive to my independence, freedom, passions, hypothesis and career development by allowing me to practice research skills, attend conferences, present my works, learn courses that interest me and introduce me to colleagues. Under her supervision during my Ph.D. years, I have been feeling well cared and been able to have a peaceful mind carrying on my research and developing myself. After this five years working with Dr. Fallon, I have been able to see my potential in being a scientist, and would like to pursue academia as my career.

Next, I'd like to thank my research committee, Dr. Ann Fallon, Dr. Tim Kurtti, Dr. Anath Das, and Dr. Marla Spivak. I have been very grateful to have this committee. All the members in this committee have been very generous and helpful in every progress I made during the pursuit of my Ph.D. degree. The knowledge they imparted, their mentorships, availabilities, supports, reviews and the discussions among us have been extremely useful for my progress and future career development. Aside from my committee, I'd like to thank everyone in the Fallon lab for treating me as a family member, a good friend and a mature co-worker, supporting me, respecting me and sharing resources with me. I want to thank Dr. John Beckmann (now a postdoctoral scientist at Yale University) and Dr. Gerald Baldridge for discussing research with me, motivating me and passing useful ideas and knowledge to me. I want to thank the "lab mother", Dr. Anna Gerenday for listening to my complaining, encouraging me and feeding me chocolates when I was stressful and hungry. I also want to thank Elissa

Carroll, Lea Graber and Cassandra Kurtz for discussing research with me, helping me with my research, letting me answer their questions and chatting with me. Thanks to everyone in the Fallon lab for providing me with a warm and peaceful working environment.

I also want to thank the University of Minnesota Department of Entomology. This is such a big and warm family that has made me, as an international student who is far away from home, feel like at home. I thank all the faculties, fellow students and staffs in the department for providing support, motivation, and help to both my work and my life during my Ph.D. years. Aside from Department of Entomology, I'd like to thank the College of Food, Agricultural and Natural Resource Sciences for awarding me the graduate fellowship, Microbial and Plant Genomics Institute for awarding me the travel fund, Entomological Society of America for awarding me the president's prize, University of Minnesota Biomedical and Genomics Center for providing the DNA sequencing and nanodrop services, and Center for Mass Spectrometry and Proteomics for providing the proteomic analysis service.

Last but not least, I'd like to give big thanks to my family in China, especially my parents Faguang Li and Suhua Yang. I'm the only child in my family, and for the past five years, there was very limited time that my parents and I could meet and be together. Instead of complaining in front of me, my parents tried their best to remove all the worries behind me and fully support me to pursue my Ph.D. education abroad. They have been offering their greatest encouragement, trust and faith to me, and I'm very proud that I have them as my parents. Aside from my parents, I also want to thank all my friends who have been staying with me, chatting with me, helping me and forgiving my insane. Mei Li, my best friend and roommate, has been very generous to me and inspiring me in many aspects including both life and work. Xindi Liu, as my roommate, has been cooking and sharing foods with me. Your and others' friendships are priceless to me. I also want to thank my pet, Cheese, for being such a cute company to me.

Abstract

Wolbachia (Rickettsiales: Anaplasmataceae) is a genus of cytoplasmically inherited alpha-proteobacterium that infects arthropods (especially insects) and filarial nematodes. In arthropods, upon infection, *Wolbachia* alters the host reproduction in a variety of ways including cytoplasmic incompatibility, parthenogenesis, male-killing and feminization to enhance its own transmission. My doctoral research has been focusing on molecular and biochemical interactions between *Wolbachia* and its arthropod host. In chapter one, I made an introduction of *Wolbachia* including its biology, phylogeny and potential in disease control. I also reviewed the studies on *Wolbachia*-host interactions with an emphasis on *Wolbachia* Type IV Secretion System (T4SS). In chapter two, I presented the research I carried out in order to understand *Wolbachia*-mosquito interactions through T4SS. I molecular cloned the T4SS coupling protein VirD4 from *w*Pip and analyzed the co-transcription between T4SS and *Wolbachia* surface protein in *w*Str. In chapter three, I amplified and sequenced five ribosomal protein (rp) genes of *w*Fol from its host *Folsomia candida*, and phylogenetic analyzed 17 *Wolbachia* strains based on the available rp sequences. I also detected a DNase activity in isolated *F. candida* DNA. In chapter four, I further studied the DNase activity that co-purified with *F. candida* DNA, including characterizing the DNase active conditions and estimating the molecular weight of the DNase. In chapter five, I described an approach to estimate the biomass of *F. candida* with a protein stain, Ponceau S.

Table of Contents

List of Tables

Chapter 2

Chapter 3

List of Figures

Chapter 1

Chapter 2

Chapter 3

Chapter 4

Chapter 5

Chapter 1

Introduction and literature review of *Wolbachia*-host interactions

Introduction

Wolbachia (Rickettsiales: Anaplasmataceae) is a genus of cytoplasmically inherited alpha-proteobacterium that infects arthropods (especially insects) and filarial nematodes. *Wolbachia* is mostly found in reproductive tissues in the host (Yen and Barr 1971, Yen and Barr 1973, O'Neill and Karr 1990) and it alters the host reproduction in a variety of ways (Werren 1997). *Wolbachia* is transmitted through the cytoplasm of eggs, and thus spreads vertically through females but not males (Werren 1997). Horizontal transfer among insect hosts also happens during the evolution of *Wolbachia* infection (Brown and Lloyd 2015, Ahmed et al. 2015), resulting in its widespread and global distribution in diverse hosts. Within insects, *Wolbachia* has been found in more than 60% of species, including each of the major insect orders (Werren 1997, Hilgenboecker et al. 2008).

Brief historical sketch of *Wolbachia*

Cytoplasmic rickettsia-like bacteria were first reported in the reproductive tissues of the mosquito *Culex pipiens* in 1924 (Hertig and Wolbach 1924), and were subsequently named *Wolbachia pipientis* (Hertig 1936). In the 1960s, certain cytoplasmically inherited incompatibility factor that results in no offspring was reported within *Culex* mosquito crosses (Laven 1951, Laven 1959, Laven 1967), but not until the 1970s, the connection between *Wolbachia* and the cytoplasmic incompatibility (CI) was formally addressed through "curing" the female with antibiotics (Yen and Barr 1971). Following the antibiotic "curing" experiments, more examples of *Wolbachia* induced CI and other types of reproductive alterations were discovered in arthropods (Trpis et al. 1981, O'Neill and Karr 1990, Stouthamer and Werren 1993, Fialho and Stevens 2000), and thus unravel the widespread distribution and versatility of *Wolbachia*.

Wolbachia in arthropods

Within arthropods, *Wolbachia* is a reproductive parasite and alters the host reproductive activities in four main ways, CI, parthenogenesis, male killing and feminization, to enhance its own transmission (Werren 1997). CI describes the phenomenon whereby eggs that are not infected by *Wolbachia*, or infected with a different type of *Wolbachia* from the male, fail to hatch when fertilized with sperms from infected males, and is the most commonly described phenomenon in *Wolbachia* induced reproductive alterations. CI is found in mosquito genera *Culex* and *Aedes* (Laven 1959, Trpis et al. 1981), wasp genus *Nasonia* (Breeuwer et al. 1992), fruit fly genus *Drosophila* (Clancy and Hoffmann 1996, O'Neill and Karr 1990) and many other arthropods (Brower 1976, Noda 1984, O'Neill 1989, Wade and Stevens 1985, Hsiao and Hsiao 1985). *Wolbachia* induced parthenogenesis or thelytoky, in which virgin females produce female offspring, is found in wasp genera including *Trichogramma* (Stouthamer and Werren 1993), *Encarsia* (Zchori-Fein et al. 1992) and *Diplolepis* (Plantard et al. 1998), thrips genus *Franklinothrips* (Arakaki et al. 2001) and mite genus *Bryobia* (Weeks and Breeuwer 2001). A parthenogenetic springtail genus *Folsomia* is also reported infected with *Wolbachia* (Vandekerckhove et al. 1999), however the direct relation of *Wolbachia* and parthenogenesis in *Folsomia* has not been determined yet because "cured" populations haven't been obtained due to the toxic effects of the antibiotics on the animal (Giordano et al. 2010). The third type of *Wolbachia* induced reproduction alteration is the killing of genetic males (male killing). Male killing *Wolbachia* has been described in beetle genus *Tribolium* (Fialho and Stevens 2000), butterfly genus *Acraea* (Jiggins et al. 2001) and pseudoscorpion genus *Cordylochernes* (Zeh et al. 2005). Feminization, conversion of the genetic male into females, is another reproductive alteration described in arthropods that are infected with *Wolbachia*. *Wolbachia*-induced feminization is commonly found in terrestrial isopod genus *Armadillidium* (Rousset et al. 1992). Among insects, *Wolbachia*-induced feminization is reported in leafhopper genus *Zyginidia* (Negri et al. 2006) and moth genus *Ostrinia* (Kageyama et al. 2002).

The molecular mechanism of *Wolbachia*-induced reproductive alterations, particularly the most common CI, is unknown yet. However, there is a general consensus that *Wolbachia* must somehow modify the sperm at an early stage of spermatogenesis before getting eliminated from the mature sperm in cytoplasmic "waste-bags" (Bressac and

Rousset 1993), since embryonic development aborts when sperm from an infected male fertilize an uninfected egg, due to the loss of properly condensed paternal chromosomes (Poinsot et al. 2003). It is also known that such modified sperm will be fully functional if *Wolbachia* are present in the egg, which indicates some sort of "rescue" is performed by those *Wolbachia* (Werren 1997). Such "mod/resc" (modification/rescue) model is a useful general concept in studying molecular mechanisms of *Wolbachia*-induced CI (Poinsot et al. 2003). Two hypotheses have been proposed based on the "mod/resc" model: the mistiming model and the lock-and-key model. The former states that *Wolbachia* modifies the sperm of infected males to induce a fatal delay of the male pronucleus during the first embryonic division, but that the bacteria can compensate the delay by slowing down mitosis in fertilized eggs. The latter states that *Wolbachia* deposit damaging "locks" on sperm DNA of infected males, but can also provide matching "keys" in infected eggs to undo the damage (Bossan et al. 2011). Among the studies aiming at unraveling the molecular mechanism of CI, the most promising one discovers a *wPip_0282* gene whose protein product associates with the sperm transferred to females by *Wolbachia* infected males, as well as a co-transcribed downstream gene *wPip_0283*. The two-gene operon (*wPip_0282* and *0283*) occurs only in insect-associated, CI-inducing *Wolbachia* indicating possible "mod/resc" pairs (Beckmann and Fallon 2013).

Wolbachia **in filarial nematodes**

Filarial nematodes are parasitic worms that can cause diseases in human and other animals. In addition to its widespread distribution in arthropods, *Wolbachia* is also documented in most of the filarial nematodes in family *Onchocercidae* that have medical and veterinary importance (Darby et al. 2012, Taylor et al. 2013). In contrast to the infection in arthropods, *Wolbachia* that infect filarial nematodes has more reduced genome size, indicating its mutualism with the host (Foster et al. 2005, Ghedin et al. 2007). Survival and reproduction of the filarial nematodes is dependent on *Wolbachia* infection (Taylor et al. 2005, Taylor et al. 2013). Due to its critical involvement in disease-causing filarial nematode biology, *Wolbachia* has become a popular target for treatments (Pfarr and Hoerauf 2006).

Wolbachia phylogeny

The inability of culturing *Wolbachia* in defined cell-free medium is the major challenge of carrying on traditional microbiological studies on *Wolbachia*. However, O'Neill and colleagues circumvented this problem by directly amplifying and sequencing *Wolbachia* genes from infected host tissue (O'Neill et al. 1992), and thus opened the new chapter of *Wolbachia* phylogeny studies using molecular methods. Nowadays, main evolutionary lineages of *Wolbachia* are defined by similarities (>97%) of the *16s rDNA*, *ftsZ*, *dnaA*, and *wsp* gene sequences (Vandekerckhove et al. 1999, Lo et al. 2002, Casiraghi et al. 2003, Lo et al. 2007). So far based on these sequences, *W. pipientis* is monophyletic relative to the other rickettsiae (Figure 1; O'Neill et al. 1992), and the genus has been divided into seven lineages (supergroups A-F and H; Fig 2). Supergroup A and B are found in a wide variety of arthropods and are among the most common endosymbionts worldwide (Lo et al. 2002). Supergroup C and D are exclusively associated with filarial nematodes (Taylor et al. 2005). Supergroup E is associated with springtail genus *Folsomia* (Vandekerckhove et al. 1999), F with two genera of termites and one genus of filarial nematode, and H with two genera of termites (Bordenstein and Rosengaus 2005). More recently, the combination of the whole and partial genome information of 11 *Wolbachia* strains (Fenn and Blaxter 2006) and the whole-genome-shotgun data (Gerth et al. 2014) reveals a more sophisticated phylogenic analysis of *Wolbachia* supergroup relations in broader evolutionary context.

W. persica originally assigned to the genus *Wolbachia* based on ultra-structural similarities is later found unrelated to true rickettsiae (O'Neill et al. 1992, Werren 1997; Fig. 1). In this thesis, I discuss only *Wolbachia pipientis* strains in the family Anaplasmataceae.

Although *Wolbachia* is generally transmitted vertically, horizontal transmissions among arthropod hosts are evident from the lack of co-cladogenesis of *Wolbachia* with its hosts and the reproductive alterations it induces (Gerth et al. 2014, Brown and Lloyd 2015). For example, different isolations of *w*Mel (from the fruit fly *Drosophila melanogaster*) that are identical or nearly identical in *ftsZ* gene sequence can be found in hosts from different insect orders including Diptera, Hymenoptera, Coleoptera and Lepidoptera (Werren et al. 1995). In supergroup B, a *Wolbachia* infected parasitoid wasp

and its blowfly host each harbor *Wolbachia* strains that are closely related phylogenetically, indicating transmission between parasites and their hosts as a possible horizontal exchange mechanism (Werren et al. 1995, Ahmed et al. 2015). Other possible mechanisms including predators, pray and competitors remain to be addressed (Werren 1997, Yun et al. 2011).

Wolbachia as a tool for insect-borne disease control

Insects such as mosquitoes are blood-sucking vectors of many human and animal pathogens such as *Plasmodium* that causes malaria, *Alphavirus* that causes chikungunya infection and *Flavivirus* that causes dengue fever and yellow fever. These vector-borne diseases account for a significant threat to human health and economic losses (Tahir et al. 2015). However current reliance on insecticides to fight against these disease-transmitting vectors is unsustainable due to increasing insecticide resistance and growing concerns about health and environmental impacts (Bourtzis et al. 2016).

Wolbachia has recently emerged as biological weapon for control of mosquito-borne diseases because of its environmental benignity, cost effectiveness, and its natural capability of interfering with viruses persisting within mosquitoes (Iturbe-Ormaetxe et al. 2011, Tahir et al. 2015). One *Wolbachia* strain (*w*MelPop from *D. melanogaster*) that over-replicates in the host induces a variety of physiological manifestations of the host such as life-shortening, egg mortality, reduced blood feeding, delayed larval development and reduced overall fitness (Ritchie et al. 2015). Therefore, *w*MelPop has been proposed as a potential tool for the control of mosquito-borne diseases through being transferred and maintained in natural mosquito populations (Iturbe-Ormaetxe et al. 2011). In addition to the potential of *w*MelPop, some other *Wolbachia* strains are discovered to be able to interfere with insect viruses in *Drosophila* and human pathogens in mosquitoes. For example, the presence of *Wolbachia* limits infections of viruses in transinfected mosquitoes including dengue virus, chikungunya virus, as well as the avian and rodent malaria parasites *Plasmodium gallinaceum* and *P. berghei* (Bian et al, 2010, Moreira et al. 2009, Kambris et al. 2010). These relatively recent findings enable *Wolbachia* as a powerful and sustainable tool for biological control.

Wolbachia-host interaction

Wolbachia, as an intracellular symbiont, has lost some of its genetic material following its adaption to the host, which partially rationalizes the difficulties of culturing *Wolbachia* without the host (Fenn and Blaxter 2006). The completed *Wolbachia* genomes (e.g. *w*Mel from the fruit fly *D. melanogaster* and *w*Bm from the nematode *Brugia malayi*) show a limited metabolic capacity, indicating a reliance on the basic metabolic pathways of the host (Wu et al. 2004, Foster et al. 2005). For example, endogenous amino acid synthesis is extremely limited and *Wolbachia* import host amino acids for protein synthesis and energy production through the tricarboxylic acid cycle and glucogenesis (Wu et al. 2004). Another example is the inability of *w*Mel to synthesize lipopolysaccharide (Wu et al. 2004). Surprisingly, given the drive towards miniaturization, the arthropod *Wolbachia* genomes also contain a large proportion of repeated sequences (Wu et al. 2004, Klasson et al. 2009). In *w*Mel, the repeats make up ~14% of the genome, and some of the repeats correspond to likely mobile elements (Wu et al. 2004). The copy number of some repeats appears to be variable between different *Wolbachia* strains. Therefore, the repeats may be useful markers for strain discrimination, and the mobile elements likely distinct *Wolbachia* strains by altering or disrupting gene functions (Wu et al. 2004).

The genomic analysis also reveals some interesting candidates that might be important for future studies of the interactions between *Wolbachia* and the hosts. The first one is the *Wolbachia* surface protein (Wsp). Wsp is one of the bacterial outer membrane proteins that perform various functions in bacteria-host interaction. *Wsp* is a mosaic gene and is important for bacterial survival and proliferation within the host as it participates in host immune responses and apoptosis inhibition (Bazzocchi et al. 2007; Pinto et al. 2012, Baldridge et al. 2016). However, the exact role that Wsp plays in the interaction between *Wolbachia* and host is unknown yet. *Wsp* is downstream of *virD4* that belongs to one of the two Type IV secretion system (T4SS) operons (Masui et al. 2000). T4SS is a large membrane-spanning protein complex and is essential for the virulence and survival of many bacteria species. It has 12 components (VirB1-11 and VirD4; Wallden et al. 2010), most of which are translated from two operons (operon *virB8-11*/*virD4* and operon *virB3-6*, Rances et al. 2008). It is widely accepted that *Wolbachia* T4SS is important for the

Wolbachia-induced reproductive alterations and the biochemical interactions between *Wolbachia* and the host through secreting DNA and a variety of protein effectors into the host cytosol.

Another interesting group of candidates that may be important for *Wolbachia*-host interactions is proteins with ankyrin-repeat domains (ANK) (Fenn and Blaxter 2006, Wu et al. 2004). The ANK is a motif of ~33 amino acids that is found in many eukaryotic proteins, often in tandem arrays, in which it mediates protein-protein interactions (Bork 1993). The *w*Mel genome contains a large number (23) of ANK genes, while *w*Bm contains nine (Wu et al. 2004, Foster et al. 2005). *Wolbachia* ANK genes might be involved in regulating the host cell cycle or in interacting with the host cytoskeleton (Elfring et al. 1997, Tram and Sullivan 2002). Some of the *w*Mel ANK genes are located within integrated prophage segments. These *Wolbachia*-specific (WO) bacteriophages were discovered in the flour moth *Ephestia kuehniella* and have been identified in many arthropod *Wolbachia* strains (Masui et al. 2000, Masui et al. 2001, Baldridge et al. 2016). There is evidence that WO phages can move both within a bacterial genome and between bacteria in multiple infected hosts, and therefore they are often a source of innovation in terms of introducing genes, in novel combinations, into novel genetic environments (Fenn and Blaxter 2006). Excitingly, genetic analysis of the CI-inducing *Wolbachia* in malaria-transmitting mosquito *C. quinquefasciatus* suggests an important role for highly variable WO-phage-associated ANK genes in the incompatibility reaction (Sinkins et al. 2005). More functions of ANK genes and WO phages in *Wolbachia*-induced host phenotypes remain to be discovered.

Wolbachia T4SS and the coupling protein VirD4

Type IV secretion system (T4SS) (Fig 3) is one of the several types of secretion systems, which bacteria use for transporting macromolecules such as proteins and DNA across the cell envelope. Details on architecture are only known for the two close related archetypical T4SSs that encoded by the Ti plasmid of *Agrobacterium tumefaciens* and by the *E. coli* plasmid pKM101. The Ti plasmid system contains 12 proteins (Fig. 3), VirB1-VirB11 and VirD4, which are referred to as the VirB/D4 proteins.

The bulk of the proteins (VirB6-B10) form the scaffold of the translocation channel that spans the entire cell envelope (Fig. 3). Structural studies have shown that VirB7, VirB9 and VirB10 assembles into a tightly associated 'core complex' containing 14 copies of each of the protein monomers (Chandran et al. 2009, Fronzes et al. 2009). Among the 'core complex' components, VirB10 forms the outer membrane channel (OMC) and inserts in both the inner and outer membranes (Chandran et al. 2009, Fronzes et al. 2009). Lipidation of the lipoprotein VirB7 is needed for correct insertion of the core complex into the outer membrane and is essential for secretion (Fronzes et al. 2009). VirB6 and VirB8 are inner membrane proteins and form the inner membrane channel (IMC). The IMC contains 24 copies of VirB6 monomers and 12 copies of VirB8 monomers (Cascales and Christie 2003). VirB3 is a small inner membrane protein that stabilized by and functions together with VirB4. Three ATPases, VirB4, VirB11 and VirD4, act as hexamers and energize the system from the cytoplasm, driving the complex assembly and substrate translocation through the channel (Wallden et al. 2010). VirB2 and VirB5 form pilus structures extending from the extracellular surface. VirB2 forms the major pilus component and is essential for substrate transfer. VirB5 is a minor pilus component possibly functions as an adhesion that, in some organism, localizes to the tip of the pilus (Eisenbrandt et al. 1999). VirB1 is a periplasmic lytic transglycosylase making holes in the peptidoglycan cell wall to allow the assembly of surface structures such as the pilus (Baron et al. 1997).

T4SS is found in both Gram-positive and Gram-negative bacteria and is essential for the survival of many pathogenic bacteria species (Wallden et al. 2010). The effector proteins transported from the bacteria through T4SS are involved in a variety of host intracellular activities so as to benefit the bacterial uptake, survival and replication. For example, studies on *Coxiella burnetii*, an intracellular pathogen of mammalian that causes Q-fever, reveal an ANK family member AnkG, interferes with the host apoptosis pathway through interacting with host p32 protein upon transported across T4SS (Lührmann et al. 2010). Another effector protein, AnkB, is found involved in bacterial nutrition intake by promoting host proteasomal degradation of proteins (Christopher and Yousef 2012). Some effectors interfere host gene transcriptions upon transported through T4SS (Zou et al. 2013).

The first sign of T4SS in *Wolbachia* is the detection of *virD4* gene in two strains of *w*Tai and *w*KueYo that infect the Taiwan cricket *Teleogryllus taiwanemma* and the Mediterranean flour moth, *Ephestia kuehniella* respectively (Masui et al. 2000). In the subsequential studies, most of the T4SS genes are identified in *Wolbachia*, and these genes are transcribed in two distinct operons. The first operon encodes *virB8-11* and *virD4*, together with upstream *ribA* gene, encoding a putative bifunctional enzyme of the riboflavin biosynthesis pathway, and downstream *wsp* gene, encoding an outer membrane protein that is important for *Wolbachia*-host interactions (see above). The second operon encodes *virB3, 4, 6* and four downstream open reading frames (ORFs) (Masui et al. 2000, Rances et al. 2008, and Felix et al. 2008). It is widely accepted that *Wolbachia* alters host reproduction and interacts with the host through secreting effector proteins through T4SS into host cells. However, there's barely any knowledge of what effectors are secreted and the mechanisms of T4SS secretion.

Hundreds of T4SS effectors have been identified in proteobacteria. As more and more T4SS effectors have been recognized, some of them are discovered to share some common features. Mimicking eukaryotic proteins through having ANK is a character that is widely found in T4SS effectors (Lührmann et al. 2010, Voth and Heinzen 2009). These proteins can hijack host cell pathways therefore altering numerous host cell activities. Another common feature shared by several T4SS effectors is having one to a few copies of the EPIYA motif (Xu et al. 2010). The translocated effectors can be phosphorylated at the tyrosine residue in the EPIYA motif and thus take over some of the host signal transduction pathways. E block, a region of 6-8 residues that are rich in glutamines (at least two), is one more common feature shared by multiple T4SS effectors (Huang et al. 2011). The E residues arrayed on an alpha-helical surface of the effector proteins are important for the translocation of the effectors. Several common signal sequences such as C-terminal translocation signal (Vergunst et al. 2005), and nuclear/mitochondria localization signals (Backert and Meyer 2006) are also found in many T4SS effectors. Based on multiple common features of T4SS effectors, larger repertoire of T4SS effector proteins have been predicted through mathematical models and computer algorithms (Xu et al. 2010, Zou et al. 2013, Lockwood et al. 2011). Studies on using experimental method to screen potential T4SS effectors are also present (Carey et al. 2011). However,

the current knowledge about *Wolbachia* T4SS effectors is insufficient to make larger effector pool predictions, as were done in other zoonotic pathogen species. The genetic screening technique is yet very time-consuming. Therefore, new and effective techniques need to be developed in order to identify *Wolbachia* T4SS effectors.

VirD4 belongs to the T4SS coupling protein (T4CP) family and is the receptor of the substrate during the secretion process (Wallden et al. 2010). Six VirD4 monomers assemble into a globular hexamer composed of two distinct domains with a ~20-Å-wide channel in the middle (Gomis-Rüth et al. 2001). T4CPs are associated with the inner membrane through an N-terminal transmembrane domain (NTD). The C-terminal portion that includes a nucleotide binding domain (NBD) and an alpha-helical bundle termed the all-alpha-domain (AAD) protrudes into the cytosol and involves in the docking of the substrates and the assembly of the T4SS (Okamoto et al. 1991; Figure 4A). Mutational analyses confirmed that the AAD is required for substrate docking and trafficking (Schröder et al. 2002, de Paz et al. 2010, Whitaker et al. 2015), and that the NTD is crucial for the assembly of T4SS especially the interaction between T4CP and other T4SS components in the membrane (Segura et al. 2013). However, more elucidation is needed concerning the function of T4CP and the interaction activities between T4CP and the substrates.

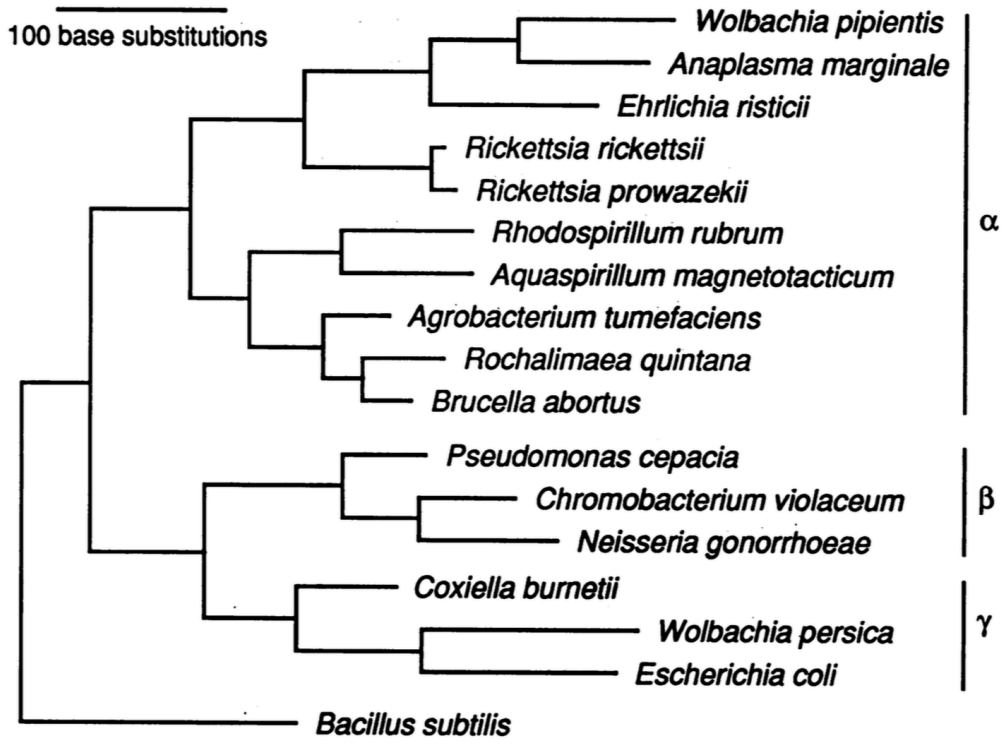

Figure 1. Phylogenetic tree derived from maximum parsimony analysis of the 16s rDNA genes from *W. pipientis* (the top) and other representative proteobacteria from the α, β and γ subdivisions. The Gram-positive bacterium *Bacillus subtilis* was used as the outgroup. This figure shows that *W. pipientis* is monophyletic relative to the other rickettsiae. Figure from O'Neill et al. 1992.

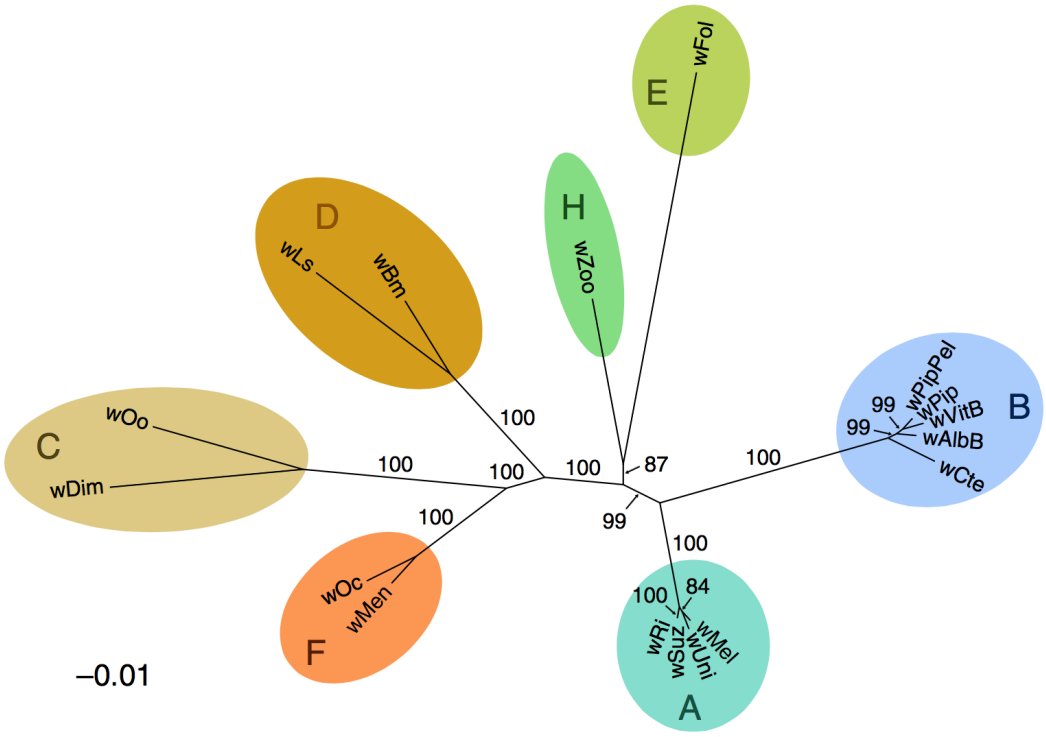

Figure 2. Unrooted phylogram showing relationships between *Wolbachia* strains. The genus *Wolbachia* has been divided into seven supergroups (A-F and H). A and B are found in insects. C and D are exclusively associated with filarial nematodes. E is associated with springtails, F with termites and filarial nematode, and H with termites. Numbers on clades correspond to bootstrap values in percent from 1,000 replicates. Supergroup affiliations are given in colored letters. Leaf labels correspond to *Wolbachia* strain names. Scale bar corresponds to inferred evolutionary changes. Figure from Gerth et al. 2014.

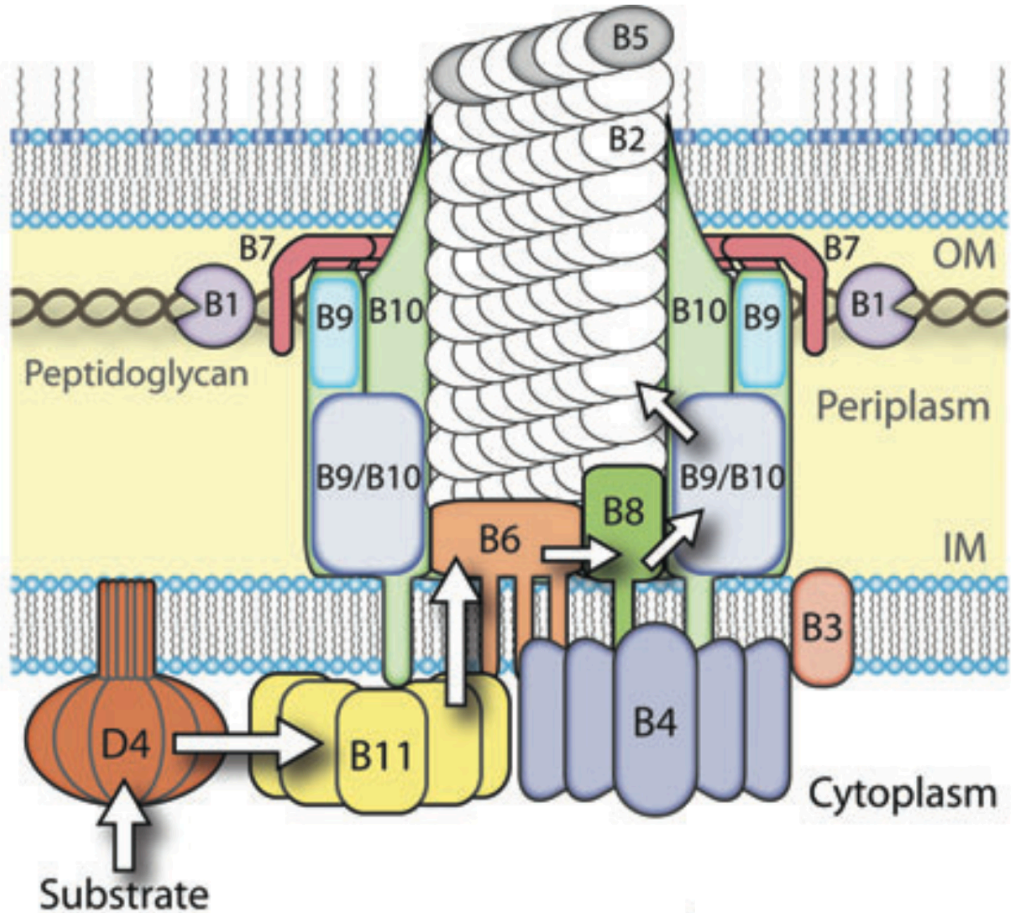

Figure 3. Schematic model of the best studied T4SS from *Agrobacterium tumefaciens.* The experimentally predicted locations of VirB/D4 components of *A. tumefaciens* relative to the bacterial membrane are shown in the figure. Arrows indicate the sequential secretion steps identified during substrate secretion through the VirB/D4 system. Figure from Wallden et al. 2010.

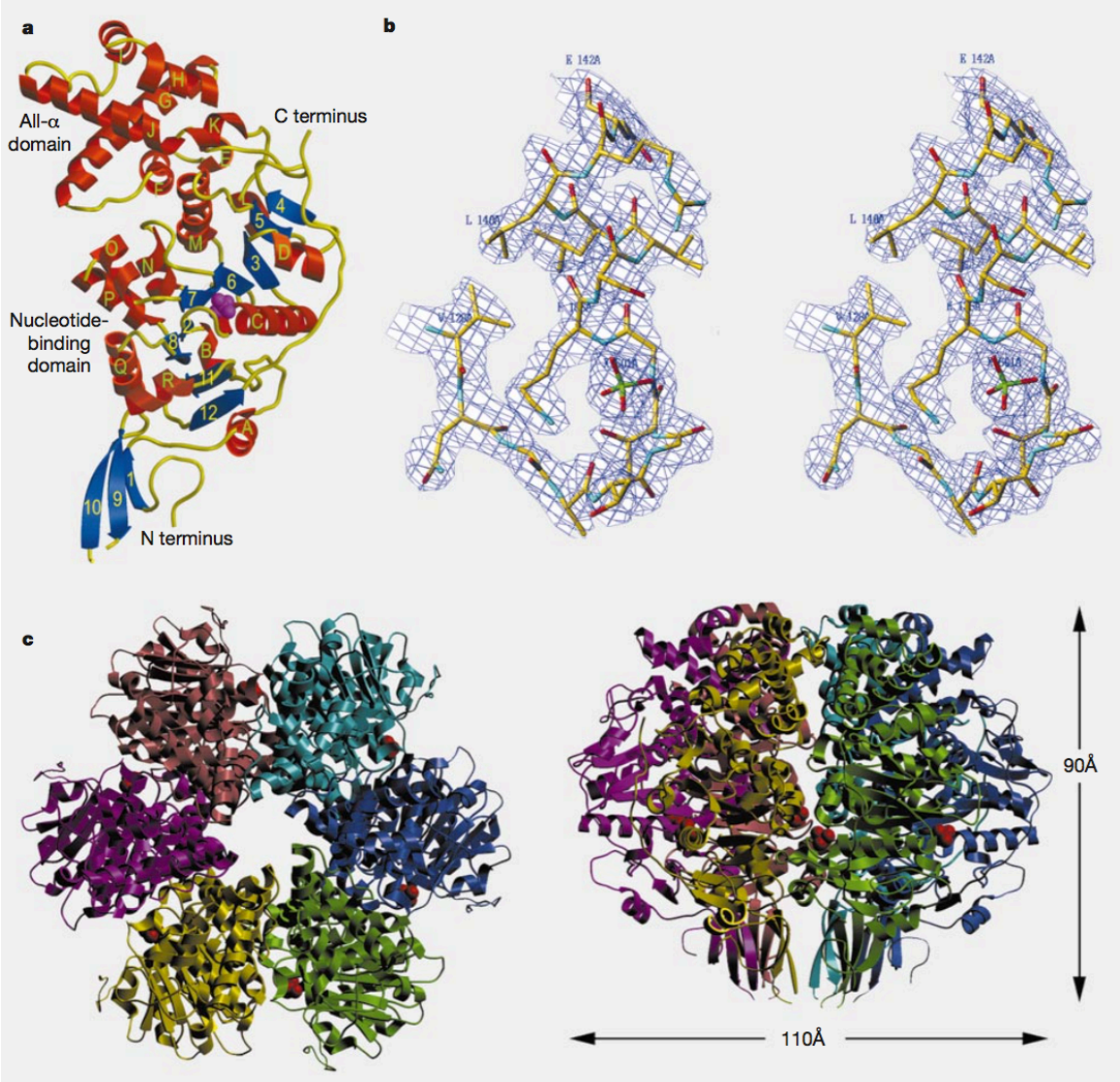

Figure 4. Structural features of a prototype in T4CP family, TrwB. TrwB is encoded by *Escherichia coli* plasmid R388. **A,** Ribbon diagram of the soluble fragment of TrwB lacking the transmembrane domain; **B,** Stereo representation of the TrwB nucleotide-binding domain; **C,** TrwB hexamer viewed from the cytoplasmic side. Left, view along the local six-fold axis; right, side view. Figure from Gomis-Rüth et al. 2001.

Chapter 2

Wolbachia-mosquito interactions through T4SS

Introduction

Wolbachia is a Gram-negative intracellular bacterium that infects arthropods and nematodes. Upon infection, it alters the host reproduction in a variety of ways including cytoplasmic incompatibility (CI), parthenogenesis, male killing and feminization to enhance its own transmission (Werren 1997). The mechanisms of *Wolbachia*-induced reproductive alterations are unknown yet. However, it is widely accepted that *Wolbachia* interact with and manipulate the host cells via secreting protein effectors across its envelope through the Type IV secretion system (T4SS) (Baldridge et al. 2016).

T4SS is one of the several types of secretion systems, which bacteria use for transporting macromolecules such as proteins and DNA across the cell envelope, and is essential for the survival, replication and virulence of many pathogenic bacteria species (Wallden et al. 2010). T4SSs are broadly distributed phylogenetically and have evolved exceptional diversity in their overall architectures, types of substrates secreted, and mechanisms employed for target cell attachment (Bhatty et al. 2013). Nowadays, the best studied T4SSs are the ones encoded by plasmids of *E. coli* (e.g. F, R388, pKM101 and RP4) and the *A. tumefaciens* T-DNA transfer system (Chapter 1, Fig. 3) (Bhatty et al. 2013).

Among the sequenced *Wolbachia* genomes, T4SS genes are organized in two operons. The first operon contains *virB3*, *virB4* and *virB6*, which encodes the inner membrane channel (IMC) component VirB6, the small inner membrane protein VirB3, and one of the inner membrane ATPases VirB4 (Chapter 1, Fig. 3). The second operon contains *virB8*, *B9*, *B10*, *B11* and *virD4*, which encodes the IMC component VirB8, the outer membrane channel (OMC) components VirB9 and VirB10, and the ATPases VirB11 and VirD4 (Chapter 1, Fig. 3). Homologs of all genes except *virB1*, *virB2*, *virB5 and virB7* of *A. tumefaciens* T4SS have been identified in *Wolbachia.* The absence of some components is probably because of the lacking of the pilus structure in *Wolbachia* T4SS.

In some *Wolbachia* genomes, the *wspB* paralog of the *wspA* major surface antigen (Fig 1; Pichon et al. 2009, Rances et al. 2008) is downstream and a member of the T4SS

virB8-11/D4 operon. In the supergroup B strain *w*Pip from mosquito *C. pipiens*, *wspB* is disrupted by a transposon and is presumably inactive (Sanogo et al. 2007, Baldridge et al. 2016). WspB is a candidate T4SS effector that may play a role in reproductive manipulation of the host (Baldridge et al. 2016). In the case of a nematode strain *w*Bm, WspB is secreted into the host cells (Bennuru et al. 2009) and co-localizes with a host protein in tissues that include embryonic nuclei (Melnikow et al. 2011).

Analysis of *Wolbachia* T4SS systems and identification of effectors will be facilitated by examining *Wolbachia* strains that grow to high abundance in cell culture, such as the strain *w*Str in supergroup B that causes strong CI in the planthopper, *Laodelphax striatellus* (Noda et al. 2001). Despite its emergence as a useful strain that grows well in vitro (Fallon et al. 2013), the *w*Str genome is not yet available. In order to demonstrate the correlation between WspB and T4SS in *w*Str, we sequenced a portion of the genome encoding T4SS components and I analyzed the transcription of *wspB* and the upstream *virD4* using reverse transcription polymerase chain reaction (RT-PCR) (Fig. 1 black line). Results were consistent with the possibility that in *w*Str, WspB is a potential T4SS effector candidate.

In parallel experiments, I cloned the T4SS effector receptor VirD4 protein from *w*Pip using the pBAD/His A vector (Invitrogen), and used an *E. coli* expression system to evaluate whether the cloned gene could be expressed at levels sufficient for recovery of interacting (putative effector) proteins using magnetic beads.

Materials and Methods

RNA extraction

Aedes albopictus C7-10 (control; Fallon and Kurtti 2005) and C/*w*Str1 (*Wolbachia* infected; Fallon et al. 2013) cells were maintained in Eagle's minimal medium supplemented with 5% fetal bovine serum at 28 °C in a 5% CO_2 atmosphere as described previously (Fallon et al. 2013). C/*w*Str1 and C7-10 cells were harvested during exponential growth, when loosely attached cells began to lift in small clumps, to favor maximal recovery of *Wolbachia* (Fallon et al. 2013, Baldridge et al. 2014). Harvested cells (2 ml) were collected into a micro centrifuge tube, frozen in liquid nitrogen and stored in -80 °C.

RNA was purified from the cells using PureLink RNA Mini Kit (Life Technologies; Catalog No. 12183018A). Purified RNA was incubated with 8U (4 µl) of DNase I (RNase free; New England Biolabs; Catalog No. M0303S) at 37 °C for 30 min. DNase I was then inactivated at 75 °C for 15 min. Purified RNAs were verified by polymerase chain reaction (PCR) for absence of genomic DNA contamination using the primer pair $S12_{F104-128}$/$S7_{R436-455}$ (Table 1) as previously described (Fallon 2008).

Reverse transcriptase PCR (RT-PCR)

Reverse transcriptase PCR (RT-PCR) was done using the GeneAmp RNA PCR Kit (Applied Biosystems; Catalog No. N8080143) using random hexamers at 42 °C for 20 min followed by 99 °C for 5 min. Samples were then treated with 10 µg (1 µl) RNase A at 37 °C for 15 min. PCR was then carried on using primers: $virD4_{F1764-1784}$ and $wspB_{R152-172}$ (Table 1). PCR reactions include initial denaturation at 95 °C for 4 min followed by 35 cycles of 95 °C for 1 min, 56 °C for 40 sec, and 72 °C for 40 sec, then final extension at 72 °C for 3 min. The PCR products were then sequenced at the University of Minnesota BioMedical Genomics Center.

DNA extraction

A *Wolbachia*-infected *C. pipiens* mosquito colony was maintained at 25 °C with a photoperiod of 16:8 (L: D). Blood meals were provided on anesthetized hamsters as described in Beckmann and Fallon (2012). An individual decapitalized mosquito was homogenized on ice in 0.2 ml distilled water in 1.5 ml micro centrifuge tube using a clean pestle (Beckmann and Fallon 2012). DNA template for PCR was extracted as described in Fallon (2008). Briefly, 0.2 ml of 20 mM Tris-HCl, pH 8.0, containing 0.2 M NaCl, 2 mM ethylenediamine tetraacetic acid (EDTA), 1% sodium dodecyl sulfate (SDS), and 10 µg (1 µl) DNAse-free RNAse A, was added. After incubating for 1 h at 37° C, proteinase K (20 µg) was added, and incubation continued at 56° C for 1 h. The samples were heated at 95° C for 10 min, extracted with phenol, and precipitated with ethanol. DNA was recovered by centrifugation, washed in 70% ethanol, dried, and resuspended in 0.1 ml of double-distilled water.

Polymerase chain reaction (PCR)

PCR primers virD4$_{F1-19}$ and virD4$_{R2228-2249}$ (Table 1) were designed based on *w*Pip complete genome sequence (GenBank: AM999887.1; range 1332043 to 1334300) downstream of six random nucleotides and the restriction enzyme cutting site (underlined in Table 1).

PCR was done in a total reaction volume of 20 µl, containing final concentrations of $MgCl_2$ at 2.5 mM, each of the four deoxyribonucleotide triphosphates at 0.2 mM, primers at 400 nM, template, and Taq polymerase (2.5 units/reaction), and up to1.5 µg of DNA template. Negative control was reaction with water in place of DNA template. Reaction conditions involved an initial denaturation at 95 °C for 4 min, followed by 35 cycles of 95 °C for 1 min, 56 °C for 40 sec, and 72 °C for 2 min, with a final extension at 72 °C for 3 min.

Molecular cloning

Molecular cloning of *virD4* gene was done using pTrcHis A and pBAD/His A vectors (Fig 3). PCR product and the vectors were first digested by XhoI (NEB; Catalog No. R0146S) in a 50 µl total volume (5 µl 10x CutSmart buffer, 10 µl DNA, 0.5 µl XhoI, 34.5 µl ddH_2O) at 37 °C for overnight followed by inactivation at 65 °C for 20 min. A total of 10 reactions were merged to make a final volume of 0.5 ml, and 50 µl 3M NaAc pH 5.2 and 1 ml 100% ethanol were added and set at -20 °C for 2 h. Sample was then centrifuged at 10,000 rpm for 10 min at 4 °C, followed by washing twice with 1 ml 70% ethanol. Sample was dried under vacuum and dissolved in 100 µl ddH_2O. Sample was then digested by EcoRI-HF (NEB; Catalog No. R3101S) in a 50 µl total volume (5 µl 10x CutSmart buffer, 10 µl DNA, 0.5 µl EcoRI-HF, 34.5 µl ddH_2O) at 37 °C for 2 h followed by inactivation at 65 °C for 20 min. 5 µl 3M NaAc pH 5.2 and 100 µl 100% ethanol were added to the merged reactions and set at -20 °C for 2 h. Sample was then centrifuged at 10,000 rpm for 10 min at 4 °C, followed by washing twice with 100 µl 70% ethanol. Sample was dried under vacuum followed by dissolving in 10 µl ddH_2O. Ligation was done in a total volume of 20 µl (9 µl ddH_2O, 2 µl 10x ligase buffer, 2 µl vector, 6 µl insert, 1 µl ligase) at 16 °C overnight followed by inactivation at 65 °C for 20 min. All of the 20 µl ligation mixture was used for transformation (see below).

The VirD4$_{79\text{-}672}$ plasmid was constructed through digesting the intact pBAD/VirD4 plasmid using SacI (NEB; Catalog No. R0156S) in a 50 ul total volume (5 µl 10x buffer, 10 µl DNA, 0.5 µl SacI, 34.5 µl ddH_2O) at 37 °C for overnight followed by inactivation at 65 °C for 20 min. Ten reactions were merged to make a final volume of 0.5 ml. 50 µl 3M NaAc pH 5.2 and 1 ml 100% ethanol were added to the combined reactions and set at -20 °C for 2 h. Sample was then centrifuged at 10,000 rpm for 10 min at 4 °C, followed by washing twice with 1 ml 70% ethanol. Sample was dried under vacuum followed by dissolving in 100 µl ddH_2O. Ligation was done in a total volume of 20 µl (9 µl ddH_2O, 2 µl 10x ligase buffer, 2 µl vector, 6 µl insert, 1 µl ligase) at 16 °C overnight followed by inactivation at 65 °C for 20 min. All of the 20 µl ligation mixture was used for transformation (see below).

Transformation

Single colony of the *E.coli* strain, TOP10 (genotype: F-, *mcr*A Δ(*mrr-hsd*RMS-*mcr*BC) Φ80*lac*ZΔM15 Δ*lac*X74 *deo*R *rec*A1 *ara*D139 Δ(*ara-leu*)7697 *gal*U *gal*K *rps*L *end*A1 nupG) or LMG194 (genotype: F- Δ*lac*X74 *gal* E *thi rps*L Δ*pho*A (*Pvu* II) Δ*ara*714 *leu*::Tn*10*), was cultured in 100 ml LB medium (1% Tryptone, 0.5% Yeast Extract, 0.5% NaCl, pH 7.0) at 37 °C with vigorous shaking. When the OD_{600} reached 0.5, 50 ml cells were collected by centrifuging at 2,600 xg for 10 min at 4 °C. The pellet was gently resuspended in 4 ml ice-cold 50 mM $CaCl_2$ and kept on ice for 30 min. $CaCl_2$ treated cells (100 µl) were aliquoted into a pre-chilled Falcon 2059 tube and the ligation mixture (see *molecular cloning* section) was added followed by incubation on ice for 30 min. The cells were then heat shocked at 42 °C for 45 sec and returned to ice for an additional 2 min. Pre-warmed SOC medium (1 ml; 2% Tryptone, 0.5% Yeast Extract, 0.05% NaCl, 2.5 mM KCl, 10 mM $MgCl_2$) was then added to the transformation mixture followed by incubation at 37 °C for 1 h with vigorous shaking. The culture (50 µl) was then plated onto pre-warmed LB plates (1% Tryptone, 0.5% Yeast Extract, 0.5% NaCl, 1.5% Agar, pH 7.0) containing 50 µg/ml ampicillin and the plates were incubated at 37°C overnight. Twenty single colonies were selected and cultured in 5 ml LB medium, RM medium (2% Casamino Acids, 0.2% glucose, 1 mM $MgCl_2$, 100 µg/ml ampicillin, 1x M9

salts (6 g/L Na_2HPO_4, 3 g/L KH_2PO_4, 0.5 g/L NaCl, 1 g/L NH_4Cl)) in the case of LMG194, containing 50 μg/ml ampicillin at 37 °C overnight with vigorous shaking.

Plasmid extraction

Plasmids were purified from the twenty cultures using bacterial alkaline lysis miniprep. Each culture (4 ml) was decanted into a micro centrifuge tube and centrifuged at 10,000 rpm for 30 sec. The supernatant was discarded leaving 50 μl of medium in the tube. The tube was then vortexed to completely resuspend the cells. TENS solution (300 μl of 10 mM Tris-HCl pH 7.5, 1 mM EDTA, 0.1 N NaOH, 0.5% SDS) was added into the tube, then 150 μl of 3 M NaAc pH 5.2 was added followed by inverting the tube for 5 times to mix completely. The tube was then centrifuged for 10 min at 10,000 rpm and the supernatant was transferred to a fresh micro centrifuge tube. Cold 100% ethanol (900 μl) was added followed by setting at -20 °C for 2 h and centrifugation for 5 min at 10,000 rpm to pellet the plasmid DNA and the RNA. The supernatant was discarded and the pellet was rinsed twice with 1 ml of 70% ethanol. The pellet was then resuspeded in 50 μl ddH_2O and 1 μg RNase A was added followed by incubation at 37 °C for 30 min. The twenty purified plasmids were then sequenced using a series of primers (Table 1) at the University of Minnesota Biomedical Genomics center. Recombinant plasmids that yielded high sequencing signals and were in frame with the N-terminal peptide were chosen for the subsequential expression experiments.

Glycerol Stock

Once the desired plasmid construct was obtained, the clones were stored at -20 °C (-80 °C for long term) as glycerol stocks. The strain containing the construct was grown to saturation (12-16 hours; OD_{600} = 1-2) in LB medium containing 50-100 μg/ml ampicillin at 37 °C with vigorous shaking. The culture (0.85 ml) was then mixed with 0.15 ml of sterile glycerol in sterile capped glass vial, and stored at -20 °C.

Protein expression

A colony that contained the recombinant plasmid was cultured in 50 ml LB medium, RM medium with glucose in the case of LMG194, and 50 μg/ml ampicillin at 37 °C with

vigorous shaking to an OD_{600}=0.5. Expression inducer (0.5 ml of 100 mM IPTG (isopropyl-β-D-thiogalactoside) for pTrcHis plasmid; 0.5 ml of 0.2% L-arabinose for pBAD plasmid) was added to the culture. The culture was then incubated at 37 °C with vigorous shaking for another 3.5 h. OD_{600} of the culture was measured every hour after the inducer was added.

Protein purification

The purification of VirD4 protein was done using the Dynabeads His-Tag Isolation & Pull down kit (Life technologies; Catalog No. 10103D). LMG194 culture (15 ml) that has the recombined VirD4 protein expressed was collected and centrifuged at 2,600 xg for 10 min. Binding/washing buffer (1 ml of 50 mM sodium phosphate pH 8.0, 300 mM NaCl, 0.01% Tween-20) was added to the pellet and mixed well by sonication for 30 sec. Dynabeads (6 mg) was transferred to a micro centrifuge tube and the tube was placed on a magnet for 2 min. The supernatant was discarded and the resuspended bacterial pellet was added into the tube. The tube was mixed well and placed on a roller for 10 min and then placed on a magnet for 20 min. The supernatant was then discarded and the beads were washed 4 times with 300 µl binding/washing buffer by placing the tube on a magnet for 5 min and discarding the supernatant. The beads were resuspended thoroughly between each washing step. The protein was eluted from the beads by adding 100 µl his-elution buffer (300 mM imidazole, 50 mM sodium phosphate pH 8.0, 300 mM NaCl, 0.01% Twen 20) and incubated on a roller for 10 min. The tube was then placed on a magnet for 2 min and the supernatant containing the eluted histidine-tagged VirD4 was transferred into a new micro centrifuge tube followed by being electrophoresed on a 10% SDS polyacrylamide gel as described by Laemmli (1970).

SDS-PAGE

SDS-PAGE was carried out as described by Laemmli (1970). Sieving gel (10%; 11 cm long, 1.5 mm thick) contained 0.1% SDS, 0.375 M Tris-HCl pH 8.8, and polymerized by 0.05% ammonium persulphate (AP) and 0.05% tetramethylethylenediamine (TEMED). Stacking gel (4%; 3 cm long, 1.5 mm thick) contained 0.1% SDS, 0.25 M Tris-HCl, pH 6.8 and polymerized by 0.05% AP and 0.05% TEMED.

The eluted histidine-tagged VirD4 was mixed with same volume of 2 x sample loading buffer (0.2% SDS, 20% glycerol, 120 mM Tris-HCl pH 6.8, 0.02% bromophenol blue), and boiled for 5 min before being loaded into the gel. Electrophoresis was carried out at 40 mA for 6 h using the running buffer (0.1% SDS, 25 mM Tris, 192 mM glycine, pH 8.3).

Western blotting

After SDS-PAGE, the proteins were transferred to nitrocellulose electrophoretically at 20 mA for 1 h in transferring buffer (25 mM Tris pH 8.3, 192 mM glycine, 20% v/v methanol). The nitrocellulose was then incubated in 10 ml blocking buffer (137 mM NaCl, 2.7 mM KCl, 10 mM Na_2HPO_4, 1.8 mM KH_2PO_4, 0.05% v/v Tween-20, 5% w/v nonfat dry milk) and gently agitated on a rocker platform for 20 min at room temperature. The nitrocellulose was washed three times in 20 ml TBST (20 mM Tris pH 7.5, 150 mM NaCl, 0.05% v/v Tween-20) for 5 min each time with gentle agitation. The nitrocellulose was transferred to a tray containing Anti-Xpress antibody (Invitrogen; Catalog No. R910-25) diluted 1:10000 in blocking buffer and incubated with gentle agitation for overnight at 4 °C. The next day, the nitrocellulose was washed three times in TBST for 5 min each time at room temperature with gentle agitation, followed by being transferred to a tray containing secondary antibody (Invitrogen; Catalog No. WP20006) diluted 1:10 in blocking buffer and incubated with gentle agitation for 1 h at room temperature. The nitrocellulose was then washed three times in TBST for 5 min each time at room temperature with gentle agitation, followed by being briefly washed with water for 2 min.

Detection was done immediately after the wash using the Immum-Star AP Chemiluminescent Protein Detection System (Bio-Rad; Catalog No. 1705010) and Kodak Biomax X-OMAT AR film with a 10-min exposure.

Results

Co-transcription of wspB *and* T4SS *in* Wolbachia supergroup B *strain* w*Str from the planthopper* L. striatellus

The robust, persistent infection of *A. albopictus* mosquito cell line, C/*w*Str1 with a CI-inducing *Wolbachia* supergroup B strain *w*Str that is isolated from the planthopper *L.*

striatellus, provides an in vitro system to study *Wolbachia*-host interactions (Fallon et al. 2013). A recent proteomic profiling of the *w*Str infection in C/*w*Str1 cell line (Baldridge et al. 2014) indicated that WspB and T4SS Vir proteins are expressed at similar, above average abundance levels. In the sequenced *Wolbachia* genomes and the available sequences from *w*Str, *wspB* is downstream of the T4SS *virB8-11/D4* operon (Fig. 1).

In order to understand the transcription status of *wspB* in *w*Str, total RNA was purified and reverse transcriptase PCR (RT-PCR) was carried out using primers $virD4_{Forward1764–1784}$ and $wspB_{Reverse152–172}$. Absence of genomic DNA contamination in purified RNA was verified by PCR (Fig. 2A lanes 2 and 3). RT-PCR results showed that a 528 bp cDNA amplicon was obtained from C/*w*Str1 (Fig. 2B lane 4), but not from the negative controls (lanes 1 and 2) or C7-10 (uninfected cell line) (lane 3). The sequence of the RT-PCR amplicon matched the expected *w*Str genomic sequence, confirming that in *w*Str, *wspB* is active and co-transcribed with the T4SS *virB8-11/D4* operon as is the case in supergroup A *w*Mel and *w*Ri from the fly *Drosophila spp.* (Rances et al. 2008, Wu et al. 2004).

Molecular cloning of the w*Pip VirD4 protein using the pTrcHis/A vector*

The co-transcription of *wspB* and T4SS in *w*Str and some other *Wolbachia* strains is consistent with the potential of WspB protein as a T4SS effector. In order to understand the *Wolbachia* host interactions through T4SS effectors, we choose to start from cloning the VirD4 protein from *w*Pip, a strain in the mosquito *Culex pipiens*, because VirD4 is the T4SS effector receptor, and *w*Pip is the best studied and genomically sequenced *Wolbachia* supergroup B strain with applications to mosquito control (Sinkins and Gould 2006). In addition, disruption of the WspB protein in *w*Pip (Sanogo et al. 2007) indicates interesting interactions with host that may differ from *w*Str and other strains. Although *w*Pip has not been adapted to cell culture, mosquito ovaries are easily available and provide an abundant source of effector proteins from *Wolbachia*-infected and 'cured' *C. pipiens* (Beckmann and Fallon 2012) for magnetic bead pull-down assays described below.

C. pipiens mosquito colony that is infected with *w*Pip was maintained in our lab. Template DNA was purified from the mosquitoes as previously described (Beckmann and Fallon 2012), and *virD4* was amplified by PCR from the purified template DNA

using primers virD4$_{F1-19}$ and virD4$_{R2228-2249}$ (Table 1). Molecular cloning was carried out using pTrcHis vector version A (Invitrogen; Catalog No. V360-20; Fig. 3A). The recombined plasmid was constructed through inserting the *virD4* gene between the restriction enzyme XhoI and EcoRI cutting sites (Fig. 3A vertical arrows). After transformation of the recombined plasmid into the *E.coli* strain TOP10, 20 ampicillin (amp) resistant single colonies were selected and cultured for plasmid extraction and protein expression. In order to make sure that the inserted *virD4* is intact, not mutated, and in frame with the N-terminal peptide, the plasmids from the picked colonies were purified and sequenced using the pTrcHis forward primer and a series of virD4 plasmid sequencing (VPS) primers (Table 1).

When expression is desired, the TOP10 colony that hosts the intact, not mutated recombined plasmid are grown to mid-log phase in a total of 50 ml LB culture followed by the addition of the inducer, IPTG, to a final concentration of 1 mM. The culture was then incubated at 37 °C with vigorous shaking for another 3.5 h. Purification of the his-tagged VirD4 protein from 10 ml of the culture was then carried out using the Dynabeads His-Tag Isolation & Pull down kit (Life Technologies; Catalog No. 10103D). SDS-PAGE stained by Coomassie shows no detectable VirD4 protein after purification, indicating either the protein was expressed at a very low level or not expressed.

Growth rate of LMG194 that hosts the recombined pBAD/A plasmid with w*Pip* virD4 *inserted*

In order to have the VirD4 protein expressed at a detectable level, we switched to the pBAD/His vector (Invitrogen; Catalog No. V430-01; Fig. 3B) and the *E. coli* strain LMG194 as plasmid host. Unlike the pTrcHis vector, the pBAD/His vector uses the araBAD promoter (PBAD) from *E. coli*. The regulatory protein for the promoter, AraC, is present in the plasmid allowing regulation of PBAD. Unlike TOP10, LMG194 is used to ensure low basal level expression of toxic genes (Guzman et al. 1995). This strain is capable of growth on minimal medium (RM medium), which allows additional repression of PBAD by glucose.

The recombined plasmid was extracted from TOP10, and transformed into LMG194. After the LMG194 colony that hosts the intact, not mutated recombined plasmid was

properly selected, the colony was grown to mid-log phase in 3 parallel cultures that each contained 50 ml RM culture followed by the addition of the inducer, L-arabinose, to a final concentration of 0%, 0.002%, and 0.2%, respectively. In order to understand the growth rate of the culture after induction, culture density was measured by OD_{600} every hour after the inducer was added (Fig. 4). Results show that the growth rate of the culture that has high inducer concentration (0.2%) is lower than the cultures that have no (0%) or low (0.002%) inducer concentrations, however the error bars of the data points are large relative to the differences among the data points at same induction time.

Detection of the VirD4 protein from LMG194 after induction

After 3.5 hours of induction, the recombined VirD4 protein was purified from 10 ml of the culture using the Dynabeads His-Tag Isolation & Pull down kit, followed by the detection of the VirD4 protein using SDS-PAGE (Fig. 5A) and western blotting (Fig. 5B). The recombined VirD4 construct should have a molecular weight of approximately 77 kDa because the total N terminal tags are 3 kDa according to the manufacturer and the 672 amino acid long VirD4 should be approximately 74 kDa assuming every amino acid is 0.11 kDa on average.

Commassie stained SDS-PAGE (Fig. 5A) shows no detectable band at ~77 kDa after induction (compare lanes 1 and 2 with lane 3), and high levels of background bands. Western blotting targets the Xpress epitope that locates downstream of the 6xhis tag and upstream of the VirD4 protein (Fig. 3B). Figure 5B shows that western blotting detected the recombined VirD4 protein in the LMG194 culture at about 75 kDa (lanes 1 and 2). Since VirD4 is the receptor of T4SS, The Dynabead attached by the his-tagged VirD4 protein is able to work as bait for future studies on *Wolbachia* T4SS effector identification. However, the expression level of the protein is low.

Molecular cloning of the soluble portion of VirD4 protein ($VirD4_{79\text{-}672}$) using the pBAD/His vector

In order to determine whether the N-terminal transmembrane domain (NTD) contributes to the low expression level of VirD4 protein through forming inclusion bodies, I truncated off the 1-78 residues from the N-terminal of the protein (Fig. 6B) via

digesting the recombined plasmid with the restriction enzyme Sac I and re-ligating the bulk rest of the plasmid. The resulting plasmid is 243 bp shorter than the original one, and the truncated protein is 81 residues (~9 kDa) shorter than the intact one (Fig. 6 compare A and B).

Western blotting confirmed the expression of the truncated protein (Fig. 7 lanes 3 and 4, star), however the expression level has no improvement compared to the intact protein (lanes 1 and 2, star), indicating the low expression level of VirD4 is not because of the NTD. In addition, western blotting also detects signal bands heavier than the VirD4 monomer (Fig. 7; VirD4 monomer is indicated by stars), indicating the monomers may form polymer or interact with other proteins after being expressed.

Discussion

In this chapter, the confirmation that the *wspB* is co-transcribed with *virD4* in *w*Str strengthens the hypothesis of interaction between WspB and T4SS. WspB might be co-localized with T4SS at the outer membrane where it functions in various *Wolbachia*-host interactions such as the inhibition of the host immune responses and apoptosis (Bazzocchi et al. 2007; Pinto et al. 2012, Baldridge et al. 2016), and the reproductive manipulations. WspB might also facilitate the T4SS assembly and secretion activities at the cell surface and be involved in the biochemical interactions between the effectors and the host cell.

In the *Wolbachia* supergroup B strain *w*Pip that causes CI in the host *C. pipiens* mosquitoes, WspB is inactivated by a transposon and thus interactions with host must be substituted by other mechanisms. In order to study these mechanisms, we cloned the VirD4 protein because it is an inner membrane ATPase and is the T4SS substrate receptor for effectors that might substitute WspB in *w*Pip. The his-tagged VirD4 protein is attached to the Dynabead and such construction is a bait for future *Wolbachia* effector identification.

However, our results indicate VirD4 expresses at a low level in *E. coli*. This may because VirD4 uses *E. coli*'s rare codons. An *E. coli* codon usage analysis (developed by Dr. Morris Maduro group, University of California, Riverside) shows 22% of *Wolbachia* VirD4 codons are below the threshold frequency (10%) used in *E. coli*. Future directions

in improving VirD4 expression include codon optimization or choosing *E.coli* mutated strains that can translate rare codons, and using in vitro expression system.

Once enough purified VirD4 protein is obtained, proteins from *w*Pip lysate that interact with VirD4 can be identified and thus more information about *w*Pip-host interactions can be obtained. It might also be interesting to study the VirD4-effector binding mechanisms so as to facilitate the discovery of more effectors from other *Wolbachia* strains. In addition, engineering VirD4 might be a new direction in order to manipulate *Wolbachia* to translocate effectors that are beneficial for biological control or to translocate therapeutic molecules for filarial nematode treatments.

Name	Sequence
$S12_{F104-128}$	5'- GCACTAAGGTGTATACTACAACTCC
$S7_{R436-455}$	5'- GCCTTATTAGCTTCAGCCAT
$virD4_{F1764-1784}$	5'- AGAGAGTAATGCTATTGAAGC
$wspB_{R152-172}$	5'- GGTTATCATCTGTAGCATCTT
$virD4_{F1-19}$	5'- ACTGCACTCGAGATGAGCAATGGAAATCACC
$virD4_{R2228-2249}$	5'- TAGTCAGAATTCACTTACCAAAGTTCAAATATTG
$virD4_{F370-385}$	5'- TGGGCATCAGAGAAAG
$virD4_{R850-866}$	5'- CTACGCATCGTACGCAC
pTrcHis F	5'- GAGGTATATATTAATGTATCG
pBAD F	5'- ATGCCATAGCATTTTTATCC
VPS1 ($virD4_{582-603}$)	5'- CTATGAAATAACAAGTGGTTGG
VPS2 ($virD4_{876-895}$)	5'- AGTTTACAATCTTGCTGTAG
VPS3 ($virD4_{1109-1127}$)	5'- TAACTCCTGATAACTTAAC
VPS4 ($virD4_{1342-1361}$)	5'- GGAATATATGAAGAAGCAGG
VPS5 ($virD4_{1645-1664}$)	5'- TATAGTGATAGCACATTCAC

Primer pair $S12_{F104-128}$/$S7_{R436-455}$ was designed by Fallon (2008)

Underlines indicate restriction enzyme cutting sites for XhoI and EcoRI.

Table 1. Primers used in the study.

Figure 1. Schematic depiction of the *Wolbachia virB8*-11/*D4* operon from *w*Str. Arrows indicate the direction of transcription. *Vir* genes are indicated in white font on a black background. Black squares indicate intergenic spacers. Black line at the bottom indicates the RT-PCR amplification product. Figure adapted from Baldridge et al. 2016.

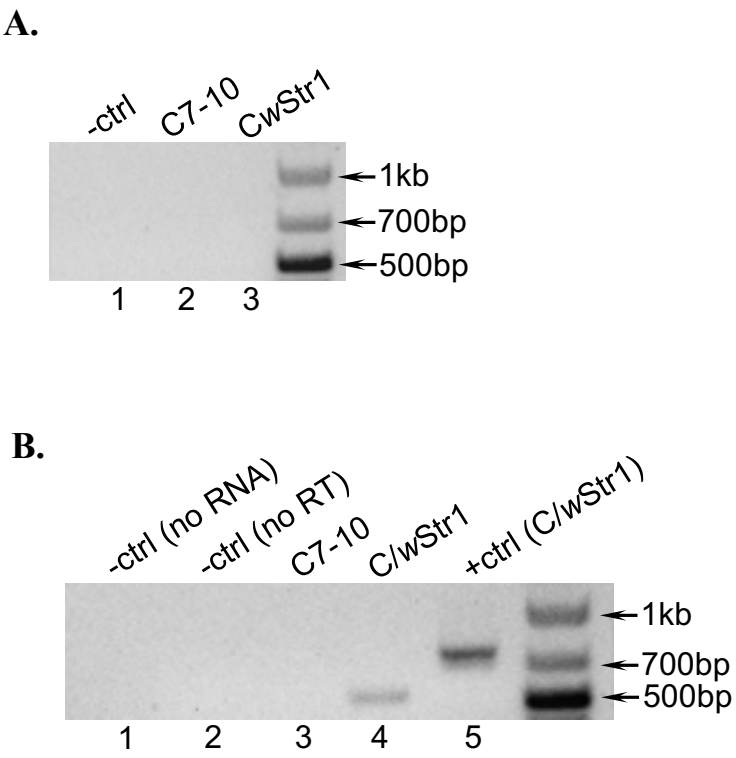

Figure 2. RT-PCR analysis of the transcription of *wspB* and *virD4*. A, PCR confirmation of no genomic DNA contamination in purified RNA samples. Lane 1, negative control with no Taq enzyme added; lane 2, C7-10 cells; lane 3, C/*w*Str1 cells. **B,** RT-PCR results. Lane 1, negative control with no RNA added; lane 2, negative control with no reverse transcriptase added; lane 3, C7-10; lane 4, C/*w*Str1; lane 5, positive control: C/*w*Str1 with *Wolbachia* primers $S12_{F104-128}$/$S7_{R436-455}$ (Table 1).

A.

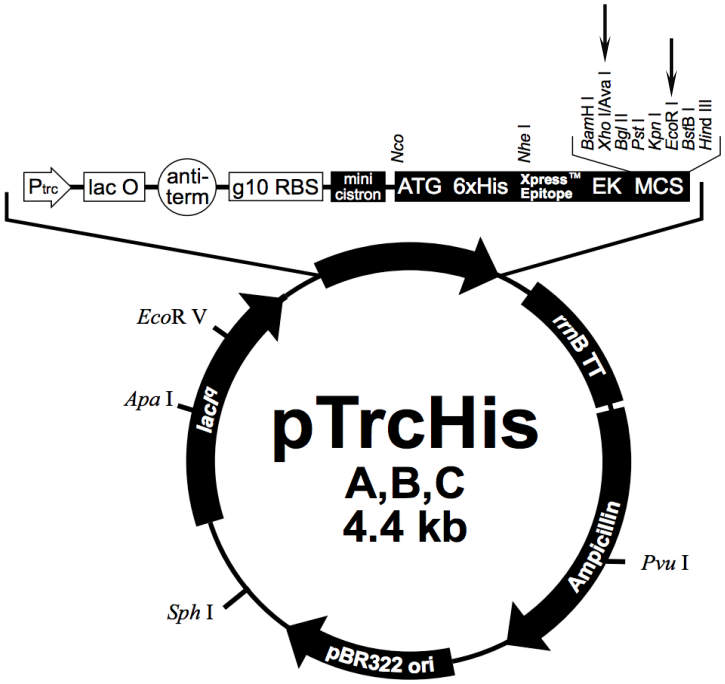
BamH I
Xho I/Ava I
Bgl II
Pst I
Kpn I
EcoR I
BstB I
Hind III
Nco
Nhe I
Ptrc
lac O
anti-term
g10 RBS
mini cistron
ATG 6xHis
Xpress™ Epitope
EK
MCS
EcoR V
Apa I
lacIq
rrnB TT
pTrcHis
A,B,C
4.4 kb
Ampicillin
Pvu I
Sph I
pBR322 ori

B.

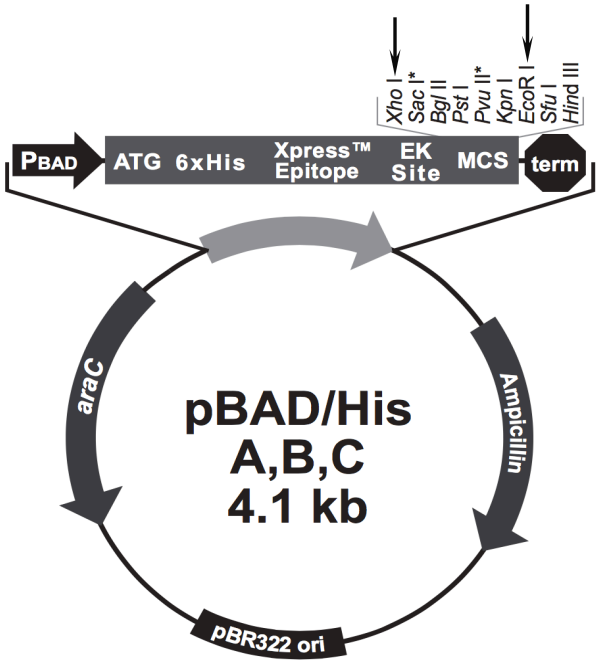
Xho I
Sac I*
Bgl II
Pst I
Pvu II*
Kpn I
EcoR I
Sfu I
Hind III
PBAD
ATG 6xHis
Xpress™ Epitope
EK Site
MCS
term
araC
pBAD/His
A,B,C
4.1 kb
Ampicillin
pBR322 ori

Figure 3. Map of the plasmid vectors. Arrows indicate the restriction enzymes used in this study. **A,** the pTrcHis vector that is a pBR322-derived expression vector using the *trc* (*trp-lac*) promoter and the *rrnB* anti-termination region. The *trc* promoter contains the -35 region of the *trp* promoter together with the -10 region of the *lac* promoter. The pTrcHis vector also contains a copy of the $lacI^q$ gene, which codes for the *lac* repressor protein. This allows for repression of transcription of the cloned insert in *E. coli* regardless of whether the strain is $lacI^{q+}$ or $lacI^{q-}$. The bacteriophage gene 10 (g10) is a translational enhancer that optimizes translation initiation. The reinitiation ribosome binding site (RBS) contains a second ribosome site for efficient reinitiation of translation into the gene of interest. Translation is enhanced by the presence of a minicistron that provides efficient translational restart into the open reading frame (ORF) of the multiple cloning sites (MCS). DNA inserts are positioned downstream and in frame with a sequence that encodes an N-terminal fusion peptide. The N-terminal peptide codes for (5´ to 3´ from the promoter) an ATG translation initiation codon, six histidine residues in series that function as a metal binding domain in the translated protein, the Xpress™ epitope (Asp-Leu-Tyr-Asp-Asp-Asp-Asp-Lys) that allows for the detection of the recombinant protein by the anti-Xpress antibody, and the Enterokinase cleavage site (Asp-Asp-Asp-Asp-Lys) that allows for the removal of the N-terminal peptide by enterokinase for production of native protein. Ampicillin resistance gene is also included in the vector allowing for the selection of the plasmid in *E.coli*. Figure adapted from the handbook of pTrcHis A, B, and C vectors (Invitrogen; Catalog no. V360-20) **B,** the pBAD/His plamid vector that is also an *E. coli* pBR322-derived expression vector but uses the *araBAD* promoter (PBAD) from *E. coli*. The regulatory protein for the promoter, AraC, is present in the plasmid allowing regulation of PBAD. Downstream of the transcription starting codon ATG are the six histidine residues, the Xpress™ epitope, the Enterokinase cleavage site, MCS, and the transcription termination region. Figure adapted from the hand book of pBAD/His A, B, and C vectors (Invitrogen; Catalog no. V430-01).

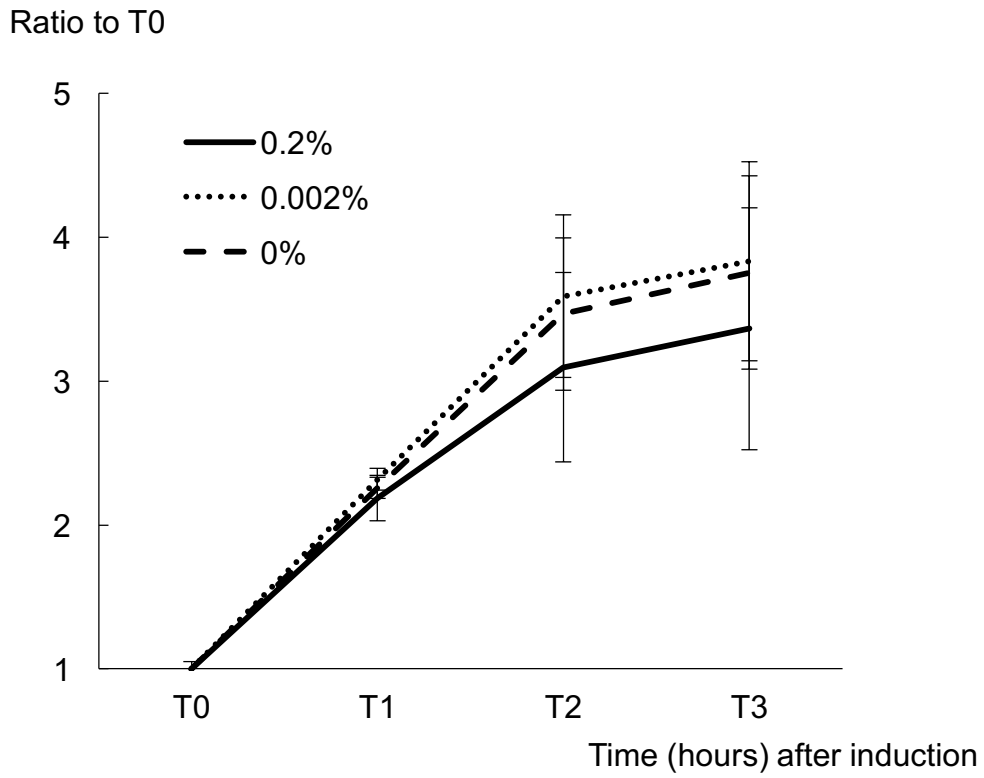

Figure 4. Growth curve (indicated by OD_{600}) of LMG194 that hosts the recombined plasmid in RM medium after induction. Glycerol stock (10 µl) was added into 50 ml RM medium and cultured at 37 °C with vigorous shaking until OD_{600} was approximately 0.4 (T0). Inducer, L-arabinose, was then added into the culture and OD_{600} was measured every hour. OD_{600} is plotted against time.

A.

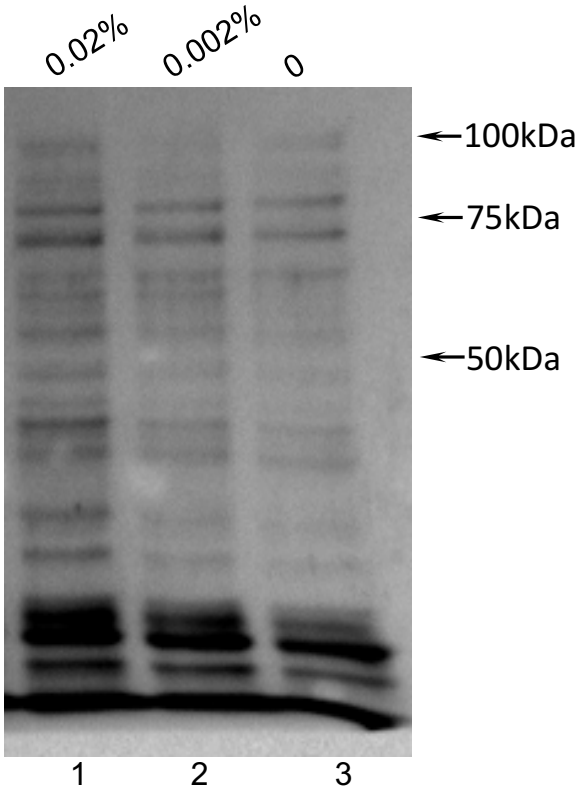

B.

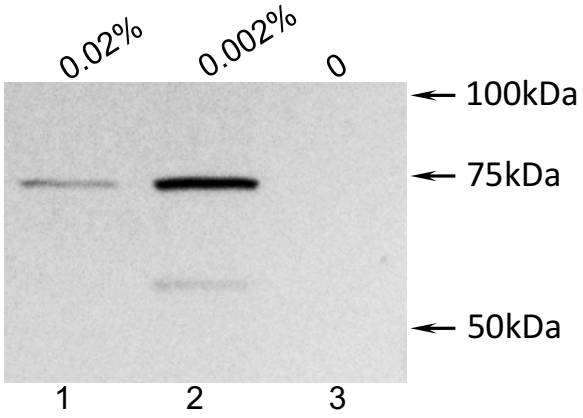

Figure 5. Commassie stained SDS-PAGE and western blotting analysis of the expression of the VirD4 recombined protein using the pBAD/His vector in LMG194 after 3.5 hours of induction. Inducer, L-arabinose, final concentrations are indicated above the lanes. **A,** Commassie stained SDS-PAGE; **B,** western blotting.

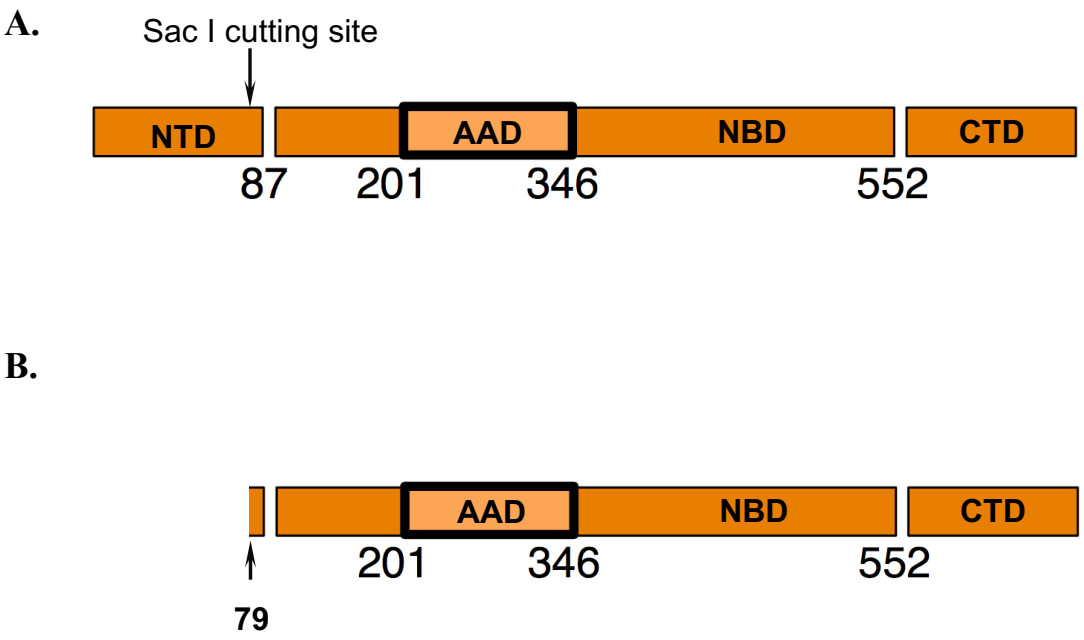

Figure 6. Map of the VirD4 insert. A, the intact VirD4 that was inserted into the pTrcHis and pBAD/His vectors; **B,** VirD4$_{79\text{-}672}$ that is inserted into the pBAD/His vector. NTD, N-termianl transmembrane domain; AAD, all-alpha domain; NBD, nucleotide binding domain; CTD, C-terminal domain.

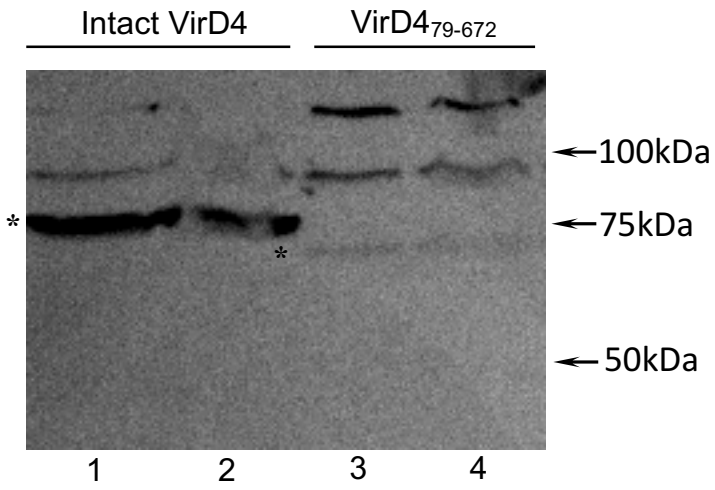

Figure 7. Western blotting analysis of the expression of the soluble portion of VirD4 protein (VirD4$_{79-672}$) using the pBAD/His vector in LMG194 after 3.5 hours of induction. Lanes 1 and 2, intact VirD4; lanes 3 and 4, the soluble portion VirD4$_{79-672}$. Inducer final concentration: 0.002%. Lanes 1 and 3, samples purified from 8 ml LMG194 culture, lanes 2 and 4, samples purified from 10 ml LMG194 culture. Stars indicate the monomer of the expressed protein.

Chapter 3

Isolation of DNA from *Folsomia candida* (Collembola: Isotomidae): detection of a DNase activity

Introduction

Wolbachia is an intracellular Gram negative alpha-proteobacterium that infects a high proportion of arthropods and some nematodes. Upon infection, *Wolbachia* alters the host reproductive activities in a variety of ways including cytoplasmic incompatibility (CI), feminization, male killing and parthenogenesis (Werren et al. 2008). In the *Wolbachia*-infected Collembolan, *Folsomia candida*, no male occurs and all individuals are parthenogenetic.

Wolbachia was first observed in *F. candida* through transmission electron microscopy (Vandekerckhove et al. 1999). Fluorescence *in situ* hybridization on microscopic sections of *F. candida* specimens confirmed that *Wolbachia* were restricted to tissues of the ovary and brain (Czarnetzki and Tebbe 2004). Sequences of *16s rDNA* and *ftsZ* proved that *w*Fol (*Wolbachia* from *Folsomia candida*) belongs to supergroup E, and is closer related to the arthropod infecting supergroup A and B than to the nematode infecting supergroup C and D (Vandekerckhove et al. 1999, Czarnetzki and Tebbe 2004).

Folsomia candida Willem 1902, is a member of the order Collembola (colloquially called springtails) that have a well-developed furca (springing organ). *F. candida* is a common and widespread arthropod that occurs in soils throughout the world (Krivtsov et al. 2003, Fountain and Hopkin 2005). The genus *Folsomia* includes species that have no anal spines and an abdomen with the posterior three segments fused (Fig. 1). The species is 1.5 to 3.0 mm in length at maturity, is white or faintly yellowish in color, and does not bear ocelli (Fountain and Hopkin 2005). Like all other collembolans, *F. candida* has a pair of thin-walled, closely apposed, eversible vesicles on the ventral side of the first abdominal segment. This structure is commonly known as the ventral tube, and is involved in fluid exchange with the external environment (Nutman 1941, Eisenbeis 1982). The ventral tube is an important exposure route for chemicals dissolved in soil pore water (Lock and Janssen 2003). The most distinguishing feature that separates *F.*

candida from other members of the genus is the presence of numerous (at least 16) stout setae on the ventral side of the manubrium of the furca (Fountain and Hopkin 2005).

F. candida has been used as a "standard" test organism for more than 40 years for estimating the effects of pesticides and environmental pollutants on nontarget soil arthropods. However, it has also been employed as a model for the investigation of numerous other phenomena such as cold tolerance, quality as a prey item, and effects of microarthropod grazing on pathogenic fungi and mycorrhizae of plant roots (Fountain and Hopkin 2005).

Populations of *F. candida* consist exclusively of diploid parthenogenetic females (Fountain and Hopkin 2005). At 20 °C they take 21-24 days to reach sexual maturity. About 30-50 eggs are laid in each batch, which take 7-10 days to hatch. The eggs are white, spherical, and 80-110 μm in diameter. The optimal temperature for hatching success is 21 °C. An adult female may go through 45 molts in her lifetime with short reproductive instars (duration 1.5 days) alternating with longer nonreproductive instars (duration 8.5 days) (Fountain and Hopkin 2005).

Currently, addition of antibiotics to the food source has been used to explore *Wolbachia*'s role in *F. candida* parthenogenesis in our lab and other groups (Pike and Kingcombe 2009, Giordano et al. 2010). However, very interestingly we observed inconsistency in amplifying *Wolbachia* genes from *F. candida* DNA, as was also the case with DNA extracted from *C. pipiens* mosquitoes (Beckmann and Fallon 2012). Literature reports only *16s rDNA* and *ftsZ* genes from *w*Fol, and the genome of *w*Fol has not been sequenced yet. The difficulty of obtaining genetic information from *w*Fol greatly hampers further studies on *Wolbachia*-*F. candida* interactions.

In order to obtain more genetic information from *w*Fol, and push forward the *Wolbachia* phylogenic and *Wolbachia*-induced parthenogenetic studies, in this chapter, we amplified five ribosomal protein genes from *w*Fol and detected evidence for a DNase activity in purified *F. candida* DNA. The discovery of the DNase that co-purifies with *F. candida* DNA shed some light on the mechanism of *Wolbachia*-induced parthenogenesis in Collambola.

Materials and Methods

F. candida *stock*

A lab culture of *F. candida* was generated from a small population initially reared in potting soil, and maintained on charcoal/agar plates. Charcoal/agar plates were made by boiling 15 g agar and 5 g of charcoal in 1 L of distilled water. When the agar dissolved, the mixture (20 ml/plate) was added to sterile petri plates and allowed to solidify. Plates were sprinkled with 20 mg of powdered yeast, and 25 large springtails were added to the plates. Within three days, communal egg masses were usually present.

F. candida *DNA purification*

In order to purify template DNA for ribosomal protein gene amplification, *F. candida* eggs were collected from 25 charcoal/agar plates into 100 ml of ice-cold distilled water. Eggs were frozen at -80 °C, thawed on ice, and broken with a mortar and pestle in 1 ml of 10 mM Tris-HCl pH 7.5 containing 100 mM NaCl, 20 mM EDTA and 10% glycerol. Samples were electrophoresed in 0.8% agarose gels, and high molecular weight DNA that migrated just below the loading wells was recovered using a Freeze 'N Squeeze DNA gel extraction column (Bio-Rad; Catalog No. 7326165).

For PCR inhibitor examination, *F. candida* eggs were collected from five charcoal/agar plates and homogenized on ice in 0.2 ml distilled water in 1.5 ml micro centrifuge tubes using a clean pestle. DNA template for PCR was extracted as described in Fallon (2008). Briefly, 0.2 ml of 2x STE buffer (20 mM Tris-HCl, pH 8.0, 0.2 M NaCl, 2 mM ethylenediamine tetraacetic acid (EDTA), 1% sodium dodecyl sulfate (SDS) and 10 µg DNase-free RNase A, was added into the sample. After 1 h at 37° C, proteinase K (20 µg) was added, and incubation continued at 56° C for 1 h. The samples were then heated at 95° C for 10 min, extracted with phenol, and precipitated with ethanol. DNA was recovered by centrifugation, washed in 70% ethanol, dried, and resuspended in 0.1 ml of double-distilled water. In the deoxyribonuclease assay (lambda test), proteinase K digestion was omitted when extracting DNA.

*Cell line (C/*w*Str1) DNA purification*

A. albopictus C/*w*Str1 cells were maintained in Eagle's minimal medium supplemented with 5% fetal bovine serum at 28 °C in a 5% CO_2 atmosphere as described previously

(Fallon et al. 2013). C/*w*Str1 cells were harvested during exponential growth, when loosely attached cells began to lift in small clumps, to favor maximal recovery of *Wolbachia* (Fallon et al. 2013, Baldridge et al. 2014). Cells (2 ml) were collected into a micro centrifuge tube, frozen in liquid nitrogen and stored in -80 °C. DNA template for PCR was extracted as described in Fallon (2008) (see above in F. candida *DNA purification* section).

C. pipiens *mosquito DNA purification*

Wolbachia-infected *C. pipiens* mosquito colony was maintained at 25 °C with a photoperiod of 16:8 (L: D). Blood meals were provided on anesthetized hamsters as described in Beckmann and Fallon (2012). Individual mosquito was collected and decapitated. DNA template for PCR was purified as described in Beckmann and Fallon (2012).

Cimex lectularius *bed bug DNA purification*

Wolbachia-infected *Cimex lectularius* bed bugs were generously provided by Dr. Stephen Kells from the Department of Entomology, University of Minnesota. Individual bed bug was homogenized on ice in 0.2 ml distilled water in 1.5 ml micro centrifuge tubes using a clean pestle. DNA template for PCR was extracted as described in Fallon (2008) (see above in F. candida *DNA purification* section).

Polymerase chain reaction (PCR)

PCR was carried out using primers listed in Table 1. PCR was done in a total reaction volume of 20 µl, containing final concentrations of $MgCl_2$ at 2.5 mM, each of the four deoxyribonucleotide triphosphates at 0.20 mM, primers at 400 nM, template, and Taq polymerase (2.5 units/reaction), and up to 9 µl of DNA template. Negative control was reaction with water in place of DNA template. Reaction conditions involved an initial denaturation at 95 °C for 4 min, followed by 35 cycles of 95 °C for 1 min, 56 °C for 1 min for primer pair $S12_{F104-128}/S7_{R436-455}$ (54 °C for 1 min for primer pairs $S13_{F68-89}/S11_{R161-180}$ and $L17_{F-34--16}/L17_{R75-93}$), and 72 °C for 2 min, with a final extension at 72 °C for 3 min. Samples were then electrophoresed on 0.8% agarose gel in buffer

containing ethidium bromide for 50 min at 105 mA and photographed with ultraviolet light illumination.

Phylogeny study of w*Fol*

PCR products were cloned into TOPO-TA cloning vectors (Invitrogen; Catalog No. K457501), amplified in *E. coli*, and sequenced by classical dideoxy Sanger sequencing at the University of Minnesota Biomedical Genomics Center. Sequences were verified using three reactions with independent DNA template preparations.

Homologous nucleotide sequences were retrieved using *w*Fol query sequences with blastn, and amino acid sequences were retrieved using tblastn to query the refseq_genomic *Wolbachia* (taxid 953) database available as of Feb 1, 2015. Sequences were assembled into a concatenate representing the five genes encoding: rpS7, rpS11, rpS12, rpS13, rpL17, aligned with clustalw2 (http://www.ebi.ac.uk/Tools/msa/clustalw2/) and saved as nexus files using default parameters for nucleotides. For amino acid sequences, pairwise parameters of 25/0.5 and multiple alignment parameters of 10/0.2 were used for gap opening and gap extension penalties, respectively.

Nexus files were analyzed using PAUP* version 4.0b10 (Swofford, 2002) to generate trees based on parsimony, using a heuristic search with bootstrapping based on 1000 replicates. Bootstrap values greater than 50% are shown. The nucleotide comparison included 325 informative characters, and the amino acid comparison included 87 parsimony-informative characters.

Deoxyribonuclease assay (lambda test)

Purified *F. candida* DNA was diluted 10x to 10,000x in double distilled water. Lambda test was carried out by mixing 0.25 µg lambda DNA (New England Biolabs; Catalog no. N3011S) and 10 µl purified *F. candida* DNA in total volume of 20 µl followed by incubating at 37 °C for 4 h. Samples were then electrophoresed on 0.8% agarose gel in buffer containing ethidium bromide for 50 min at 105 mA and photographed with ultraviolet light illumination.

Results

Streptomycin resistance and phylogeny analysis of w*Fol using ribosomal protein genes*

The parthenogenetic *F. candida* is infected with *Wolbachia* (designed *w*Fol). *w*Fol belongs to supergroup E based on *16s rDNA* and *ftsZ* genes. However, no more gene sequence is available from *w*Fol. In order to obtain more genetic information from *w*Fol and further address its phylogeny, we amplified portions of *w*Fol DNA that encode ribosomal protein (rp) genes using PCR. Primer pairs used are listed in Table 1. Product of primer pair $S12_{F104\text{-}128}/S7_{R436\text{-}455}$ contains $rpS12_{104\text{-}372}$ (accession no. KP746937.1) and $rpS7_{1\text{-}455}$ (accession no. KP746938.1). Product of primer pair $S13_{F68\text{-}89}/S11_{R161\text{-}180}$ contains $rpS13_{68\text{-}366}$ (accession no. KP746939.1) and $rpS11_{1\text{-}180}$ (accession no. KP746940.1). Product of primer pair $L17_{F\text{-}34\text{--}16}/L17_{R75\text{-}93}$ contains $rpL17_{1\text{-}93}$ (accession no. KP746936.1).

The five rp gene (*rpS12*, *rpS7*, *rpS13*, *rpS11*, *rpL17*) sequences were translated into amino acids using ExPASy translate tool. All of the *Wolbachia* strains thus far examined encode rpS12 with a K42R point mutation that confers streptomycin resistance (Fallon et al. 2013). Although the ecological significance of streptomycin resistance in *Wolbachia* is unknown, rpS12 from *w*Fol also contains this mutation.

Sequences, both nucleotides and amino acids, were assembled into a concatenate and aligned with homologs from 16 *Wolbachia* strains using clustalW2. The trees shown in Fig. 2 were generated based on these alignments. Both trees clearly distinguished between supergroup A and B strains from insects, and C and D strains from filarial worms. Although bootstrap support is stronger with nucleotide sequences, trees show good congruence with the possible exception of *w*Lec, from the bedbug. These analyses place *w*Fol as a sister group to insect-associated *Wolbachia* strains in supergroup B.

Detection of PCR inhibitor in purified F. candida *DNA*

During the amplification of *w*Fol rp genes, recovery of *w*Fol DNA was erratic as was also the case with DNA extracted from *C. pipiens* mosquitoes (Beckmann and Fallon 2012). To test for an inhibitor in *w*Fol DNA, template DNAs for PCR were purified from *F. candida* eggs, an *A. albopictus* mosquito cell line (C/*w*Str1) that is infected with a CI-inducing *Wolbachia* supergroup B strain *w*Str (Fallon et al. 2013), decapitated *C. pipiens*

mosquitoes that are infected with supergroup B strain *w*Pip, and *Cimex lectularius* bed bugs that are infected with supergroup F strain *w*Lec (Rasgon and Scott 2004).

PCR was carried out using the various template DNAs with primer pair $S12_{F104-128}$/$S7_{R436-455}$ as previously described (Fallon, 2008). Figure 3A shows that PCR with *F. candida* DNA obtains no product (lane 2) while the other DNA templates obtain intense product bands (lanes 3-5).

PCR was then carried out using mixed templates composed of 1 µl C/*w*Str1 DNA and 0, 4-7 µl *F. candida* DNA. Figure 3B shows that the intensity of the PCR product band decreases as increasing amounts of *F. candida* DNA were added (compare lane 2 with lanes 3-6). These results indicate PCR inhibitor in purified *F. candida* DNA.

Detection of a DNase activity in purified F. candida *DNA*

According to the previous results, we speculated the possibility of the PCR inhibitor being a DNase. In order to test this, DNA was purified from *F. candida* eggs as described by Fallon (2008) omitting the protease K digestion (see Materials and Methods). Deoxyribonuclease assay (lambda test) was carried out by mixing different dilutions of the purified *F. candida* DNA with 0.25 µg lambda DNA, an *E. coli* bacteriophage DNA, and incubating at 37 °C for 4 h. Fig. 4 shows that lambda DNA was degraded by 10x to 1000x dilutions of the purified *F. candida* DNA, indicating DNase activity in *F. candida* DNA.

Discussion

Like other *Wolbachia*, *w*Fol encodes a mutation, K42R substitution, in ribosomal protein S12, which is associated with resistance to streptomycin, one of several metabolites secreted by the Gram-positive soil bacterium, *Streptomyces griseus*. Structural and biochemical studies have identified rpS12, as well as specific nucleotides in 16S rRNA, as a critical molecular contributor in distinguishing between cognate and near-cognate tRNA species as well as in promoting more global rearrangements in the ribosomal small subunit. Streptomycin targets rpS12, and the K42 residue interacts directly with streptomycin (Sharma et al. 2007). Because *Wolbachia* grows only within eukaryotic host cells, which are generally thought to exclude aminoglycoside antibiotics

such as streptomycin, it is surprising to note that *Wolbachia* is resistant to streptomycin. *Wolbachia*'s resistance to this antibiotic may confer an advantage to establishment of an infection, and provides a phenotype useful for adapting *Wolbachia* isolated from insect tissues to cell culture, as most contaminating microbes would be expected to be streptomycin sensitive.

Our phylogenetic analysis based on rp sequences places supergroup E strain *w*Fol as a sister group to insect-associated *Wolbachia* strains in supergroup B. The close relationship between supergroup E and supergroups A and B *Wolbachia* is confirmed by many studies. However, Gerth et al. (2014) recently used a set of 90 short loci with average length of 300 bp and found robust support for placement of supergroup E at the base of the *Wolbachia* phylogenetic tree. Further studies will be needed to resolve this discrepancy caused by differences in the lengths of the loci being used for phylogenetic studies.

The discovery of the DNase activity in *Wolbachia*-infected *F. candida* DNA elucidates the difficulty of obtaining genetic information of *w*Fol from *F. candida*, and is the first molecular indication of the mechanism of *Wolbachia*-induced parthenogenesis in Collembolan. In addition to the results described above, we obtained some primary understanding of this DNase activity based on several interesting observations. For example, we speculate that the DNase might bind to and interact with the DNA with extremely high affinity because it was able to survive the traditional DNA purification procedures including phenol/chloroform extraction and ethanol precipitation that in most cases could remove contaminating proteins. The DNase activity was also able to survive the digestion with the broad-spectrum serine proteinase K indicating the association with DNA might protect it from exposing to protease binding. We also speculate that the DNase activity does not have sequence specificity for binding or digesting because the DNA templates all turned into short pieces (~100 bp) after incubating with high DNase activity (Fig 4 lanes 2 and 3) and didn't show any band pattern after incubating with low DNase activity (Fig 4 lanes 4). These observations and speculations indicated the DNase activity that co-purifies with *F. candida* DNA is very powerful and interesting. However, more studies need to be addressed to purify, identify and further characterize this DNase activity.

Name	Sequence
$S12_{F104-128}$	5'- GCACTAAGGTGTATACTACAACTCC
$S7_{R436-455}$	5'- GCCTTATTAGCTTCAGCCAT
$S13_{F68-89}$	5'- ATGGTATAGG(C/T)ATTGCTACTGC
$S11_{R161-180}$	5'- AGCATAAGGTGT(A/G)GA(C/T)TTTC
$L17_{F-34--16}$	5'- GCTA(A/G)ACAACATACTGATG
$L17_{R75-93}$	5'- CTAGAATACCCACCTTTAC

Primer pair $S12_{F104-128}$/$S7_{R436-455}$ was designed by Fallon (2008)

Table 1. Primers used in this study

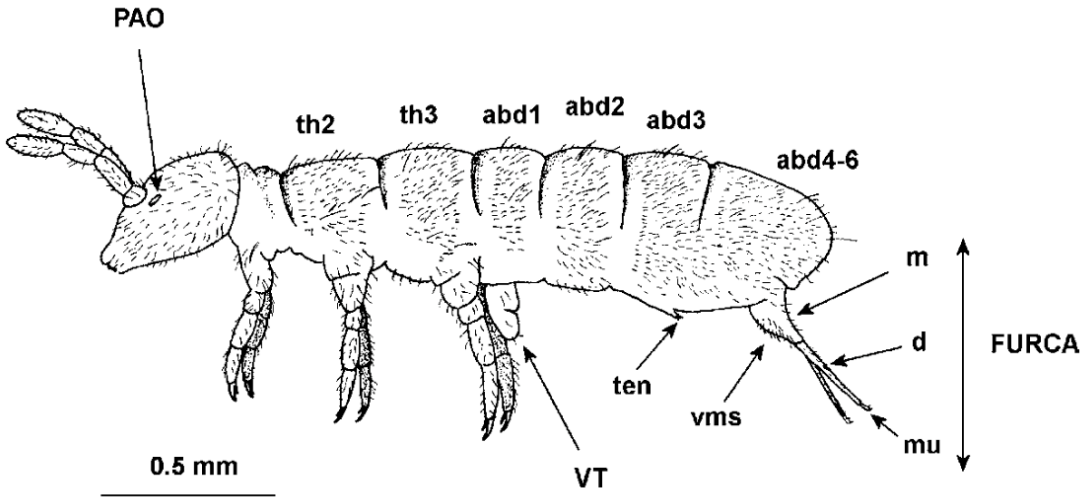

Figure 1. Adult female *F. candida*. In the living animal the furca is held in place under the body by the tenaculum (ten). The first thoracic segment is reduced dorsally compared with the second (th2) and third (th3). The last three abdominal segments (abd4-6) are fused together. d, dens; m, manubrium; mu, mucro; PAO, post-antennal organ; vms, ventral manubrial setae; VT, ventral tube. Figure from Fountain and Hopkin 2005.

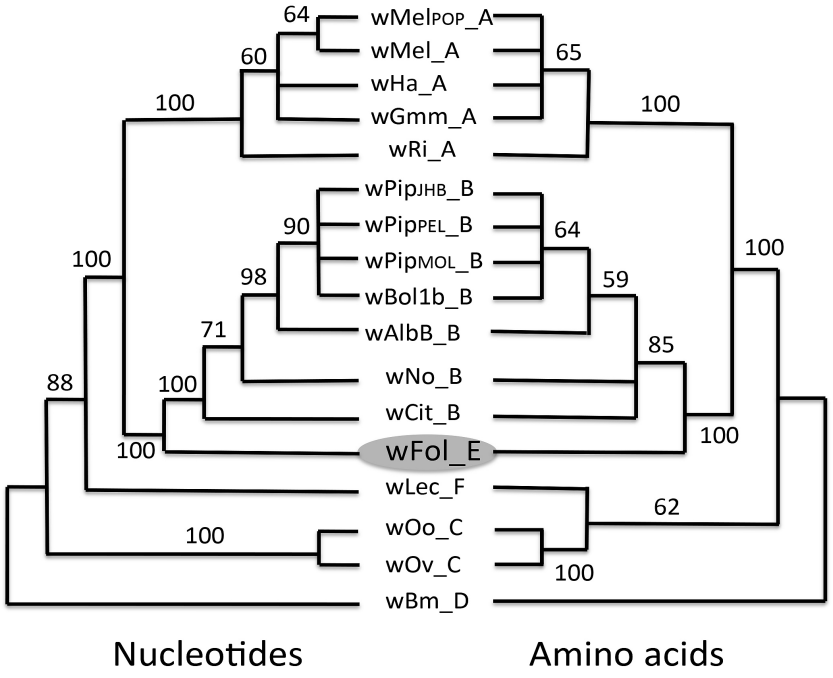

Figure 2. Phylogenetic analysis of *w*Fol compared to other *Wolbachia* strains. Supergroup is indicated next to the "_" following the strain name. Trees were generated using PAUP* based on parsimony, using a heuristic search with bootstrapping based on 1000 replicates. Bootstrap values greater than 50% are shown. *w*Fol is indicated by the grey oval.

A.

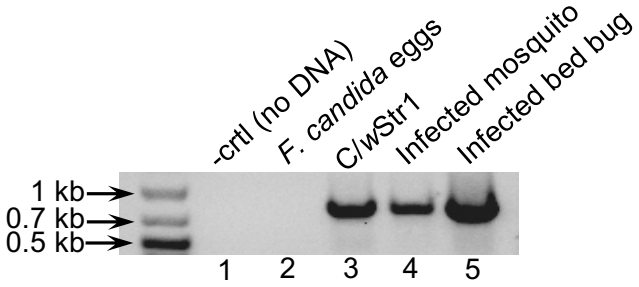

B.

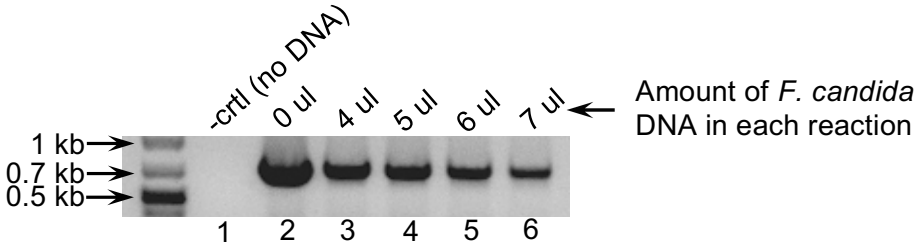

Figure 3. Detection of PCR inhibitor in purified *F. candida* DNA. A, PCR using template DNA from various sources; **B,** PCR using mixed templates composed of 1 µl C/*w*Str1 DNA and 0, 4-7 µl *F. candida* DNA.

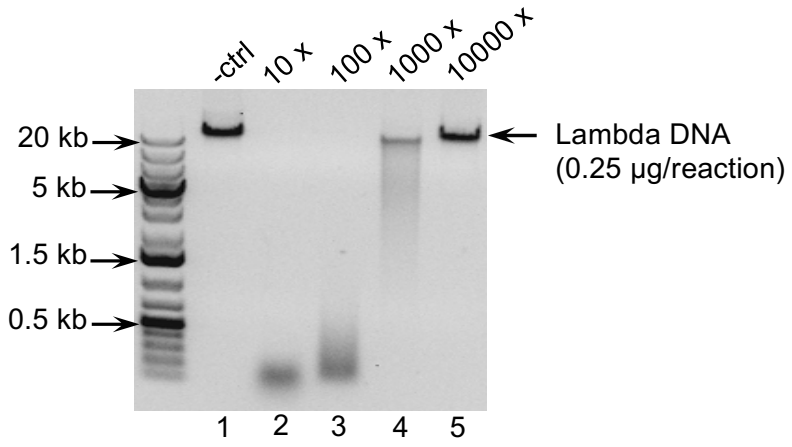

Figure 4. DNase activity in dilutions of purified *F. candida* DNA. Dilutions of *F. candida* DNA are indicated above the lanes.

Chapter 4

Primary characterization and molecular weights of the DNases in purified *Folsomia candida* DNA

Introduction

Folsomia candida Willem (Collembola: Isotomidae) typically reproduces by parthenogenesis and has been widely used in soil pollution and ecotoxicological studies (Fountain and Hopkin 2005). *Wolbachia* has been observed in *F. candida* (Vandekerckhove et al. 1999), and its potential role in parthenogenesis has been studied by addition of antibiotics to the food source (Pike and Kingcombe 2009, Giordano et al. 2010). *Wolbachia* is currently divided into several supergroups (A-F and H) (Lo et al. 2002). *Wolbachia* from *F. candida* (*w*Fol) is assigned to supergroup E based on sequence of *16s rDNA* and *ftsZ* genes (Czarnetzki and Tebbe 2004). Few additional genes have been characterized form *w*Fol, and the *w*Fol genome has not been sequenced, limiting phylogenetic studies and exploration of *Wolbachia*'s role in parthenogenesis.

In the last chapter, we amplified five ribosomal protein genes from *w*Fol and detected evidence for a DNase activity associated with purified *F. candida* DNA. The discovery of the DNase activity may contribute to the difficulty of obtaining genetic information from *w*Fol and its host, *F. candida*. In this chapter, I further characterized and biochemically analyzed the DNase activity, and estimated the molecular weights of the DNases.

Materials and Methods

F. candida *stock*

A lab culture of *F. candida* was generated from a small population initially reared in potting soil, and maintained on charcoal/agar plates. Charcoal/agar plates were made by boiling 15 g agar and 5 g of charcoal in 1 L of distilled water. When the agar dissolved, the mixture (20 ml/plate) was added to sterile petri plates and allowed to solidify. Plates were sprinkled with 20 mg of powdered yeast, and 25 large springtails were added to the plates. Within three days, communal egg masses were usually present.

Sample preparation

Preparation of F. candida *egg extract-F.candida* eggs were collected from 25 charcoal/agar plates into 100 ml of ice-cold distilled water, frozen at -80 °C, thawed on ice, and broken with a mortar and pestle in 1 ml of 10 mM Tris-HCl pH 7.5 containing 100 mM NaCl, 20 mM EDTA and 10% glycerol. Protein concentration of the egg extract was about 1.6 mg/ml as measured using the Bio-Rad Protein Assay (BIO-RAD, catalog no. 500-0006). The egg extract was used in the biochemical assays as described below.

Preparation of purified F. candida *DNA-F. candida* eggs were collected from 10 charcoal/agar plates and homogenized on ice in 0.2 ml distilled water in 1.5 ml micro centrifuge tubes using a clean pestle. DNA template for PCR was extracted as described in Fallon (2008) omitting the proteinase K digestion. Briefly, 0.2 ml of 2x STE buffer (20 mM Tris-HCl pH 8.0, 0.2 M NaCl, 2 mM ethylenediamine tetraacetic acid (EDTA), 1% sodium dodecyl sulfate (SDS)) and 10 µg DNase-free RNase A was added into the sample. After 1 h at 37 °C, the sample was then extracted with phenol, and precipitated with ethanol. DNA was recovered by centrifugation, washed in 70% ethanol, dried, and resuspended in 0.2 ml of double-distilled water. The sample has DNA concentration about 1.8 µg/µl, and was used in the gel-based assays as described below.

Biochemical assay (lambda test)

Lambda test was carried out by mixing 0.25 µg lambda DNA (48 kb in size; New England Biolabs; Catalog No. N3011S) and 10 µl diluted *F. candida* egg extracts in total volume of 20 µl followed by incubating at various conditions, e.g. temperature, $MgCl_2$ concentrations, $CaCl_2$ concentrations, NaCl concentrations, and pH, as described below. The activity of the DNase is determined by the degradation of the lambda DNA in each reaction, as shown by the densitometry of the DNA bands (see below) after electrophoresing in a 0.8% agarose gel. The stronger the DNase activity was; the less intact lambda DNA was left in each reaction.

In order to determine the proper amount of the egg extract (original sample has protein concentration of 1.6 mg/ml) used for the reactions in each condition, e.g. temperature, $MgCl_2$ concentrations, $CaCl_2$ concentrations, NaCl concentrations, and pH, pilot

experiments were carried out with different dilutions (10 x to 1000 x) of the egg extract at different conditions. The dilutions that best describe the strongest DNase activity in each condition are reported in the Results.

Densitometry of DNA bands

After lambda test (see above), samples were electrophoresed on 0.8% agarose gel in buffer containing ethidium bromide (EB) for 50 min at 105 mA and photographed with ultraviolet light illumination. Densitometry of the DNA bands were measured using Adobe Photoshop CS6. Briefly, the image was opened as white bands on black background in Photoshop. The marquee tool was used to outline each DNA band, and the Mean value in the histogram window (Window>>Histogram) was collected. The Mean value represents the density of the area selected.

Polynucleotide-polyacrylamide gel electrophoresis (PPAGE)

A summary of gel preparation, electrophoresis, and visualization of the DNase activity is shown in Fig. 1. Sieving gel (10%; 11 cm long, 1.5 mm thick) contained 0.375 M Tris-HCl pH 8.8 and 0.03% DNA (Sigma, Lot No. 49F70551), and polymerized by 0.05% ammonium persulphate (AP) and 0.05% tetramethylethylenediamine (TEMED). Stacking gel (4%; 3 cm long, 1.5 mm thick) contained 0.25 M Tris-HCl pH 6.8 and polymerized by 0.05% AP and 0.05% TEMED.

F. candida egg extract was diluted 10 x, and was mixed with same volume of 2 x sample loading buffer (20% glycerol, 120 mM Tris-HCl pH 6.8, 0.02% bromophenol blue). Samples (200 µl, 100 µl, 60 µl, 50 µl, 40 µl) were loaded into the gel. Electrophoresis was carried out at 40 mA at 4 °C (DNase inactive) for 4.5 h using the running buffer (25 mM Tris, 192 mM glycine pH 8.3). After electrophoresis, the sieving gel was separated from the stacking gel and was incubated overnight in the DNase buffer (20 mM $MgCl_2$, 10 mM Tris-HCl pH 5.0) at 45 °C (DNase active). The gel was then stained with Pyronin Y (0.1% Pyronin Y in 7% acetic acid) at room temperature for 6-8 h followed by being destained with 7% acetic acid at room temperature for 4 h.

For comparing the DNase activities in *F. candida* egg extract and purified *F. candida* DNA, *F. candida* egg extract (15 µl of 10 x diluted as described above) and purified *F.*

candida DNA (100 µl; 1.8 µg/µl) was mixed with same volume of 2x sample loading buffer (20% glycerol, 120 mM Tris-HCl pH 6.8, 0.02% bromophenol blue) followed by being loaded into the gel. Electrophoresis was carried out at 40 mA at 4 °C (DNase inactive) for 4.5 h using the running buffer (25 mM Tris, 192 mM glycine pH 8.3). After electrophoresis, the sieving gel was separated from the stacking gel and was incubated overnight in the DNase buffer (20 mM $MgCl_2$, 10 mM Tris-HCl pH 5.0) at 45 °C (DNase active). The gel was then stained with Pyronin Y (0.1% Pyronin Y in 7% acetic acid) at room temperature for 6-8 h followed by being destained with 7% acetic acid at room temperature for 4 h.

Native polyacrylamide gel electrophoresis (PAGE)

Native PAGE was carried out as described by Laemmli (1970) without SDS. Sieving gel (7%, 7.5%, 8%, or 10%; 11 cm long, 1.5 mm thick) contained 0.375 M Tris-HCl pH 8.8, and polymerized by 0.05% AP and 0.05% TEMED. Stacking gel (4%; 3 cm long, 1.5 mm thick) contained 0.25 M Tris-HCl pH 6.8 and polymerized by 0.05% AP and 0.05% TEMED.

Purified *F. candida* DNA (1.8 µg/µl, see above) or protein standards (see below) were mixed with same volume of 2 x sample loading buffer (20% glycerol, 120 mM Tris-HCl pH 6.8, 0.02% bromophenol blue). Samples (50 µl, 100 µl, or 200 µl) were loaded onto the gel, and electrophoresis was carried out at 40 mA at 4 °C for 5 h using the running buffer (25 mM Tris, 192 mM glycine, pH 8.3; DNase inactive). Eight protein standards representing eight different molecular weights were used. The 20 kDa, 146 kDa, 242 kDa, and 480 kDa standards were from NativeMark Unstained Protein Standard (10 µl/lane; Thermo Fisher Scientific; Catalog No. LC0725). The 66 kDa, 132 kDa, 198 kDa, and 264 kDa were bovine serum albumin (BSA; 20 µg/lane) monomer, dimer, trimer, and tetramer respectively.

After electrophoresis, the sieving gel was separated from the stacking gel. Lanes that contained purified *F. candida* DNA was incubated in the DNase buffer (20 mM $MgCl_2$, 10 mM Tris-HCl pH 5.0) at 45 °C (DNase active) for overnight. The sieving gel was washed by distilled water briefly followed by being stained with Pierce™ Color Silver

Stain Kit (Thermo Fisher Scientific, catalog no. 24597). Lanes that contained protein standards were stained with Coomassie brilliant blue.

The agarose overlay

Purified *F. candida* DNA (1.8 µg/µl, see above) was mixed with same volume of 2 x sample loading buffer (20% glycerol, 120 mM Tris-HCl pH 6.8, 0.02% bromophenol blue). Native PAGE was carried out using the samples (50 µl, 100 µl, or 200 µl; see above). After electrophoresis, the sieving gel was separated from the stacking gel. The agarose overlay was made by boiling 0.5% agarose, and when the agarose dissolved, substrate DNA (Sigma, Lot No. 49F70551) was added to 0.03% final concentration. Before solidification, a thin layer (~2 mm) of the overlay was poured on the surface of the sieving gel. After the overlay was solidified (about 30 min), the sieving gel (with the overlay attached) was soaked into the DNase buffer (20 mM $MgCl_2$, 10 mM Tris-HCl pH 5.0) and incubated at 45 °C (DNase active) for overnight. The overlay was then carefully peeled off from the sieving gel and stained with Pyronin Y (0.1% Pyronin Y in 7% acetic acid) at room temperature for 6-8 h followed by being destained with 7% acetic acid at room temperature for 4 h. The sieving gel was stained with Pierce™ Color Silver Stain Kit (Thermo Fisher Scientific; Catalog No. 24597).

SDS-PAGE

SDS-PAGE was carried out as described by Laemmli (1970). Sieving gel (10%; 11 cm long, 1.5 mm thick) contained 0.1% SDS, 0.375 M Tris-HCl pH 8.8, and polymerized by 0.05% AP and 0.05% TEMED. Stacking gel (4%; 3 cm long, 1.5 mm thick) contained 0.1% SDS, 0.25 M Tris-HCl pH 6.8 and polymerized by 0.05% AP and 0.05% TEMED.

F. candida DNA was purified from the eggs as described above with or without SDS in the 2 x STE buffer. Purified *F. candida* DNA (1.8 µg/µl, see above) were mixed with same volume of 2 x sample loading buffer (0.2% SDS, 20% glycerol, 120 mM Tris-HCl pH 6.8, 0.02% bromophenol blue). Sample (200 µl) were boiled for 5 min before being loaded onto the gel. Electrophoresis was carried out at 40 mA for 6 h using the running buffer (0.1% SDS, 25 mM Tris, 192 mM glycine pH 8.3). After electrophoresis, the

sieving gel was separated from the stacking gel, and was stained by Coomassie brilliant blue.

Results

Biochemical assays (lambda tests)

In the last chapter, I described a DNase activity that co-purifies with *F. candida* DNA. The DNase activity may contribute to the inconsistency in amplifying *Wolbachia* genes from *F. candida* DNA. In order to better understand the DNase activity so as to find ways to remove it from DNA purified from *F. candida* eggs, motivated by Brown et al. (1982), we decided to start with visualizing the DNase activity using polynucleotide-polyacrylamide gel electrophoresis (PPAGE; Brown et al. 1982). The *F. candida* colony in our lab can provide abundant eggs as resource for the technique.

The visualization of the DNase activity using PPAGE requires inactivating and activating the DNase activity at different steps (Brown et al. 1982). Therefore, looking for conditions that inactivates and activates the DNase activity was needed. We decided to characterize the DNase activity at different conditions using lambda tests (see Materials and Methods). In order to have abundant DNase resource to work with, we prepared *F. candida* egg extract (see Materials and Methods). We used the egg extract instead of purified DNA as the DNase resource for the lambda tests.

Effects of temperature on the DNase activity

Lambda DNA (0.25 μg) was mixed with 10 μl 800 x diluted egg extract in a total volume of 20 μl that contained 1 mM $MgCl_2$ and 20 mM Tris-HCl pH 7.0, and was incubated at different temperatures (4 °C, 15 °C, 23 °C, 30 °C, 37 °C, 45 °C, 56 °C, 69 °C) for 1h. Samples and a new batch of lambda DNA (0.25 μg; no treatment) were then electrophoresed on 0.8% agarose gel in buffer containing ethidium bromide (EB) for 50 min at 105 mA and photographed with ultraviolet light illumination. Densitometry of the bands were measured (see Materials and Methods). DNase activity was calculated as subtracting the band density in each treatment from the band density of the new batch of lambda DNA (0.25 μg; no treatment). All the reactions were repeated 3 times with

different *F. candida* egg samples. Fig. 2 shows that the DNase has the highest activity at 45 °C.

Effects of pH on the DNase activity

Lambda DNA (0.25 μg) was mixed with 10 μl 200 x diluted egg extract in a total volume of 20 μl that contained 1 mM $MgCl_2$ and 20 mM Tris-HCl with different pH (5.0-9.0 with 0.5 intervals), and was incubated at 45 °C for 30 min. Samples and a new batch of lambda DNA (0.25 μg; no treatment) were then electrophoresed on 0.8% agarose gel in buffer containing ethidium bromide (EB) for 50 min at 105 mA and photographed with ultraviolet light illumination. Densitometry of the bands were measured (see Materials and Methods). DNase activity was calculated as subtracting the lambda band density in each treatment from the band density of the new batch of lambda DNA (0.25 μg; no treatment). All the reactions were repeated 3 times with different *F. candida* egg samples.

Fig. 3 shows that the DNase activity was more active at low pH (5.0) and pH 7.5, indicating two different activities might be involved. The DNase activity was partially inhibited at pH 6.0 and high pH (9.0). However, the effects of pH on the DNase activity is not as significant as the effects of temperature because the difference between the lowest and highest band density in Fig. 3 is only 15, while in Fig. 2 is 51.

Effects of $MgCl_2$ on the DNase activity

Lambda DNA (0.25 μg) was mixed with 10 μl 200 x diluted egg extract in a total volume of 20 μl that contained 0-80 mM (0 mM, 0.25 mM, 0.5 mM, 5 mM, 20 mM, 40 mM, 60 mM, 80 mM) $MgCl_2$ and 20 mM Tris-HCl pH 7.0, and was incubated at 45 °C for 30 min. Samples and a new batch of lambda DNA (0.25 μg; no treatment) were then electrophoresed on 0.8% agarose gel in buffer containing ethidium bromide (EB) for 50 min at 105 mA and photographed with ultraviolet light illumination. Densitometry of the bands were measured (see Materials and Methods). DNase activity was calculated as subtracting the lambda band density in each treatment from the band density of the new batch of lambda DNA (0.25 μg; no treatment). All the reactions were repeated 3 times with different *F. candida* egg samples.

Fig. 4 shows that the DNase has high activity in $MgCl_2$ final concentrations ranging from 0.25 mM to 40 mM.

Effects of $CaCl_2$ on the DNase activity

Lambda DNA (0.25 μg) was mixed with 10 μl 50 x diluted egg extract in a total volume of 20 μl that contained 0-100 mM (0 mM, 5 mM, 10 mM, 20 mM, 40 mM, 60 mM, 100 mM) $CaCl_2$ and 20 mM Tris-HCl pH 7.0, and was incubated at 45 °C for 30 min. Samples and a new batch of lambda DNA (0.25 μg; no treatment) were then electrophoresed on 0.8% agarose gel in buffer containing ethidium bromide (EB) for 50 min at 105 mA and photographed with ultraviolet light illumination. Densitometry of the bands were measured (see Materials and Methods). DNase activity was calculated as subtracting the lambda band density in each treatment from the band density of the new batch of lambda DNA (0.25 μg; no treatment). All the reactions were repeated 3 times with different *F. candida* egg samples.

Fig. 5 shows that the activity of the DNase was low at high $CaCl_2$ final concentrations.

The biochemical assays above show that the DNase has high activity at 45 °C (Fig. 2) and at $MgCl_2$ final concentrations ranging from 0.25 to 40 mM (Fig. 4). The activity of the DNase was low at high $CaCl_2$ final concentrations (Fig. 5). The effects of pH on the DNase activity is less significant and more complicated than the effects of the other conditions (Fig. 3), which maybe because more than one DNase activity was involved.

Visualization of the DNase activity using polynucleotide-polyacrylamide gel electrophoresis (PPAGE)

In order to visualize the DNase activity, PPAGE was carried out as described in Materials and Methods. Visualization of the DNase activity was made possible by the inclusion of 0.03% high molecular weight DNA (Sigma, Lot No. 49F70551) substrate within the sieving gel. No protein denaturant was used in this technique. Electrophoresis was carried out using conditions under which the DNase was inactive (4 °C, no $MgCl_2$). The position of the DNase was revealed by incubation of the sieving gel in the DNase buffer (20 mM $MgCl_2$, 10 mM Tris-HCl, pH 5.0) at 45 °C (DNase active) followed by

staining for intact DNA. The colorless regions on the gel indicated absence of intact high molecular weight DNA and thus corresponded to the presence of the DNase activity. A summary of this technique is shown in Fig. 1.

Visualization of the DNase activity in F. candida *egg extract using PPAGE*

PPAGE was carried out using 10 x diluted *F. candida* egg extract (see Materials and Methods). In order to better show all the DNase activities of different strengths, different amounts of the sample were loaded into the gel (as indicated above the lanes in Fig. 6A). Fig. 6A reveals a pattern of at least 7 DNase activities (letters a-g) of different strengths in *F. candida* egg extract. Activity a was high molecular weight and weak. Activity b was strong and wavy compared to other activities, and had a tail. Activity d, e, and g were also weak. These DNase activities should include the DNase activity that co-purifies with *F. candida* DNA and may contributes to the difficulties of obtaining genetic information from *w*Fol and its host.

Visualization of the DNase activity in purified F. candida *DNA using PPAGE*

PPAGE revealed 7 DNase activities in *F. candida* egg extract (Fig. 6A; letters a-g). In order to narrow down the activities that were co-purified with *F. candida* DNA and may contributed to the difficulties of obtaining genetic information from *w*Fol and its host, we carried out PPAGE using purified *F. candida* DNA (see Materials and Methods). We modified DNA purification procedures from Fallon (2008) by using no proteinase so that the proteins in the sample were intact. Since phenol extraction was carried out in purified *F. candida* DNA preparation (see Materials and Methods), most of the proteins that did not interact with DNA were removed. Therefore, the proteins left in the sample were intact DNA binding proteins, and likely contains the DNase that may contributes to the difficulties of obtaining genetic information from *w*Fol and its host.

In order to compare the DNase activities pattern between *F. candida* egg extract and purified *F. candida* DNA, PPAGE was carried out using both samples as described in Materials and Methods. Fig. 6B (lane 1) showed same DNase activity pattern as Fig. 6A (lane 5) in the egg extract. Only two colorless bands (DNase activities) were shown in purified *F. candida* DNA (Fig. 6B; arrows). The two colorless bands (DNase activities)

(Fig. 6B; arrows) correspond to band b and f in the egg extract (lane 1). We noticed that the two DNase activities in lane 2 migrated slightly slower than the corresponding band b and f in lane 1. This may be because more DNA was interacting with the DNases in purified *F. candida* DNA sample than in the egg extract sample.

Localization of the two DNase activities on native polyacrylamide gel electrophoresis (PAGE)

PPAGE reveals two DNase activities in purified *F. candida* DNA (Fig. 6B lane 2), but did not tell the molecular weights (MWs) of the two bands. In order to know the MWs, localization of the two DNase activities on native PAGE was needed.

Native polyacrylamide gel electrophoresis (PAGE) with agarose overlay

Motivated by Hernandez et al. (1994), native PAGE was carried out using purified *F. candida* DNA at a condition under which the DNases were inactive (4 °C, and no $MgCl_2$), and after electrophoresis, the sieving gel was overlaid with a thin (~2 mm) layer of agarose (0.5%) that contained 0.03% high MW DNA (Sigma, Lot No. 49F70551) substrate. The sieving gel, with the agarose overlay attached, was then incubated in the DNase buffer (20 mM $MgCl_2$, 10 mM Tris-HCl pH 5.0) at 45 °C for overnight. During incubation, the DNases diffused from the sieving gel into the overlay, and degraded the DNA substrate in the overlay. After staining the overlay with Pyronin Y for DNA, the positions of the DNase activities were revealed by colorless area on the overlay. The sieving gel was then stained with Pierce™ Color Silver Stain Kit (Thermo Fisher Scientific; Catalog no. 24597). The positions of the DNase bands on the sieving gel were revealed by localizing the colorless areas of the overlay on the sieving gel.

A few colorless areas (Fig, 7B) were shown on the agarose overlay, indicating the DNase activities in corresponding areas on the native PAGE sieving gel (Fig. 7A). We also noticed that the degraded DNA substrate in the overlay diffused into the sieving gel and got stained after silver staining (Fig. 7A; the circled area). Two strongest DNase activities were shown on the overlay (Fig. 7B; arrows), as is also the case in PPAGE (Fig. 6B lane 2). The areas on the native PAGE sieving gel that corresponded to the strongest DNase activities on the overlay were indicated by arrows (Fig. 7A; arrows).

Interestingly, we noticed some slightly under-stained area on the native PAGE sieving gel after silver staining (Fig. 7A; boxes). Two of these unstained areas corresponded to the positions of the strongest DNase activities (Fig. 7A; arrows). Since DNA was stained by silver staining as described by the manufacturer, we suspected that the DNase activities degraded the surrounding *F. candida* DNA that also migrated into the sieving gel, and the unstained area (Fig. 7A; boxes) on the sieving gel directly indicated the absence of DNA and thus were the positions of the DNase activities.

Positions of the DNase activities on native PAGE

In order to understand whether the under-stained areas on native PAGE correspond to the DNase activities, 10% native PAGE were carried out using purified *F. candida* DNA as described in Materials and Methods. After electrophoresis, the sieving gel was incubated in the DNase buffer (20 mM $MgCl_2$, 10 mM Tris-HCl pH 5.0) at 45 °C (DNase active) for overnight, followed by being stained with Pierce™ Color Silver Stain Kit (Thermo Fisher Scientific; Catalog No. 24597).

The 10% native PAGE clearly showed 3 unstained areas (Fig. 8; boxes) that corresponded to the unstained areas in Fig. 7A (boxes), indicating DNase activities. Among the three areas, the bottom two contained the strongest DNase activities, as was the case in Fig. 7A (the bottom two boxes).

Estimation of the molecular weights of the two strongest DNase activities using native PAGE

Based on the fact that the unstained areas in native PAGE indicated the positions of the DNases after silver staining, in order to know the molecular weights (MWs) of the DNases in purified *F. candida* DNA, four different native PAGE (7%, 7.5%, 8%, and 10%) was carried out as described in Materials and Methods. Samples loaded into the native PAGE were purified *F. candida* DNA and protein standards (see Materials and Methods). After electrophoresis, lanes containing protein standards were removed and stained by Coomassie brilliant blue. The lanes containing *F. candida* DNA were incubated in the DNase buffer (20 mM $MgCl_2$, 10 mM Tris-HCl pH 5.0) at 45 °C (DNase

active) for overnight, followed by being stained with Pierce™ Color Silver Stain Kit (Thermo Fisher Scientific; Catalog No. 24597).

After staining, migration rates (Rm), distance of protein migration divided by distance of loading dye migration, of all the protein bands were measured. The data were treated as described in Hedrick and Smith (1968). For all the protein standards and the two DNases, log of Rm was plotted against gel concentrations (Fig. 9). Standard line representing the linear relationship between the log of Rm and gel concentration for each protein was generated from each of the plots (Fig. 9). The slopes of the standard lines (Fig. 9; underlined in the equation in each plot) of the eight protein standards were then plotted against the molecular weights of the protein standards (Fig 10). A standard line representing the linear relationship between slope and molecular weight (Fig. 10) of the eight protein standards was then generated. The slopes of the standard lines of the two DNases in Fig. 9 (underlined in the equation in the bottom two plots) were plotted in the standard lines in Fig. 10 (white triangle markers), and according to the linear relationship between the slopes and molecular weights of the eight protein standards, the molecular weights of the two DNases in purified *F. candida* DNA are 95 kDa and 72 kDa.

Very interestingly, we found that the two unstained areas in 10% gel were merged into one big unstained area in 7.5% gel (Fig. 11; bars). Within the big unstained area (Fig. 11; bars), two protein bands (arrows) each contained two different activities (stars) were shown. The distance between the top of the gel and the center of the two activities within each band was measured as the distance of protein migration. These protein bands were very likely to be the DNases that co-purify with *F. candida* DNA. The bands were cut from the gel, trypsin digested and analyzed by University of Minnesota Center of Mass Spectrometry and Proteomics. No nuclease hit was identified when searching against *Drosophila melanogaster* or *Wolbachia* databases.

Visualization of the two DNases on SDS-PAGE

We estimated the molecular weights (MWs) of the two DNase activities using native PAGE (see above). In order to verify these results, we wanted to carry on SDS-PAGE (Laemmli 1970) using purified *F. candida* DNA hoping to obtain specific bands close to

95 kDa and 72 kDa. Obtaining the DNase bands on SDS-PAGE could aid future characterization of the DNase such as mass spectrometry analysis and sequencing.

In the *F. candida* DNA purification procedures discussed above, 1% sodium dodecyl sulfate (SDS) was added in the 2 x STE buffer (see Materials and Methods). The SDS (0.5% final concentration) in STE buffer functioned in breaking the cell and partially denaturing proteins. Therefore, part of the DNases was denatured and removed from the DNA sample during purification. In order to have as much as the DNases associated with the purified *F. candida* DNA, we removed the SDS from the STE buffer. We electrophoresed the purified DNA sample using SDS-PAGE, and compared with same amount of the sample that purified using STE buffer that contained SDS (Fig. 12).

Treating the eggs in STE buffer without SDS resulted in incomplete breakage of the cells, as indicated by the less total protein amount in lane 1 than in lane 2 (Fig. 12; compare lane 1 and 2). However, two proteins bands (Fig. 12; starts) was more abundant in lane 1 than in lane 2, and the molecular weights of the two bands (Fig. 12; starts) were very close to 95 kDa and 72 kDa, raising the possibility that the two bands were the DNases that co-purify with *F. candida* DNA.

Discussion

In this chapter, I characterized the DNase activity under different conditions using *F. candida* egg extract as resource of the DNases. We found that the DNases had the highest activity at 45 °C (Fig. 2B), and $MgCl_2$ activated (Fig. 4B) while $CaCl_2$ inhibited (Fig. 5B) the DNase activity. The effects of pH on the DNase activity was not as significant as the above conditions (Fig. 3B). Taking advantage of these results, PPAGE revealed 7 DNase activities of different strength in *F. candida* egg extract, but only two DNase activities in purified *F. candida* DNA (Fig. 6). Localization of the two DNase activities that co-purified with *F. candida* DNA on native PAGE was made possible by incubating the sieving gel in 20 mM $MgCl_2$ at 45 °C overnight (DNase active) and looking for unstained area after silver staining (Fig. 8). Molecular weights of the two DNase activities were estimated as 95 kDa and 72 kDa according to Hedrick and Smith (1986) (Fig. 9 and 10). SDS-PAGE of the purified *F. candida* DNA that was treated without SDS in STE buffer

also revealed two protein bands (Fig. 12) corresponded to the estimated MWs of the DNases.

In *Wolbachia*-infected *C. pipiens* mosquitoes, some promising CI effector proteins were identified (Beckmann et al. 2013, Beckmann and Fallon 2013). However, in the parthenogenetic *F. candida*, no effector has been reported because the "cured" population is not available yet. It will be interesting to understand the role of the DNases in *Wolbachia*-induced reproductive alterations in arthropods, particularly in *F. candida* parthenogenesis, and identify its correlation with the possible CI effectors.

In order to understand the role of the DNases in interactions between *w*Fol and its host, one question awaits to be answered: Are the DNases encoded by *w*Fol or the host? We attempted to answer this question via analyzing the unstained bands on the 10% native PAGE (Fig. 8; arrows) and the protein bands (Fig. 11 stars) in the unstained area on the 7.5% native PAGE using mass spectrometry in the University of Minnesota Center for Mass Spectrometry and Proteomics, but no hit related to nuclease was found when searching against *Drosophila melanogaster* or *Wolbachia* databases. Future attempts are needed upon obtaining more abundant and purified DNases.

The inability of culturing *Wolbachia* in cell-free medium makes the host genomic DNA extract the most common resource for amplifying *Wolbachia* genes (O'Neill et al. 1992). However, the presence of the DNases that co-purify with *F. candida* DNA hampers the access of genomic information from *w*Fol and thus obstructs the study on *Wolbachia* supergroup E and the mechanism of the *Wolbachia*-induced parthenogenesis. Therefore, searching for standardized method for obtaining *w*Fol genomic information is needed, which includes a standardized method to remove the DNases from purified *F. candida* DNA. We attempted to purify the *F. candida* DNA using different procedures including guanidine isothiocyanate preparation and Livak (1984), but were unable to completely remove the DNases, which makes the DNases very interesting regarding its interaction mechanism with DNA. Future attempts are needed to understand the interaction mechanism of the DNases with DNA so as to find more targeted methods on removing these DNases from *F. candida* DNA.

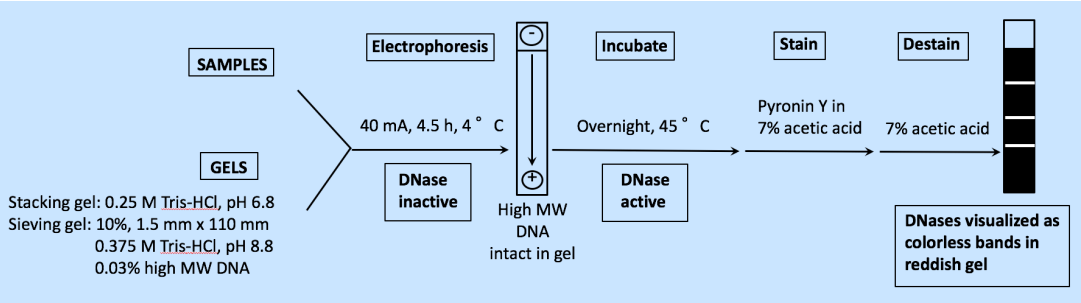

Figure 1. Polynucleotide-polyacrylamide gel electrophoresis (PPAGE) flow chart.

Figure adapted from Brown et al. (1982).

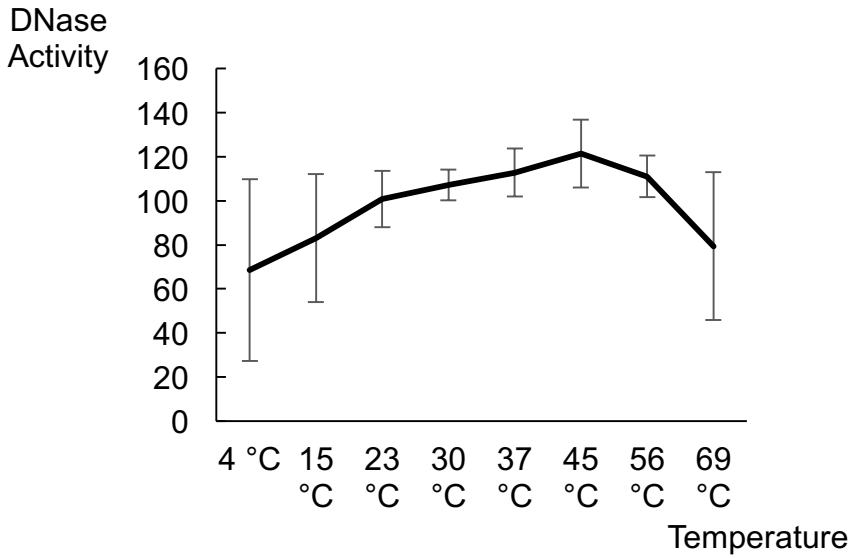

Figure 2. DNase activity at different temperatures. Lambda DNA (0.25 μg) was mixed with 10 μl 800 x diluted egg extract in a total volume of 20 μl that contained 1 mM $MgCl_2$ and 20 mM Tris-HCl pH 7.0, and was incubated at different temperatures (4 °C, 15 °C, 23 °C, 30 °C, 37 °C, 45 °C, 56 °C, 69 °C) for 1h. DNase activity was calculated as subtracting the band density in each treatment from the band density of the new batch of lambda DNA (0.25 μg; no treatment). All the reactions were repeated 3 times with different *F. candida* egg samples.

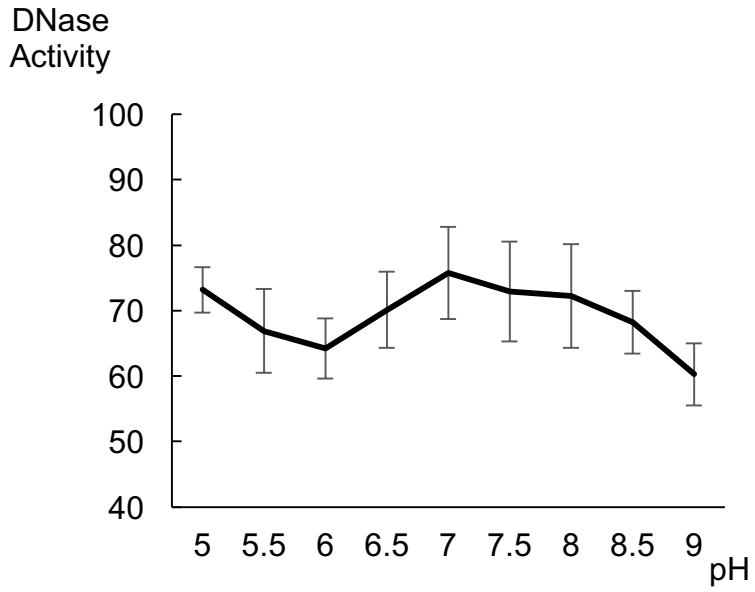

Figure 3. DNase activity at different pHs. Lambda DNA (0.25 μg) was mixed with 10 μl 200 x diluted egg extract in a total volume of 20 μl that contained 1 mM $MgCl_2$ and 20 mM Tris-HCl with different pHs (5.0-9.0 with 0.5 interval) at 45 °C for 30 min. DNase activity was calculated as subtracting the band density in each treatment from the band density of the new batch of lambda DNA (0.25 μg; no treatment). All the reactions were repeated 3 times with different *F. candida* egg samples.

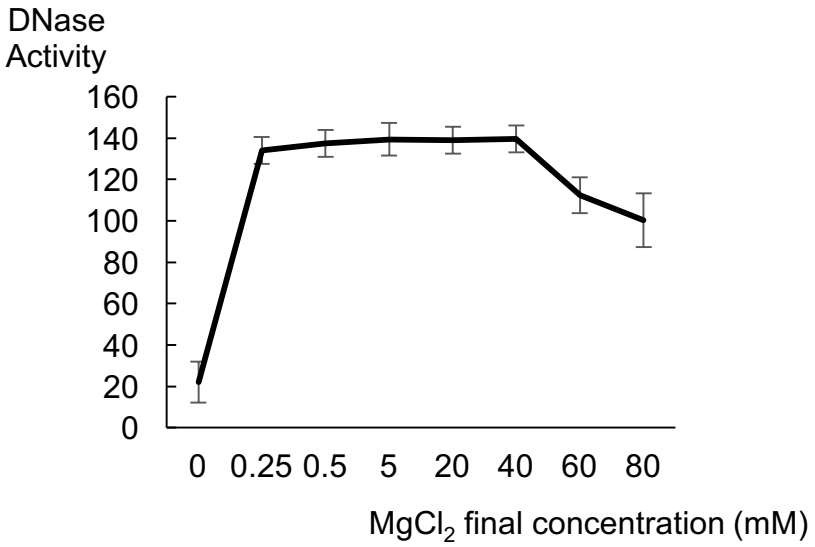

Figure 4. DNase activity at different $MgCl_2$ concentrations. Lambda DNA (0.25 μg) was mixed with 10 μl 200 x diluted egg extract in a total volume of 20 μl that contained 0-80 mM $MgCl_2$ and 20 mM Tris-HCl pH 7.0, and was incubated at 45 °C for 30 min. DNase activity was calculated as subtracting the band density in each treatment from the band density of the new batch of lambda DNA (0.25 μg; no treatment). All the reactions were repeated 3 times with different *F. candida* egg samples.

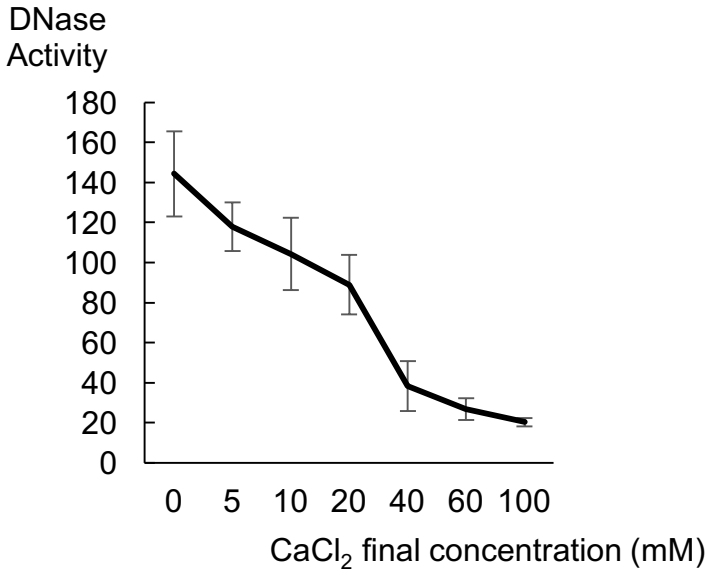

Figure 5. DNase activity at different $CaCl_2$ concentrations. Lambda DNA (0.25 μg) was mixed with 10 μl 50 x diluted egg extract in a total volume of 20 μl that contained 0-100 mM $CaCl_2$ and 20 mM Tris-HCl pH 7.0, and was incubated at 45 °C for 30 min. DNase activity was calculated as subtracting the band density in each treatment from the band density of the new batch of lambda DNA (0.25 μg; no treatment). All the reactions were repeated 3 times with different *F. candida* egg samples.

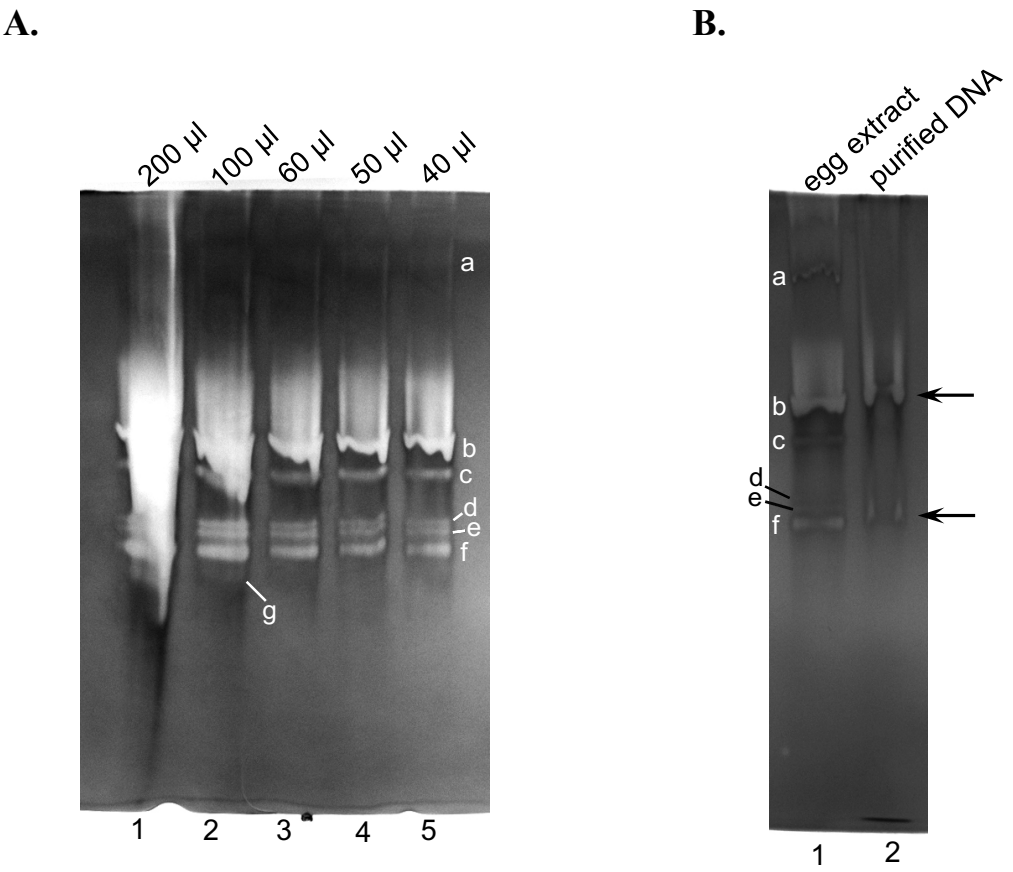

Figure 6. Polynucleotide-polyacrylamide gel electrophoresis (PPAGE; 10%) of *F. candida* egg extract (A, and lane 1 of B) and purified *F. candida* DNA (lane 2 of B). **A,** PPAGE of *F. candida* egg extract. Amounts of the samples (10 x dilution of original preparation mixed with same volume of 2x sample loading buffer) loaded into the gel are indicated above the lanes. Letters (a-g) indicate the colorless bands (DNase activities) detected in the samples; **B,** PPAGE comparing the *F. candida* egg extract sample (lane 1) and the purified DNA sample (lane 2). *F. candida* egg extract sample (30 µl) loaded into the gel was same as in **A**. DNA sample loaded in lane 2 was purified *F. candida* DNA (100 µl) mixed with same volume of 2 x sample loading buffer. Letters (a-f) that indicate colorless bands (DNase activities) in **B** correspond to the letters in **A**. Arrows on the right pointing to the two colorless bands (DNase activities) in purified DNA sample (lane 2) that correspond to band b and f in lane 1.

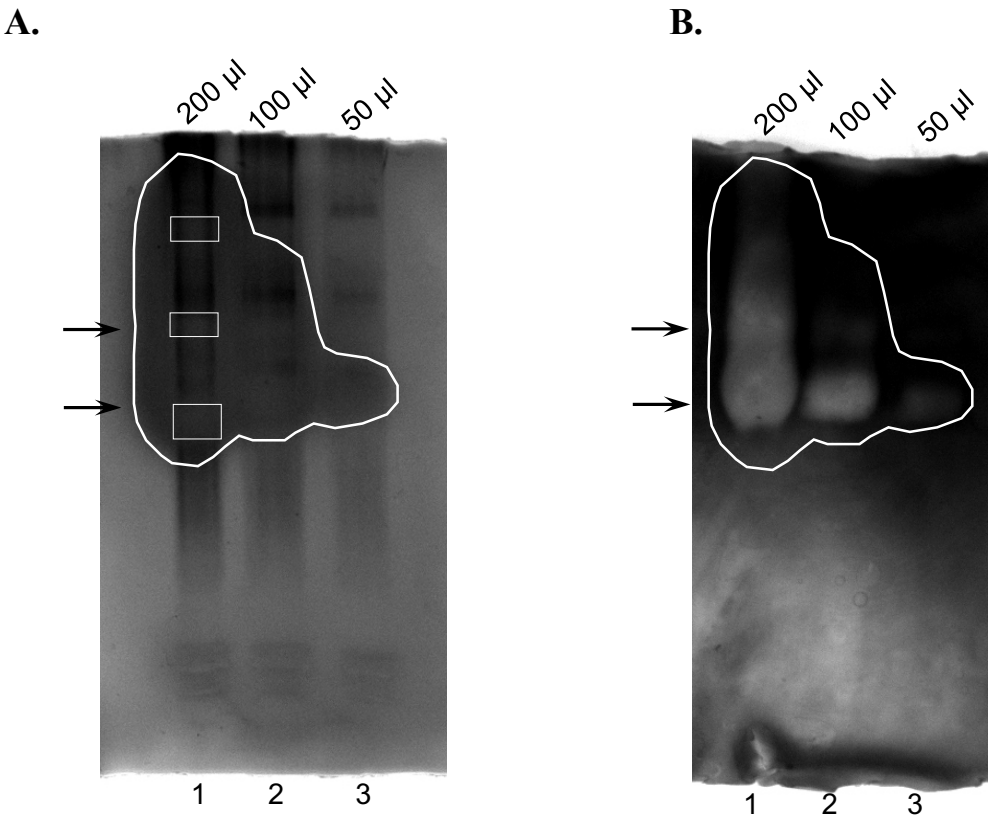

Figure 7. Native PAGE and the corresponding agarose overlay. The purified *F. candida* DNA samples (50 µl, 100 µl, 200 µl as indicated above the lanes) were electrophoresed in 10% native PAGE. After electrophoresis, the stacking gel was removed from the sieving gel. The agarose overlay was made as described in Materials and Methods. After the overlay was solidified, the sieving gel (with the overlay attached) was soaked into the DNase buffer (20 mM $MgCl_2$, 10 mM Tris-HCl pH 5.0) and incubated at 45 °C (DNase active) for overnight. The overlay was then carefully peeled off from the sieving gel and stained with Pyronin Y for intact DNA substrate (**B**). The sieving gel (**A**) was stained with Pierce™ Color Silver Stain Kit (Thermo Fisher Scientific; Catalog No. 24597). **A,** 10% native PAGE sieving gel; **B,** 0.5% agarose overlay with 0.03% DNA substrate. Lanes in **A** and **B** correspond to each other. The DNase activity in the sieving gel diffused into the overlay and degraded the DNA substrate in the overlay. The degraded DNA substrate in the overlay diffused back into

the sieving gel, therefore was silver stained as well (see the dark area as circled in **A**). The circled areas in **A** and **B** correspond to each other. The boxes in **A** indicate unstained area. Arrows indicate highest DNase activities. This assay was repeated 3 times with different *F. candida* DNA samples.

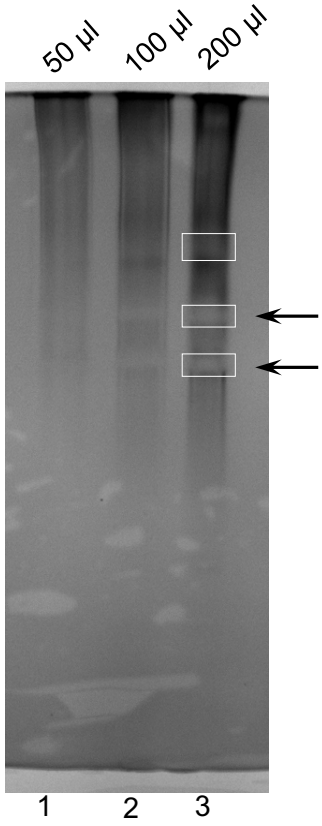

Figure 8. Positions of the DNase activities were revealed by the unstained areas on native PAGE (10%). Boxes indicate unstained areas, and correspond to the boxed area in Fig. 7A. Arrows indicate the strongest DNase activities that also correspond to Fig. 7A (arrows). Amounts of the samples loaded into the gel are indicated above the lanes.

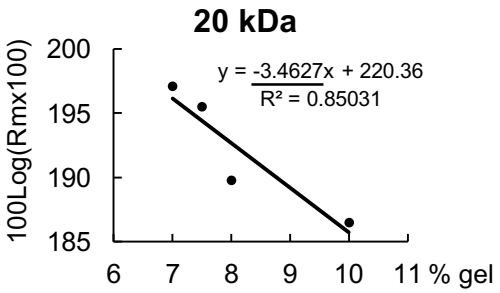
20 kDa
y = -3.4627x + 220.36
R² = 0.85031
100Log(Rmx100)
200
195
190
185
6 7 8 9 10 11 % gel

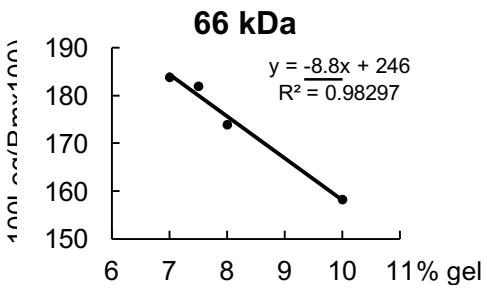
66 kDa
y = -8.8x + 246
R² = 0.98297
190
180
170
160
150
6 7 8 9 10 11% gel

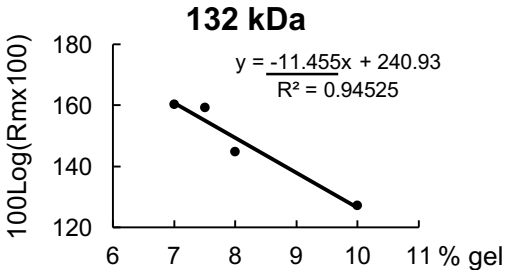
132 kDa
y = -11.455x + 240.93
R² = 0.94525
100Log(Rmx100)
180
160
140
120
6 7 8 9 10 11 % gel

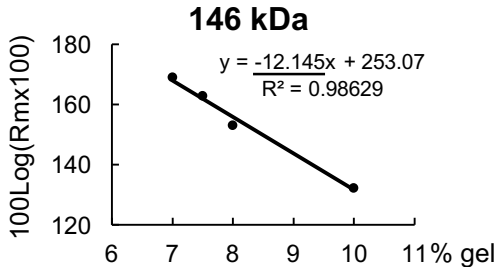
146 kDa
y = -12.145x + 253.07
R² = 0.98629
100Log(Rmx100)
180
160
140
120
6 7 8 9 10 11% gel

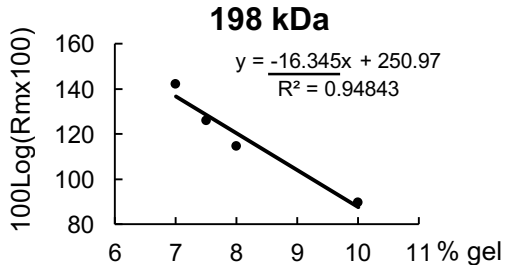
198 kDa
y = -16.345x + 250.97
R² = 0.94843
100Log(Rmx100)
160
140
120
100
80
6 7 8 9 10 11 % gel

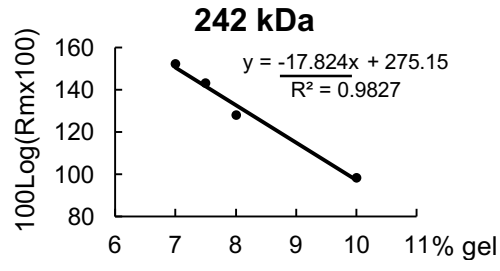
242 kDa
y = -17.824x + 275.15
R² = 0.9827
100Log(Rmx100)
160
140
120
100
80
6 7 8 9 10 11% gel

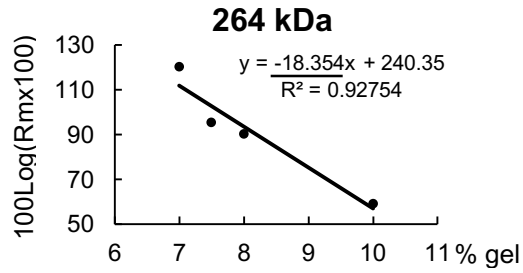
264 kDa
y = -18.354x + 240.35
R² = 0.92754
100Log(Rmx100)
130
110
90
70
50
6 7 8 9 10 11 % gel

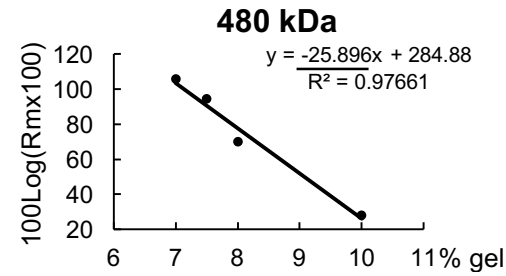
480 kDa
y = -25.896x + 284.88
R² = 0.97661
100Log(Rmx100)
120
100
80
60
40
20
6 7 8 9 10 11% gel

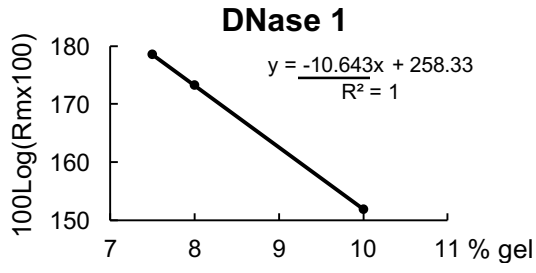
DNase 1
y = -10.643x + 258.33
R² = 1
100Log(Rmx100)
180
170
160
150
7 8 9 10 11 % gel

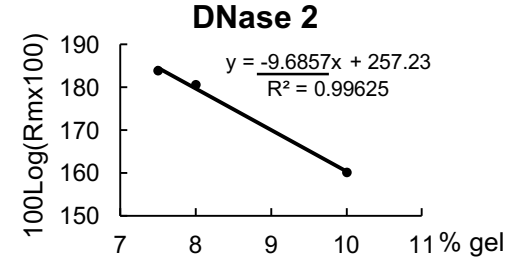
DNase 2
y = -9.6857x + 257.23
R² = 0.99625
100Log(Rmx100)
190
180
170
160
150
7 8 9 10 11 % gel

Figure 9. Linear relationships of the log of protein mobility against gel concentrations. For the eight protein standards and the two DNases in purified *F. candida* DNA, migration rates (Rm), distance of protein migration divided by distance of loading dye migration, were measured. Log of Rm were plotted against gel concentrations. Standard lines were generated from these plots. Absolute value of the slopes (underlined in the equation in each plot) of these standard lines were used in Fig. 10.

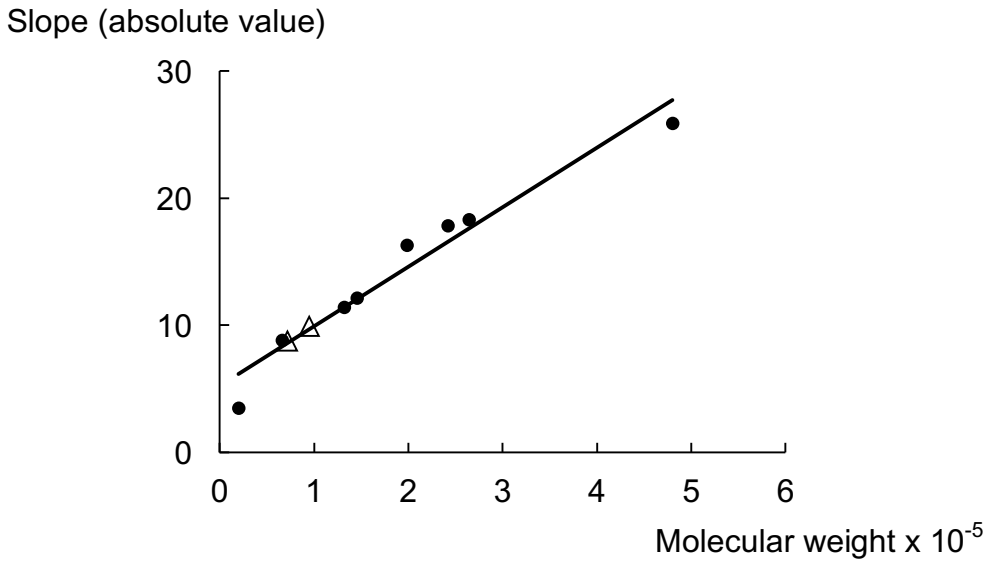

Figure 10. Linear relationship of the slopes and molecular weights of the protein standards and estimation of the molecular weights of the DNases in purified *F. candida DNA*. Slopes of the standard lines of the eight protein standards in Fig. 9 were plotted against the molecular weights of the protein standards. Each black circle data point represents one protein standard. A standard line representing the linear relationship between slope and molecular weight was generated according to these data points. The slopes of the standard lines of the two DNases in Fig. 9 (bottom) were then plot on the standard line, as indicated by the white triangle markers. According to the linear relationship between the slopes and molecular weights of the eight protein standards, the molecular weights of the two DNases in purified *F. candida* DNA are 95 kDa and 72 kDa.

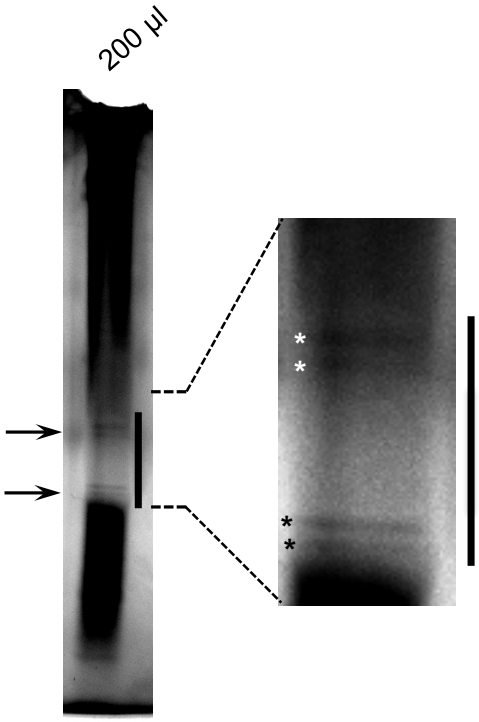

Figure 11. Native PAGE (7.5%) of purified *F. candida* DNA. Amount of the sample loaded into the gel is indicated above the lane on the left. Two close-located activities (indicated by starts in the zoomed in figure on the right) of each of the two protein bands (arrows in figure on the left) were shown within the one big unstained area (indicated by the black bar in both figures). Starts are either black or white to contrast the background.

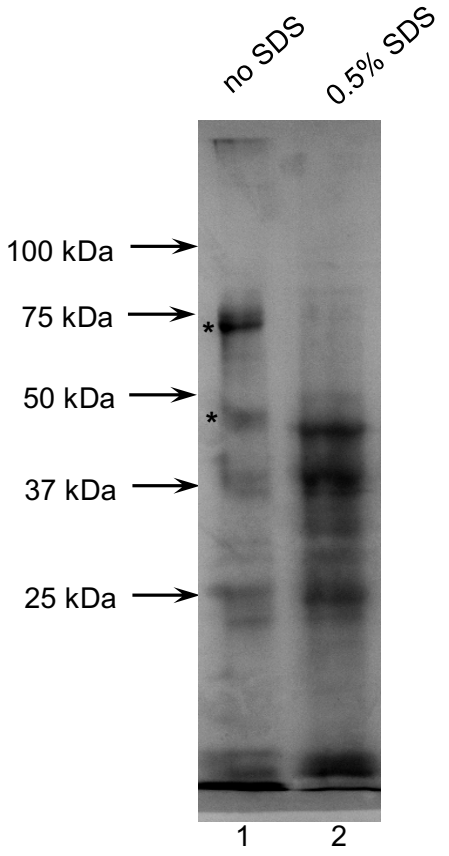

Figure 12. SDS polyacrylamide gel electrophoresis (SDS-PAGE; 10%) of purified *F. candida* DNA. Final percentages of SDS used in the STE buffer were indicated above the lanes. Treating the eggs in STE buffer without SDS resulted in incomplete breakage of the cells, as indicated by the less total protein amount in lane 1 than in lane 2. However, two proteins bands (starts) was more abundant in lane 1 than in lane 2, and the molecular weights of the two bands were very close to 95 kDa and 72 kDa.

Chapter 5

Estimating biomass of *Folsomia candida* by protein staining with Ponceau S

Introduction

Folsomia candida Willem (Collembola: Isotomidae) occurs in soils throughout the world. The species is easy to rear and has been widely used in soil pollution and ecotoxicological studies (Fountain and Hopkin 2005). *F. candida* typically reproduces by parthenogenesis (Fountain and Hopkin 2005, Marshall and Kevan 1962), and the absence of males simplifies mass production and facilitates use of *F. candida* as a model organism. In addition to its longstanding use for testing pesticide effects on non-target species in artificial soils according to established international standards (ISO 1999; OECD 2009), more recent studies have applied physiological and molecular approaches to investigate growth, reproduction and gene expression in *F. candida*. For example, Maria et al. (2014) describe biomarkers associated with toxicant exposure, and Chen et al. (2014) used *F. candida* transcriptomics as an additional measure of soil quality. Finally, several studies describe incorporation of antibiotics into the food source to investigate the possible role of an intracellular bacterium, *Wolbachia pipientis*, in *F. candida* parthenogenesis (Czarnetzki and Tebbe 2004; Giordano et al. 2010; Pike and Kingcombe 2009).

In standard toxicological studies, *F. candida* are introduced into artificial soil containing the test contaminant and allowed to reproduce (Alves et al. 2014; Ardestani and van Gestel 2013; Bur et al. 2012; Idinger 2002). The standard protocol is terminated after several days by flooding the soil samples with water, and counting floating individuals (survivors and progeny) on a photographic image to establish an experimental end point. Improved evaluation methods include automated analysis of Collembola images (Mallard et al. 2013) and biomass estimation using real-time polymerase chain reaction (Hou et al. 2014). As a complementary protocol, we describe a biochemical approach to quantifying *F. candida* biomass, using the reversible protein stain, Ponceau S.

Materials and Methods

F. candida *stock*

A lab culture of *F. candida* was generated from a small population initially reared in potting soil, and maintained on charcoal/agar plates. Charcoal/agar plates were made by boiling 15 g agar and 5 g of charcoal in 1 L of distilled water. When the agar dissolved, the mixture (20 ml/plate) was added to sterile petri plates and allowed to solidify. Plates were sprinkled with 20 mg of powdered yeast, and 25 large springtails were added to the plates. Within three days, communal egg masses were usually present.

Handling F. candida

As noted by others, the small size and high activity of *F. candida* make them difficult to handle. *F. candida* were recovered from stock plates by tapping the plate on the edge of a 250 ml beaker. In a pooled mixture of *F. candida*, larger individuals tend to aggregate at the surface, and for egg production, these can be enriched by gently tapping the larger individuals into a new beaker, with occasional remixing of the population. Likewise, remaining juveniles (which are sensitive to desiccation during handling) can be plated to provide populations of uniformly staged immature individuals of desired size. *F. candida* were added to plates with a simple aspirator made by joining the narrow end of a 1 ml plastic pipet tip (inner diameter 8 mm) to a 12 ml syringe with parafilm. *F. candida* were recovered by positioning the wide end of the pipet tip over the massed *F. candida*, applying gentle suction with the syringe, and releasing the *F. candida* (a pipet-tip equivalent) onto the surface of an agar plate.

Protein staining with Ponceau S

For staining, *F. candida* were collected into a dry 250 ml beaker. Dead individuals adhered to the agar plates, and were not assayed. The pooled *F. candida* were submerged under ~5 ml of hexanes (Thermo Fisher Scientific; Catalog No. H292-1), which was evaporated to dryness under a fume hood. A 0.1 % solution of Ponceau S (Alfa Aesar; Catalog No. J60744) was prepared in 5 % acetic acid, and Triton-X 100 was added to a final concentration of 1 %. Staining solution (15 ml) was added to the hexane-dried *F.*

candida, which were hydrated by gentle agitation while heating to 60 °C on a slide warmer. Beakers were covered, and heating was continued with occasional agitation for 1–2 h. Samples were held at room temperature overnight.

For destaining, the dye in the original beakers was diluted to ~150 ml with distilled water, and the *F. candida* were collected onto filter paper discs by vacuum filtration. The beaker and filtered *F. candida* were rinsed with an additional 150 ml of distilled water. Damp filters (Fig. 1A) were placed in clean petri plates, and 25 ml of 25 mM NaOH was added (Fig. 1B). Plates were gently agitated at 60 °C on a slide warmer until the *F. candida* became pale to ensure uniform distribution of the dye (~1 h), and *F. candida* were removed by filtering 3-4 ml of the solution through a flow cytometry cell strainer tube (35 μm nylon mesh; Falcon, Catalog No. 352235 from Thermo Fisher Scientific). Within a 30 min interval, absorbance of the dissolved dye was read at 570 nm with a spectrophotometer. Because the color of the stain gradually changes from purple to pink with time, it is important to process and read the samples in a single batch.

Results

As an alternative to estimating *F. candida* numbers by photography, we developed a protein-based biochemical method for quantifying biomass. Ponceau S is a reversible stain commonly used for western blots. By trial and error, we determined that pre-extraction of *F. candida* with hexanes, adding 1 % Triton-X 100 to the dye and gentle heating at 60 °C facilitated penetration of dye through the cuticle.

To test linearity of staining, we pooled, stained, and filtered *F. candida* en masse. Dry *F. candida* were weighed in batches and destained in 25 ml of 25 mM NaOH. Absorbance at 570 nm was determined by spectrophotometry, with dilution as necessary. Figure 2 shows data from a typical experiment. In replicate experiments using different batches of stained *F. candida*, staining was linear with biomass up to at least 100 mg (R^2 = 0.9859).

In addition, to evaluate data based on numbers of individuals from a uniform population, *F. candida* at maximum size (3 mm; see Fountain and Hopkin 2001) were counted under a dissection microscope while damp, dried, and destained in 2 ml of 25

mM NaOH (Fig. 3). Again the R^2 value (0.98459) indicated good linearity of the staining reaction.

Discussion

Aside from its responses to pesticides and environmental toxins, *F. candida* is becoming a model organism for investigating basic biology and species diversity, where survival of the *F. candida* is not the key experimental endpoint. Recent studies include efforts to uncover biochemical and molecular mechanisms underlying cold tolerance (Waagner et al. 2013), responses to antioxidants (Maria et al. 2014), developmental processes (Schaeper et al. 2013), evolution (Timmermans et al. 2008; Zhang et al. 2014), and gene-based biomarkers for exposure to toxic substances (Nakamori et al. 2010). In addition, several studies describe incorporation of antibiotics into the food source to investigate the possible role of an intracellular bacterium, *Wolbachia pipientis*, in *F. candida* parthenogenesis (Czarnetzki and Tebbe 2004; Giordano et al. 2010; Pike and Kingcombe 2009). In chapter 3 and 4, we also discovered interesting DNases that co-purify with *F. candida* DNA.

Given the increased interest in aspects of *F. candida* biology other than soil toxicity, we anticipate that the methods describe here will facilitate ongoing efforts to expand the applications of *F. candida* as a model hexapod.

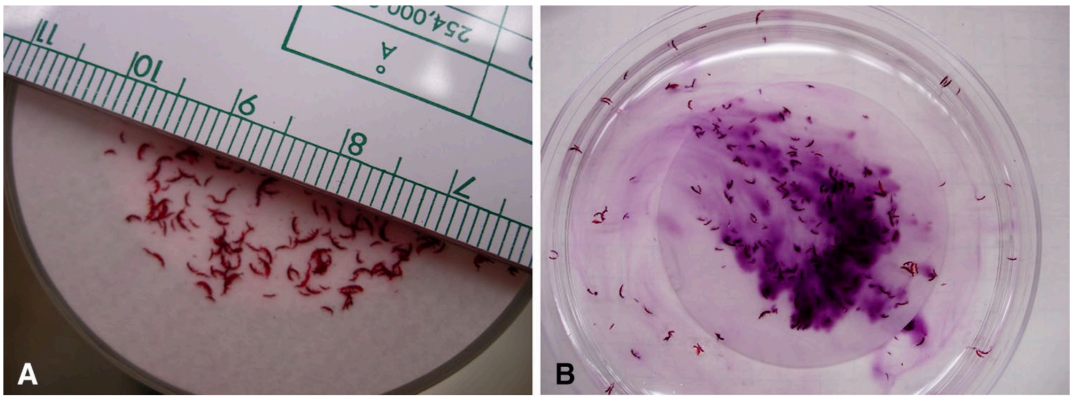

Figure 1. Staining and destaining *F. candia*. A, Ponceau S stained *F. candida* after filtation. Scale shows mm; **B,** Reversibility of the staining reaction after ~5 min in 25 mM NaOH. Figure from Li and Fallon (2016).

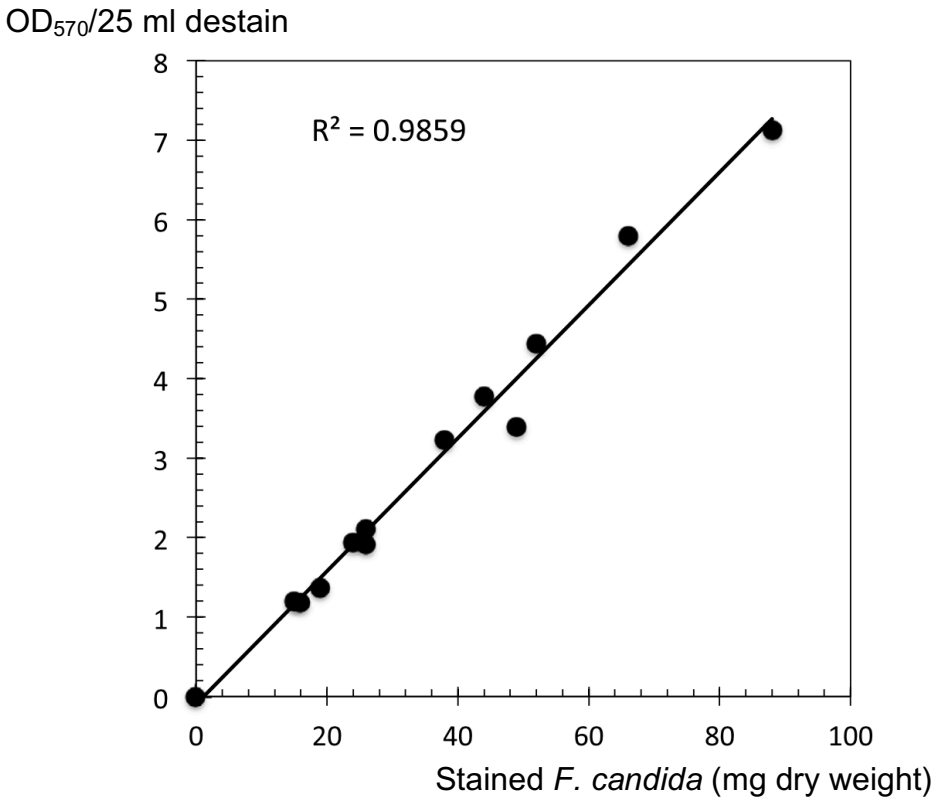

Figure 2. Linearity of the staining reaction. From a total of ~500 mg of stained, dried *F. candida*. Various portions of the sample were weighted and destained in 25 ml of 25 mM NaOH. OD_{570} is plotted against biomass. Individual data points are shown. Figure adapted from Li and Fallon (2016).

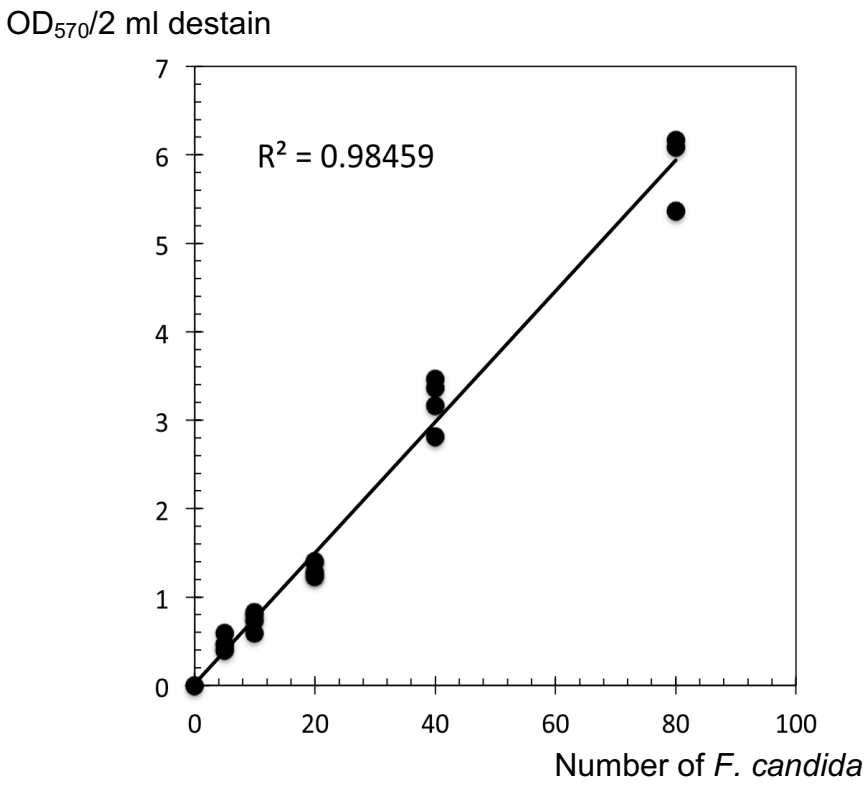

Figure 3. Linearity of the staining reaction as a function of *F. candida* number. Maximum-size (3 mm), stained *F. candida* were counted under a dissection microscope, dried and destained in 2 ml of 25 mM NaOH. OD_{570} is plotted against number of individuals. Individual data points are shown. Figure adapted from Li and Fallon (2016).

Bibliography

Ahmed, M. Z., Li, S. J., Xue, X., Yin, X. J., Ren, S. X., Jiggins, F. M., ... & Qiu, B. L. (2015). The intracellular bacterium *Wolbachia* uses parasitoid wasps as phoretic vectors for efficient horizontal transmission. PLoS Pathog, 11(2), e1004672.

Alvarez-Martinez, C. E., & Christie, P. J. (2009). Biological diversity of prokaryotic type IV secretion systems. Microbiology and Molecular Biology Reviews, 73(4), 775-808.

Alves, P. R. L., Cardoso, E. J., Martines, A. M., Sousa, J. P., & Pasini, A. (2014). Seed dressing pesticides on springtails in two ecotoxicological laboratory tests. Ecotoxicology and environmental safety, 105, 65-71.

Amann, E., Brosius, J., & Ptashne, M. (1983). Vectors bearing a hybrid trp-lac promoter useful for regulated expression of cloned genes in *Escherichia coli*. Gene, 25(2), 167-178.

Arakaki, N., Miyoshi, T., & Noda, H. (2001). Wolbachia-mediated parthenogenesis in the predatory thrips *Franklinothrips vespiformis* (Thysanoptera: Insecta). Proceedings of the Royal Society of London B: Biological Sciences, 268(1471), 1011-1016.

Ardestani, M. M., & van Gestel, C. A. (2013). Toxicodynamics of copper and cadmium in *Folsomia candida* exposed to simulated soil solutions. Environmental Toxicology and Chemistry, 32(12), 2746-2754.

Backert, S., & Meyer, T. F. (2006). Type IV secretion systems and their effectors in bacterial pathogenesis. Current opinion in microbiology, 9(2), 207-217.

Baldo, L., Lo, N., & Werren, J. H. (2005). Mosaic nature of the *Wolbachia* surface protein. Journal of Bacteriology, 187(15), 5406-5418.

Baldridge, G. D., Baldridge, A. S., Witthuhn, B. A., Higgins, L., Markowski, T. W., & Fallon, A. M. (2014). Proteomic profiling of a robust *Wolbachia* infection in an *Aedes albopictus* mosquito cell line. Molecular microbiology, 94(3), 537-556.

Baldridge, G. D., Li, Y. G., Witthuhn, B. A., Higgins, L., Markowski, T. W., Baldridge, A. S., & Fallon, A. M. (2016). Mosaic composition of *ribA* and *wspB* genes flanking the virB8-D4 operon in the *Wolbachia* supergroup B-strain, *w*Str. Archives of Microbiology, 198(1), 53-69.

Baldridge, G. D., Markowski, T. W., Witthuhn, B. A., Higgins, L., Baldridge, A. S., & Fallon, A. M. (2016). The *Wolbachia* WO bacteriophage proteome in the *Aedes albopictus* C/wStr1 cell line: evidence for lytic activity?. In Vitro Cellular & Developmental Biology-Animal, 52(1), 77-88.

Baron, C., Llosa, M., Zhou, S., & Zambryski, P. C. (1997). VirB1, a component of the T-complex transfer machinery of Agrobacterium tumefaciens, is processed to a C-terminal secreted product, VirB1. Journal of bacteriology, 179(4), 1203-1210.

Bazzocchi, C., Comazzi, S., Santoni, R., Bandi, C., Genchi, C., & Mortarino, M. (2007). *Wolbachia* surface protein (WSP) inhibits apoptosis in human neutrophils. Parasite immunology, 29(2), 73-79.

Beare, P. A., Broschat, S. L., Brown, W. C., Voth, D. E., Brayton, K. A., Lockwood, S., & Heinzen, R. A. (2011). Identification of *Anaplasma marginale* type IV secretion system effector proteins.

Beckmann, J. F., & Fallon, A. M. (2012). Decapitation improves detection of *Wolbachia pipientis* (Rickettsiales: Anaplasmataceae) in *Culex pipiens* (Diptera: Culicidae) mosquitoes by the polymerase chain reaction. Journal of medical entomology, 49(5), 1103-1108.

Beckmann, J. F., & Fallon, A. M. (2013). Detection of the *Wolbachia* protein WPIP0282 in mosquito spermathecae: implications for cytoplasmic incompatibility. Insect biochemistry and molecular biology, 43(9), 867-878.

Beckmann, J. F., Markowski, T. W., Witthuhn, B. A., & Fallon, A. M. (2013). Detection of the *Wolbachia*-encoded DNA binding protein, HU beta, in mosquito gonads. Insect biochemistry and molecular biology, 43(3), 272-279.

Bennuru, S., Semnani, R., Meng, Z., Ribeiro, J. M., Veenstra, T. D., & Nutman, T. B. (2009). *Brugia malayi* excreted/secreted proteins at the host/parasite interface: stage- and gender-specific proteomic profiling. PLoS Negl Trop Dis, 3(4), e410.

Bhatty, M., Gomez, J. A. L., & Christie, P. J. (2013). The expanding bacterial type IV secretion lexicon. Research in microbiology, 164(6), 620-639.

Bian, G., Xu, Y., Lu, P., Xie, Y., & Xi, Z. (2010). The endosymbiotic bacterium *Wolbachia* induces resistance to dengue virus in *Aedes aegypti*. PLoS pathog, 6(4), e1000833.

Bordenstein, S., & Rosengaus, R. B. (2005). Discovery of a novel *Wolbachia* supergroup in Isoptera. Current microbiology, 51(6), 393-398.

Bork, P. (1993). Hundreds of ankyrin-like repeats in functionally diverse proteins: Mobile modules that cross phyla horizontally?. Proteins: Structure, Function, and Bioinformatics, 17(4), 363-374.

Bossan, B., Koehncke, A., & Hammerstein, P. (2011). A new model and method for understanding *Wolbachia*-induced cytoplasmic incompatibility. PLoS One, 6(5), e19757.

Bourtzis, K. (2008). *Wolbachia*-based technologies for insect pest population control. In Transgenesis and the management of vector-borne disease (pp. 104-113). Springer New York.

Bourtzis, K., Lees, R. S., Hendrichs, J., & Vreysen, M. J. (2016). More than one rabbit out of the hat: Radiation, transgenic and symbiont-based approaches for sustainable management of mosquito and tsetse fly populations. Acta tropica.

Breeuwer, J. A. J., Stouthamer, R., Barns, S. M., Pelletier, D. A., Weisburg, W. G., & Werren, J. H. (1992). Phylogeny of cytoplasmic incompatibility microorganisms in the parasitoid wasp genus *Nasonia* (Hymenoptera: Pteromalidae) based on 16S ribosomal DNA sequences. Insect molecular biology, 1(1), 25-36.

Bressac, C., & Rousset, F. (1993). The reproductive incompatibility system in *Drosophila simulans*: DAPI-staining analysis of the *Wolbachia* symbionts in sperm cysts. Journal of invertebrate pathology, 61(3), 226-230.

Brower, J. H. (1976). Cytoplasmic Incompatibility: Occurrence in a Stored-product Pest *Ephestia cautella*. Annals of the Entomological Society of America, 69(6), 1011-1015.

Brown, A. N., & Lloyd, V. K. (2015). Evidence for horizontal transfer of *Wolbachia* by a *Drosophila* mite. Experimental and Applied Acarology, 66(3), 301-311.

Brown, G. E., Karpetsky, T. P., Rahman, A., McFarland, E., & Haroth, M. B. (1982). Characterization of intracellular deoxyribonucleases using polynucleotide-polyacrylamide gel electrophoresis. Electrophoresis, 3(3), 151-157.

Bur, T., Crouau, Y., Bianco, A., Gandois, L., & Probst, A. (2012). Toxicity of Pb and of Pb/Cd combination on the springtail *Folsomia candida* in natural soils:

Reproduction, growth and bioaccumulation as indicators. Science of the Total Environment, 414, 187-197.

Carey, K. L., Newton, H. J., Lührmann, A., & Roy, C. R. (2011). The *Coxiella burnetii* Dot/Icm system delivers a unique repertoire of type IV effectors into host cells and is required for intracellular replication. PLoS Pathog, 7(5), e1002056.

Cascales, E., & Christie, P. J. (2003). The versatile bacterial type IV secretion systems. Nature Reviews Microbiology, 1(2), 137-149.

Casiraghi, M., Werren, J. H., Bazzocchi, C., Biserni, A., & Bandi, C. (2003). dnaA gene sequences from *Wolbachia pipientis* support subdivision into supergroups and provide no evidence for recombination in the lineages infecting nematodes. Parassitologia, 45(1), 13-18.

Chandran, V., Fronzes, R., Duquerroy, S., Cronin, N., Navaza, J., & Waksman, G. (2009). Structure of the outer membrane complex of a type IV secretion system. Nature, 462(7276), 1011-1015.

Chen, C., Banga, S., Mertens, K., Weber, M. M., Gorbaslieva, I., Tan, Y., ... & Samuel, J. E. (2010). Large-scale identification and translocation of type IV secretion substrates by *Coxiella burnetii*. Proceedings of the National Academy of Sciences, 107(50), 21755-21760.

Chen, G., de Boer, T. E., Wagelmans, M., van Gestel, C. A., van Straalen, N. M., & Roelofs, D. (2014). Integrating transcriptomics into triad-based soil-quality assessment. Environmental toxicology and chemistry, 33(4), 900-909.

Christie, P. J. (2004). Type IV secretion: the *Agrobacterium* VirB/D4 and related conjugation systems. Biochimica et Biophysica Acta (BBA)-Molecular Cell Research, 1694(1), 219-234.

Christie, P. J., & Vogel, J. P. (2000). Bacterial type IV secretion: conjugation systems adapted to deliver effector molecules to host cells. Trends in microbiology, 8(8), 354-360.

Clancy, D. J., & Hoffmann, A. A. (1996). Cytoplasmic incompatibility in *Drosophila simulans*: evolving complexity. Trends in Ecology & Evolution, 11(4), 145-146.

Czarnetzki, A. B., & Tebbe, C. C. (2004). Detection and phylogenetic analysis of *Wolbachia* in Collembola. Environmental microbiology, 6(1), 35-44.

Darby, A. C., Armstrong, S. D., Bah, G. S., Kaur, G., Hughes, M. A., Kay, S. M., ... & Tanya, V. N. (2012). Analysis of gene expression from the *Wolbachia* genome of a filarial nematode supports both metabolic and defensive roles within the symbiosis. Genome research, 22(12), 2467-2477.

De La Cruz, F., Frost, L. S., Meyer, R. J., & Zechner, E. L. (2010). Conjugative DNA metabolism in Gram-negative bacteria. FEMS microbiology reviews, 34(1), 18-40.

de Paz, H. D., Larrea, D., Zunzunegui, S., Dehio, C., de la Cruz, F., & Llosa, M. (2010). Functional dissection of the conjugative coupling protein TrwB. Journal of bacteriology, 192(11), 2655-2669.

Eisenbeis, G. (1982). Physiological absorption of liquid water by Collembola: absorption by the ventral tube at different salinities. Journal of Insect Physiology, 28(1), 11-20.

Eisenbrandt, R., Kalkum, M., Lai, E. M., Lurz, R., Kado, C. I., & Lanka, E. (1999). Conjugative pili of IncP plasmids, and the Ti plasmid T pilus are composed of cyclic subunits. Journal of Biological Chemistry, 274(32), 22548-22555.

Elfring, L. K., Axton, J. M., Fenger, D. D., Page, A. W., Carminati, J. L., & Orr-Weaver, T. L. (1997). *Drosophila* PLUTONIUM protein is a specialized cell cycle regulator required at the onset of embryogenesis. Molecular biology of the cell, 8(4), 583-593.

Fallon, A. M. (2008). Cytological properties of an *Aedes albopictus* mosquito cell line infected with *Wolbachia* strain *w*AlbB. In Vitro Cellular & Developmental Biology-Animal, 44(5-6), 154-161.

Fallon, A. M., Baldridge, G. D., Higgins, L. A., & Witthuhn, B. A. (2013). *Wolbachia* from the planthopper *Laodelphax striatellus* establishes a robust, persistent, streptomycin-resistant infection in clonal mosquito cells. In Vitro Cellular & Developmental Biology-Animal, 49(1), 66-73.

Fallon, A. M., & Kurtti, T. J. (2005). Cultured cells as a tool for analysis of gene expression. Biology of disease vectors. 2nd ed. Elsevier, New York, 539-549.

FALLON, U. I. (1998). Culture of mosquito cells in Eagle's medium. In Vitro Cell. Dev. Biol.-Animal, 34, 629-630.

Félix, C., Pichon, S., Braquart-Varnier, C., Braig, H., Chen, L., Garrett, R. A., ... & Grève, P. (2008). Characterization and transcriptional analysis of two gene clusters for type IV secretion machinery in *Wolbachia* of *Armadillidium vulgare*. Research

in microbiology, 159(6), 481-485.

Fenn, K., & Blaxter, M. (2006). *Wolbachia* genomes: revealing the biology of parasitism and mutualism. Trends in parasitology, 22(2), 60-65.

Fialho, R. F., & Stevens, L. (2000). Male-killing *Wolbachia* in a flour beetle. Proceedings of the Royal Society of London B: Biological Sciences, 267(1451), 1469-1473.

Fountain, M. T., & Hopkin, S. P. (2001). Continuous monitoring of *Folsomia candida* (Insecta: Collembola) in a metal exposure test. Ecotoxicology and environmental safety, 48(3), 275-286.

Fountain, M. T., & Hopkin, S. P. (2005). *Folsomia candida* (Collembola): A "Standard" soil arthropod. Annu. Rev. Entomol., 50, 201-222.

Foster, J., Ganatra, M., Kamal, I., Ware, J., Makarova, K., Ivanova, N., ... & Vincze, T. (2005). The *Wolbachia* genome of *Brugia malayi*: endosymbiont evolution within a human pathogenic nematode. PLos biol, 3(4), e121.

Fronzes, R., Christie, P. J., & Waksman, G. (2009). The structural biology of type IV secretion systems. Nature Reviews Microbiology, 7(10), 703-714.

Ge, J., & Shao, F. (2011). Manipulation of host vesicular trafficking and innate immune defence by *Legionella* Dot/Icm effectors. Cellular microbiology, 13(12), 1870-1880.

Gerth, M., Gansauge, M. T., Weigert, A., & Bleidorn, C. (2014). Phylogenomic analyses uncover origin and spread of the *Wolbachia* pandemic. Nature communications, 5.

Ghedin, E., Wang, S., Spiro, D., Caler, E., Zhao, Q., Crabtree, J., ... & Angiuoli, S. V. (2007). Draft genome of the filarial nematode parasite *Brugia malayi*. Science, 317(5845), 1756-1760.

Giordano, R., Weber, E., Waite, J., Bencivenga, N., Krogh, P. H., & Soto-Adames, F. (2010). Effect of a high dose of three antibiotics on the reproduction of a parthenogenetic strain of *Folsomia candida* (Isotomidae: Collembola). Environmental entomology, 39(4), 1170-1177.

Gomis-Rüth, F. X., Moncalián, G., Pérez-Luque, R., González, A., Cabezón, E., de la Cruz, F., & Coll, M. (2001). The bacterial conjugation protein TrwB resembles ring helicases and F_1-ATPase. Nature, 409(6820), 637-641.

Guglielmini, J., de la Cruz, F., & Rocha, E. P. (2012). Evolution of conjugation and type IV secretion systems. Molecular biology and evolution, mss221.

Guzman, L. M., Belin, D., Carson, M. J., & Beckwith, J. O. N. (1995). Tight regulation, modulation, and high-level expression by vectors containing the arabinose P_{BAD} promoter. Journal of bacteriology, 177(14), 4121-4130.

Hedrick, J. L., & Smith, A. J. (1968). Size and charge isomer separation and estimation of molecular weights of proteins by disc gel electrophoresis. Archives of Biochemistry and Biophysics, 126(1), 155-164.

Hernandez, V. P., Gerenday, A., & Fallon, A. M. (1994). Secretion of an inducible cecropin-like activity by cultured mosquito cells. The American journal of tropical medicine and hygiene, 50(4), 440-447.

Hertig, M. (1936). The rickettsia, *Wolbachia pipientis* (gen. et sp. n.) and associated inclusions of the mosquito, *Culex pipiens*. Parasitology, 28(04), 453-486.

Hertig, M., & Wolbach, S. B. (1924). Studies on rickettsia-like micro-organisms in insects. The Journal of medical research, 44(3), 329.

Hilgenboecker, K., Hammerstein, P., Schlattmann, P., Telschow, A., & Werren, J. H. (2008). How many species are infected with *Wolbachia*?-a statistical analysis of current data. FEMS microbiology letters, 281(2), 215-220.

Hopkin, S. P. (1997). Biology of the Springtails:(Insecta: Collembola). OUP Oxford.

Hou, L. B., Yanagisawa, Y., Yachi, S., Kaneko, N., & Nakamori, T. (2014). Biomass estimation of the terrestrial ecotoxicological species *Folsomia candida* (Collembola) using a real-time polymerase chain reaction. Ecotoxicology and environmental safety, 101, 59-63.

Hsiao, C., & Hsiao, T. H. (1985). Rickettsia as the cause of cytoplasmic incompatibility in the alfalfa weevil, *Hypera postica*. Journal of invertebrate pathology, 45(2), 244-246.

Huang, L., Boyd, D., Amyot, W. M., Hempstead, A. D., Luo, Z. Q., O'Connor, T. J., ... & Isberg, R. R. (2011). The E Block motif is associated with *Legionella pneumophila* translocated substrates. Cellular microbiology, 13(2), 227-245.

Idinger, J. (2002). Laboratory studies to detect effects of selected plant protection products on *Folsomia candida* (Collembola: Isotomidae)/Laborstudien zur Auswirkung von ausgewählten Pflanzenschutzmitteln auf *Folsomia candida* (Collembola: Isotomidae). Zeitschrift für Pflanzenkrankheiten und

Pflanzenschutz/Journal of Plant Diseases and Protection, 512-529.

ISO, I. (1999). 11267: Soil Quality. Inhibition of Reproduction of Collembola (*Folsomia candida*) by Soil Pollutants. International Organization for Standardization, Geneve, Switzerland.

Iturbe-Ormaetxe, I., Walker, T., & LO'Neill, S. (2011). *Wolbachia* and the biological control of mosquito-borne disease. EMBO reports, 12(6), 508-518.

Jiggins, F. M., Hurst, G. D., Schulenburg, J. H. G., & Majerus, M. E. (2001). Two male-killing *Wolbachia* strains coexist within a population of the butterfly *Acraea encedon*. Heredity, 86(2), 161-166.

Kageyama, D., Nishimura, G., Hoshizaki, S., & Ishikawa, Y. (2002). Feminizing *Wolbachia* in an insect, *Ostrinia furnacalis* (Lepidoptera: Crambidae). Heredity, 88(6), 444-449.

Kambris, Z., Blagborough, A. M., Pinto, S. B., Blagrove, M. S., Godfray, H. C. J., Sinden, R. E., & Sinkins, S. P. (2010). *Wolbachia* stimulates immune gene expression and inhibits *Plasmodium* development in *Anopheles gambiae*. PLoS pathog, 6(10), e1001143.

Kambris, Z., Cook, P. E., Phuc, H. K., & Sinkins, S. P. (2009). Immune activation by life-shortening *Wolbachia* and reduced filarial competence in mosquitoes. Science, 326(5949), 134-136.

Klasson, L., Westberg, J., Sapountzis, P., Näslund, K., Lutnaes, Y., Darby, A. C., ... & Bourtzis, K. (2009). The mosaic genome structure of the *Wolbachia w*Ri strain infecting *Drosophila simulans*. Proceedings of the National Academy of Sciences, 106(14), 5725-5730.

Krivtsov, V., Illian, J. B., Liddell, K., Garside, A., Bezginova, T., Salmond, R., ... & Brendler, A. (2003). Some aspects of complex interactions involving soil mesofauna: analysis of the results from a Scottish woodland. Ecological Modelling, 170(2), 441-452.

Laemmli, U. K. (1970). Cleavage of structural proteins during the assembly of the head of bacteriophage T4. nature, 227, 680-685.

Laven, H. (1951). Crossing experiments with *Culex* strains. Evolution, 5(4), 370-375.

Laven, H. (1959, January). SPECIATION IN MOSQUITOES Speciation by Cytoplasmic

Isolation in the *Culex Pipiens*-Complex. In Cold Spring Harbor Symposia on Quantitative Biology (Vol. 24, pp. 166-173). Cold Spring Harbor Laboratory Press.

Laven, H. A. N. N. E. S. (1967). Speciation and evolution in *Culex pipiens*. Genetics of insect vectors of disease, 251-275.

Li, S. C., Squires, C. L., & Squires, C. (1984). Antitermination of *E. coli* rRNA transcription is caused by a control region segment containing lambda nut-like sequences. Cell, 38(3), 851-860.

Li, Y. G., & Fallon, A. M. (2016). Rearing the soil arthropod *Folsomia candida* (Collembola: Isotomidae) on agar plates and estimating biomass by protein staining with Ponceau S. Applied Entomology and Zoology, 1-6. DOI: 10.1007/s13355-016-0405-8.

Li, Z., & Carlow, C. K. (2012). Characterization of transcription factors that regulate the type IV secretion system and riboflavin biosynthesis in *Wolbachia* of *Brugia malayi*. PLoS One, 7(12), e51597.

Livak, K. J. (1984). Organization and mapping of a sequence on the *Drosophila melanogaster* X and Y chromosomes that is transcribed during spermatogenesis. Genetics, 107(4), 611-634.

Llosa, M., Roy, C., & Dehio, C. (2009). Bacterial type IV secretion systems in human disease. Molecular microbiology, 73(2), 141-151.

Lo, N., Casiraghi, M., Salati, E., Bazzocchi, C., & Bandi, C. (2002). How many *Wolbachia* supergroups exist?. Molecular biology and evolution, 19(3), 341-346.

Lo, N., Paraskevopoulos, C., Bourtzis, K., O'Neill, S. L., Werren, J. H., Bordenstein, S. R., & Bandi, C. (2007). Taxonomic status of the intracellular bacterium *Wolbachia pipientis*. International journal of systematic and evolutionary microbiology, 57(3), 654-657.

Lock, K., & Janssen, C. R. (2003). Effect of new soil metal immobilizing agents on metal toxicity to terrestrial invertebrates. Environmental Pollution, 121(1), 123-127.

Lockwood, S., Voth, D. E., Brayton, K. A., Beare, P. A., Brown, W. C., Heinzen, R. A., & Broschat, S. L. (2011). Identification of *Anaplasma marginale* type IV secretion system effector proteins. PLoS One, 6(11), e27724.

Locht, C., Coutte, L., & Mielcarek, N. (2011). The ins and outs of pertussis toxin. FEBS

Journal, 278(23), 4668-4682.

Lührmann, A., Nogueira, C. V., Carey, K. L., & Roy, C. R. (2010). Inhibition of pathogen-induced apoptosis by a *Coxiella burnetii* type IV effector protein. Proceedings of the National Academy of Sciences, 107(44), 18997-19001.

Mallard, F., Le Bourlot, V., & Tully, T. (2013). An automated image analysis system to measure and count organisms in laboratory microcosms. PloS one, 8(5), e64387.

Maria, V. L., Ribeiro, M. J., & Amorim, M. J. (2014). Oxidative stress biomarkers and metallothionein in *Folsomia candida*-responses to Cu and Cd. Environmental research, 133, 164-169.

Marshall, V. G., & Kevan, D. K. M. (1962). Preliminary observations on the biology of *Folsomia candida* Willem, 1902 (Collembola: Isotomidae). The Canadian Entomologist, 94(06), 575-586.

Masui, S., Kamoda, S., Sasaki, T., & Ishikawa, H. (2000). Distribution and evolution of bacteriophage WO in *Wolbachia*, the endosymbiont causing sexual alterations in arthropods. Journal of molecular evolution, 51(5), 491-497.

Masui, S., Kuroiwa, H., Sasaki, T., Inui, M., Kuroiwa, T., & Ishikawa, H. (2001). Bacteriophage WO and virus-like particles in *Wolbachia*, an endosymbiont of arthropods. Biochemical and biophysical research communications, 283(5), 1099-1104.

Masui, S., Sasaki, T., & Ishikawa, H. (2000). Genes for the type IV secretion system in an intracellular symbiont, *Wolbachia*, a causative agent of various sexual alterations in arthropods. Journal of bacteriology, 182(22), 6529-6531.

Maturana, P., Graham, J. G., Sharma, U. M., & Voth, D. E. (2013). Refining the plasmid-encoded type IV secretion system substrate repertoire of *Coxiella burnetii*. Journal of bacteriology, 195(14), 3269-3276.

Melnikow, E., Xu, S., Liu, J., Li, L., Oksov, Y., Ghedin, E., ... & Lustigman, S. (2011). Interaction of a *Wolbachia* WSP-like protein with a nuclear-encoded protein of *Brugia malayi*. International journal for parasitology, 41(10), 1053-1061.

Moreira, L. A., Iturbe-Ormaetxe, I., Jeffery, J. A., Lu, G., Pyke, A. T., Hedges, L. M., ... & Hugo, L. E. (2009). A *Wolbachia* symbiont in *Aedes aegypti* limits infection with dengue, Chikungunya, and *Plasmodium*. Cell, 139(7), 1268-1278.

Nagai, H., & Kubori, T. (2011). Type IVB secretion systems of *Legionella* and other Gram-negative bacteria. *Legionella*: from protozoa to humans, 52.

Nakamori, T., Fujimori, A., Kinoshita, K., Ban-nai, T., Kubota, Y., & Yoshida, S. (2010). mRNA expression of a cadmium-responsive gene is a sensitive biomarker of cadmium exposure in the soil collembolan *Folsomia candida*. Environmental pollution, 158(5), 1689-1695.

Negri, I., Pellecchia, M., Mazzoglio, P. J., Patetta, A., & Alma, A. (2006). Feminizing *Wolbachia* in *Zyginidia pullula* (Insecta, Hemiptera), a leafhopper with an XX/X0 sex-determination system. Proceedings of the Royal Society of London B: Biological Sciences, 273(1599), 2409-2416.

Noda, H. (1984). Cytoplasmic incompatibility in allopatric field populations of the small brown planthopper, *Laodelphax striatellus*, in Japan. Entomologia experimentalis et applicata, 35(3), 263-267.

Noda, H., Koizumi, Y., Zhang, Q., & Deng, K. (2001). Infection density of *Wolbachia* and incompatibility level in two planthopper species, *Laodelphax striatellus* and *Sogatella furcifera*. Insect biochemistry and molecular biology, 31(6), 727-737.

Nutman, S. R. (1941). Function of the ventral tube in *Onychiurus armatus* (Collembola). Nature, 148, 168-169.

Okamoto, S., Toyoda-Yamamoto, A., Ito, K., Takebe, I., & Machida, Y. (1991). Localization and orientation of the VirD4 protein of *Agrobacterium tumefaciens* in the cell membrane. Molecular and General Genetics MGG, 228(1-2), 24-32.

O'Neill, S. L. (1989). Cytoplasmic symbionts in *Tribolium confusum*. Journal of Invertebrate Pathology, 53(1), 132-134.

O'Neill, S. L., Giordano, R., Colbert, A. M., Karr, T. L., & Robertson, H. M. (1992). *16S rRNA* phylogenetic analysis of the bacterial endosymbionts associated with cytoplasmic incompatibility in insects. Proceedings of the National Academy of Sciences, 89(7), 2699-2702.

O'Neill, S. L., & Karr, T. L. (1990). Bidirectional incompatibility between conspecific populations of *Drosophila* simulans.

OECD (2009) Test no. 232: collembolan reproduction test in soil. OECD Publishing, Paris

Pfarr, K. M., & Hoerauf, A. M. (2006). Antibiotics which target the *Wolbachia* endosymbionts of filarial parasites: a new strategy for control of filariasis and amelioration of pathology. Mini reviews in medicinal chemistry, 6(2), 203-210.

Pichon, S., Bouchon, D., Cordaux, R., Chen, L., Garrett, R. A., & Grève, P. (2009). Conservation of the Type IV secretion system throughout *Wolbachia* evolution. Biochemical and biophysical research communications, 385(4), 557-562.

Pike, N., & Kingcombe, R. (2009). Antibiotic treatment leads to the elimination of *Wolbachia* endosymbionts and sterility in the diplodiploid collembolan *Folsomia candida*. BMC biology, 7(1), 54.

Pinto, S. B., Mariconti, M., Bazzocchi, C., Bandi, C., & Sinkins, S. P. (2012). *Wolbachia* surface protein induces innate immune responses in mosquito cells. BMC microbiology, 12(1), 1.

Plantard, O., Rasplus, J. Y., Mondor, G., Le Clainche, I., & Solignac, M. (1998). *Wolbachia*-induced thelytoky in the rose gallwasp *Diplolepis spinosissimae* (Giraud) (Hymenoptera: Cynipidae), and its consequences on the genetic structure of its host. Proceedings of the Royal Society of London B: Biological Sciences, 265(1401), 1075-1080.

Poinsot, D., Charlat, S., & Mercot, H. (2003). On the mechanism of *Wolbachia*-induced cytoplasmic incompatibility: Confronting the models with the facts. Bioessays, 25(3), 259-265.

Price, C. T., & Kwaik, Y. A. (2010). Amoebae and mammals deliver protein-rich Atkins diet meals to Legionella cells. Issues.

Rancès, E., Voronin, D., Tran-Van, V., & Mavingui, P. (2008). Genetic and functional characterization of the type IV secretion system in *Wolbachia*. Journal of bacteriology, 190(14), 5020-5030.

Rasgon, J. L., & Scott, T. W. (2004). Phylogenetic characterization of *Wolbachia* symbionts infecting *Cimex lectularius* L. and *Oeciacus vicarius* Horvath (Hemiptera: Cimicidae). Journal of medical entomology, 41(6), 1175-1178.

Ritchie, S. A., Townsend, M., Paton, C. J., Callahan, A. G., & Hoffmann, A. A. (2015). Application of *w*MelPop *Wolbachia* Strain to Crash Local Populations of *Aedes aegypti*. PLoS Negl Trop Dis, 9(7), e0003930.

Rousset, F., Bouchon, D., Pintureau, B., Juchault, P., & Solignac, M. (1992). *Wolbachia* endosymbionts responsible for various alterations of sexuality in arthropods. Proceedings of the Royal Society of London B: Biological Sciences, 250(1328), 91-98.

Sanogo, Y. O., Dobson, S. L., Bordenstein, S. R., & Novak, R. J. (2007). Disruption of the *Wolbachia* surface protein gene wspB by a transposable element in mosquitoes of the Culex pipiens complex (Diptera, Culicidae). Insect molecular biology, 16(2), 143-154.

Schaeper, N. D., Wimmer, E. A., & Prpic, N. M. (2013). Appendage patterning in the primitively wingless hexapods *Thermobia domestica* (Zygentoma: Lepismatidae) and *Folsomia candida* (Collembola: Isotomidae). Development genes and evolution, 223(6), 341-350.

Schröder, G., Krause, S., Zechner, E. L., Traxler, B., Yeo, H. J., Lurz, R., ... & Lanka, E. (2002). TraG-like proteins of DNA transfer systems and of the *Helicobacter pylori* type IV secretion system: inner membrane gate for exported substrates?. Journal of bacteriology, 184(10), 2767-2779.

Segura, R. L., Águila-Arcos, S., Ugarte-Uribe, B., Vecino, A. J., de la Cruz, F., Goñi, F. M., & Alkorta, I. (2013). The transmembrane domain of the T4SS coupling protein TrwB and its role in protein-protein interactions. Biochimica et Biophysica Acta (BBA)-Biomembranes, 1828(9), 2015-2025.

Sharma, D., Cukras, A. R., Rogers, E. J., Southworth, D. R., & Green, R. (2007). Mutational analysis of S12 protein and implications for the accuracy of decoding by the ribosome. Journal of molecular biology, 374(4), 1065-1076.

Sinkins, S. P. (2004). *Wolbachia* and cytoplasmic incompatibility in mosquitoes. Insect biochemistry and molecular biology, 34(7), 723-729.

Sinkins, S. P., & Gould, F. (2006). Gene drive systems for insect disease vectors. Nature Reviews Genetics, 7(6), 427-435.

Sinkins, S. P., Walker, T., Lynd, A. R., Steven, A. R., Makepeace, B. L., Godfray, H. C. J., & Parkhill, J. (2005). *Wolbachia* variability and host effects on crossing type in *Culex mosquitoes*. Nature, 436(7048), 257-260.

Stingl, K., Müller, S., Scheidgen-Kleyboldt, G., Clausen, M., & Maier, B. (2010).

Composite system mediates two-step DNA uptake into *Helicobacter pylori*. Proceedings of the National Academy of Sciences, 107(3), 1184-1189.

Stouthamer, R., Breeuwer, J. A., & Hurst, G. D. (1999). *Wolbachia pipientis*: microbial manipulator of arthropod reproduction. Annual Reviews in Microbiology, 53(1), 71-102.

Stouthamer, R., & Kazmer, D. J. (1994). Cytogenetics of microbe-associated parthenogenesis and its consequences for gene flow in *Trichogramma* wasps. Heredity, 73(3), 317-327.

Stouthamer, R., Luck, R. F., & Hamilton, W. D. (1990). Antibiotics cause parthenogenetic *Trichogramma* (Hymenoptera/Trichogrammatidae) to revert to sex. Proceedings of the National Academy of Sciences, 87(7), 2424-2427.

Stouthamer, R., & Werren, J. H. (1993). Microbes associated with parthenogenesis in wasps of the genus *Trichogramma*. Journal of Invertebrate Pathology, 61(1), 6-9.

Tahir, U., Khan, U. H., & Zubair, M. S. (2015). *Wolbachia pipientis*: A potential candidate for combating and eradicating dengue epidemics in Pakistan. Asian Pacific journal of tropical medicine, 8(12), 989-998.

Taylor, M. J., Bandi, C., & Hoerauf, A. (2005). *Wolbachia*. Bacterial endosymbionts of filarial nematodes. Advances in parasitology, 60, 245-284.

Taylor, M. J., Voronin, D., Johnston, K. L., & Ford, L. (2013). *Wolbachia* filarial interactions. Cellular microbiology, 15(4), 520-526.

Terradot, L., & Waksman, G. (2011). Architecture of the *Helicobacter pylori* Cag-type IV secretion system. FEBS Journal, 278(8), 1213-1222.

Timmermans, M. J., & Ellers, J. (2009). *Wolbachia* endosymbiont is essential for egg hatching in a parthenogenetic arthropod. Evolutionary ecology, 23(6), 931-942.

Timmermans, M. J. T. N., Roelofs, D., Mariën, J., & Straalen, N. V. (2008). Revealing pancrustacean relationships: Phylogenetic analysis of ribosomal protein genes places Collembola (springtails) in a monophyletic Hexapoda and reinforces the discrepancy between mitochondrial and nuclear DNA markers. BMC Evolutionary Biology, 8(1), 1.

Tram, U., & Sullivan, W. (2002). Role of delayed nuclear envelope breakdown and mitosis in *Wolbachia*-induced cytoplasmic incompatibility. Science, 296(5570),

1124-1126.

Trpis, M., Perrone, J. B., Reissig, M., & Parker, K. L. (1981). Control of cytoplasmic incompatibility in the *Aedes scutellaris* complex Incompatible crosses become compatible by treatment of larvae with heat or antibiotics. Journal of Heredity, 72(5), 313-317.

Vandekerckhove, T. T., Watteyne, S., Willems, A., Swings, J. G., Mertens, J., & Gillis, M. (1999). Phylogenetic analysis of the *16S rDNA* of the cytoplasmic bacterium *Wolbachia* from the novel host *Folsomia candida* (Hexapoda, Collembola) and its implications for wolbachial taxonomy. FEMS microbiology letters, 180(2), 279-286.

Vavre, F., De Jong, J. H., & Stouthamer, R. (2004). Cytogenetic mechanism and genetic consequences of thelytoky in the wasp *Trichogramma cacoeciae*. Heredity, 93(6), 592-596.

Vergunst, A. C., van Lier, M. C., den Dulk-Ras, A., Stüve, T. A. G., Ouwehand, A., & Hooykaas, P. J. (2005). Positive charge is an important feature of the C-terminal transport signal of the VirB/D4-translocated proteins of *Agrobacterium*. Proceedings of the National Academy of Sciences of the United States of America, 102(3), 832-837.

Voth, D. E., & Heinzen, R. A. (2009). *Coxiella* type IV secretion and cellular microbiology. Current opinion in microbiology, 12(1), 74-80.

Waagner, D., Holmstrup, M., Bayley, M., & Sørensen, J. G. (2013). Induced cold-tolerance mechanisms depend on duration of acclimation in the chill-sensitive *Folsomia candida* (Collembola). The Journal of experimental biology, 216(11), 1991-2000.

Wade, M. J., & Stevens, L. (1985). Microorganism mediated reproductive isolation in flour beetles (genus *Tribolium*). Science, 227(4686), 527-528.

Wallden, K., Rivera-Calzada, A., & Waksman, G. (2010). Microreview: Type IV secretion systems: versatility and diversity in function. Cellular microbiology, 12(9), 1203-1212.

Weeks, A. R., & Breeuwer, J. A. J. (2001). *Wolbachia*-induced parthenogenesis in a genus of phytophagous mites. Proceedings of the Royal Society of London B: Biological Sciences, 268(1482), 2245-2251.

Werren, J. H. (1997). Biology of *Wolbachia*. Annual review of entomology, 42(1), 587-609.

Werren, J. H., Baldo, L., & Clark, M. E. (2008). *Wolbachia*: master manipulators of invertebrate biology. Nature Reviews Microbiology, 6(10), 741-751.

Werren, J. H., & Bartos, J. D. (2001). Recombination in *Wolbachia*. Current Biology, 11(6), 431-435.

Werren, J. H., Zhang, W., & Guo, L. R. (1995). Evolution and phylogeny of *Wolbachia*: reproductive parasites of arthropods. Proceedings of the Royal Society of London B: Biological Sciences, 261(1360), 55-63.

Whitaker, N., Chen, Y., Jakubowski, S. J., Sarkar, M. K., Li, F., & Christie, P. J. (2015). The all-alpha domains of coupling proteins from the *Agrobacterium tumefaciens* VirB/VirD4 and *Enterococcus faecalis* pCF10-encoded type IV secretion systems confer specificity to binding of cognate DNA substrates. Journal of bacteriology, 197(14), 2335-2349.

Wu, M., Sun, L. V., Vamathevan, J., Riegler, M., Deboy, R., Brownlie, J. C., ... & Wiegand, C. (2004). Phylogenomics of the reproductive parasite *Wolbachia pipientis w*Mel: a streamlined genome overrun by mobile genetic elements. PLoS Biol, 2(3), e69.

Xu, S., Zhang, C., Miao, Y., Gao, J., & Xu, D. (2010). Effector prediction in host-pathogen interaction based on a Markov model of a ubiquitous EPIYA motif. BMC genomics, 11(3), 1.

Yen, J. H., & Barr, A. R. (1971). New hypothesis of the cause of cytoplasmic incompatibility in *Culex pipiens* L.

Yen, J. H., & Barr, A. R. (1973). The etiological agent of cytoplasmic incompatibility in *Culex pipiens*. Journal of invertebrate pathology, 22(2), 242-250.

Yun, Y., Peng, Y., Liu, F. X., & Lei, C. (2011). *Wolbachia* screening in spiders and assessment of horizontal transmission between predator and prey. Neotropical entomology, 40(2), 164-169.

Zchori-Fein, E., Roush, R. T., & Hunter, M. S. (1992). Male production induced by antibiotic treatment in *Encarsia formosa* (Hymenoptera: Aphelinidae), an asexual species. Experientia, 48(1), 102-105.

Zeh, D. W., Zeh, J. A., & Bonilla, M. M. (2005). *Wolbachia*, sex ratio bias and apparent male killing in the harlequin beetle riding pseudoscorpion. Heredity, 95(1), 41-49.

Zhang, F., Chen, Z., Dong, R. R., Deharveng, L., Stevens, M. I., Huang, Y. H., & Zhu, C. D. (2014). Molecular phylogeny reveals independent origins of body scales in Entomobryidae (Hexapoda: Collembola). Molecular Phylogenetics and Evolution, 70, 231-239.

Zou, L., Nan, C., & Hu, F. (2013). Accurate prediction of bacterial type IV secreted effectors using amino acid composition and PSSM profiles. Bioinformatics, 29(24), 3135-3142.